THE UNIVERSITY
of EDINBURGH

Post-transcriptional regulation of miRNA biogenesis

Angela Downie

Thesis presented for the degree of Doctor of Philosophy

2019

Declaration

I declare that this thesis was compose by myself, that the work contained herein is my own except where explicitly stated otherwise in the text, and that this work has not been submitted for any other degree or processional qualification except as specified.

The work presented in the results chapter, *Post-transcriptional regulation of 14q32 cluster microRNAs*, has been published in Molecular Therapy Nucleic Acids, Volume 14, p329-338, March 2019, under the title "Posttranscriptional Regulation of 14q32 MicroRNAs by the CIRBP and HADHB during Vascular Regeneration after Ischemia" by authors, Angela Downie Ruiz Velasco, Sabine M.J Welten, Eveline A.C Goossens, Paul H.A Quax, Juri Rappsilber, Gracjan Michlewski and A. Yaël Nossent.

The work presented in the results chapter, *Lin28a regulation of miRNAs during neurogenesis*, has been published in RNA, 2017 Mar, 23(3): 317-332, under the title "Lin28a uses distinct mechanisms of binding to RNA and affects miRNA levels positively and negatively" by authors Jakub Stanislaw Nowak, Furzsina Hobor, Angela Downie Ruiz Velasco, Nila Roy Choudhury, Gregory Heikel, Alastair Kerr, Andres Ramos and Gracjan Michlewski.

The work presented in the results chapter, *Oleic acid regulation of miRNA biogenesis by inhibition of RNA binding activity of RBPs,* has been published in Journal of Molecular Biology, Volume 429, Issue 11, June 2017, p1638-1649 under the title "Oleic Acid Induces MiR-7 Processing through Remodelling of Pri-MiR-7/Protein Complex" by authors Santosh Kumar, Angela Downie Ruiz Velasco and Gracjan Michlewski.

Angela Downie

Edinburgh

June 2019

Contents

Acknowledgments

Firstly, I would like to thank my supervisor Dr. Gracjan Michlewski for his extensive support, advice and patience. I am lucky to have had the opportunity to carry out my PhD under someone I look up to as both a scientist and a mentor and will look back fondly at this part of my career, despite its challenges.

I would also like to thank Dr. Nila Roy Choudhury who was always there to fix any constantly arising problems. Her knowledge and experience in the lab where invaluable problem solving tools and her emotional support was a guiding light in the dark and confusing points of my PhD.

Thanks as well to the many members of the lab who weaved in and out during my 4 years there, you were all great to work with, providing levity when needed and each of you teaching me valuable lessons. In particular, thanks to Gregory Heikel, who I got to share this journey with from the beginning to the end, and then further.

I would like to thank everyone at both the WCCB and the DIPM who ever offered help both in and out of the lab. I would especially like to thank the members of my thesis committee Dr. Atlanta Cook and Dr. David Finnegan for your advice and suggestions. I would also like to thank Sarah Keer-Keer as the opportunity to participate in public engagement constantly reminded me that science *is* in fact, really cool, when I might have forgotten it and provided me with great personal growth.

Thank you to the funding bodies who made my PhD possible; the Mexican National Commission of Science and Technology (CONACYT) and the University of Edinburgh's Principal's Career Development Scholarship.

Finally I would like to thank all of my friends and family. I was lucky enough to meet incredible people in Edinburgh who made my time there a very enjoyable one through many dinners, parties, climbing sessions, trips near and far and many a pub quiz.

And the most special thanks to my parents, the people I admire the most in the world and the best role models I could hope for. I would not be where I am without your love and support. I am so lucky to have you to turn to when things get hard and I love you enormously.

"And you are made of a hundred trillion cells. We are, each of us, a multitude." -Carl Sagan

Abstract

MicroRNAs (miRNAs) are short non-coding RNA molecules of ~22 nt in length that function as regulators of gene expression. They bind to the 3' UTR of target mRNAs in a non-perfect complimentary manner, leading to either their degradation or translational repression. Over half of all protein coding genes contain miRNA target sites, meaning that miRNAs are involved in the regulation of virtually every cellular pathway. Because of this, miRNAs themselves are under strict regulation, often expressed in temporal or tissue-specific manners.

MiRNAs are transcribed as long primary transcripts (pri-miRs) with stem-loop structures that are processed in the nucleus into ~70nt hairpins (pre-miRs), exported into the cytoplasm and cleaved into miRNA duplexes. MiRNA duplexes are incorporated into Ago proteins which retain single stranded mature miRNA in a functional RISC complex. Regulation of miRNA biogenesis occurs both at a transcriptional and post-transcriptional level. Various proteins that function in the post-transcriptional regulation of miRNA biogenesis have been described. However, in recent years, proteome-wide studies have expanded our knowledge of RNA-binding proteins (RBPs). Many non-canonical RBPs with unknown roles in RNA metabolism have been identified. This expanded repertoire of RBP represents a new pool of potential miRNA biogenesis regulators. One group of interest amongst newly identified non-canonical RBPs are metabolic enzymes which are beginning to show a role in RNA metabolism, providing a link between gene regulation and cellular metabolism that is not yet fully understood.

This study has focused on better understanding the post-transcriptional regulation of miRNA biogenesis in several systems. Firstly, protein factors involved in the regulation of miRNA cluster 14q32 were sought. This cluster represents the largest mammalian miRNA cluster and is important in mediating the response to ischemia. In this study, two proteins, cold-induced RNA binding protein (CIRBP) and hydroxyacyl-CoA dehydrogenase trifunctional multienzyme complex subunit beta

(HADHB), were identified as post-transcriptional regulators of selected 14q32 miRNAs and further validated in cellular systems.

Next, the mechanism underlying the control of miRNA biogenesis by known RBP regulator, cell lineage abnormal 28a (Lin28a), was explored in further detail. Lin28a represents the best-studied example of post-transcriptional miRNA regulation, influencing both nuclear and cytoplasmic let-7 processing as well as mediating pre-let-7 uridylation and subsequent degradation. Lin28a can also regulate neuro-specific miR-9 which differs in sequence and structure from let-7. Here we showed that both miRNA precursors interact with different domains of Lin28a and the mechanisms regulation are different. This shows how a single RBP can have extensive effects in the regulation of miRNA biogenesis in different cellular contexts.

Finally, in this study the inhibition by oleic acid (OA) of HuR and MSI2 binding to pri-miR-7 was explored. MSI2 in a complex with HuR inhibits biogenesis of neuro-enriched miR-7. OA is the most abundant fatty acid and had previously been shown to inhibit the RNA-binding of MSI2 homolog, MSI1. Here this knowledge was extended to show that OA also inhibits MSI2 and HuR binding to pri-miR-7, increasing its processing. This gives an example of a mechanism regulating the interaction of miRNA precursors with regulatory proteins, modulating the effect of these proteins on miRNA biogenesis. This also provided additional links between metabolism and regulation of RNA processing.

In general, these investigations add to the current knowledge on post-transcriptional regulation of miRNAs and highlight the complexity of this system. Different mechanisms governing regulation of miRNA processing coexists in cells. Therefore, better understanding the individual factors at play will allow to generate a better picture of the regulatory networks mediating miRNA biogenesis.

Lay summary

Every cell in our body contains an identical copy of DNA, however these cells have to carry out different functions depending on their stage of development, the organ they belong to or the environmental stress they are subjected to. To achieve this, our cells employ various mechanisms to control which genes (or bits of DNA) are actively being used. One of these mechanisms involves the use of special regulatory molecules named microRNAs (or miRNAs for short).

Our DNA is made up of four different bases; these bases serve as a four-letter code that our cells are able to interpret in order to make useful molecules named proteins out of our genes. In order to carry out this process, cells create a copy of our DNA which is known as RNA. The RNA copy of a gene is known as messenger RNA and it has the same sequence of bases as DNA; but unlike DNA each cell can have multiple RNA copies of a single gene, meaning more of that type of protein will be produced. Like messenger RNA, miRNAs are made up of RNA, but they do not code for proteins. Instead miRNAs can bind to messenger RNAs with similar sequences to them and destroy them. This is very important for our cells as it ensures that only the necessary proteins for each cell-type and developmental stage are produced and the levels of these can be fine-tuned according to the needs of the cell. Because of this, expression of miRNAs in incorrect temporal and spatial patterns can lead to many diseases including cardiovascular diseases, neurodegenerative diseases and cancer.

The focus of this thesis has been to understand how cells control which miRNAs are produced. I have looked at the regulatory mechanisms behind the expression of miRNAs in three different scenarios. Firstly, I looked at a group of miRNAs whose levels increase when there is a lack of blood flow to the tissue and have identified two new proteins involved in regulation of miRNA. Secondly, I explored the roles of a known protein called Lin28a in controlling the levels of different miRNAs during the development of the brain. Finally, I looked at how fatty acids, which are common

components of our cells and our diets can affect the proteins that bind to and control the production of miRNAs.

Because miRNAs are found dysregulated in a variety of diseases, identifying the regulators of miRNA biogenesis provides potential targets for the future development of novel therapies.

Abbreviations

AD	Alzheimer's disease
ADAR	adenosine deaminases acting on RNA
AGO	argonaute
ARE	AU-rich element
ATP	adenosine triphosphate
CIP	creatine phosphate
CIRBP	cold-induced RNA-binding protein
CSD	cold-shock domain
CTL	conserved terminal loop
EA	elaidic acid
EMSA	electrophoretic mobility shift assay
ES/ESC	embryonic stem (cells)
FACS	fluorescence-activated cell sorting
GAPDH	glyceraldehyde 3-phosphate dehydrogenase
GFP	green fluorescent protein
GSO	gene-silencing oligonucleotides
HADHA	hydroxyacyl-CoA dehydrogenase trifunctional multienzyme complex subunit alpha
HADHB	hydroxyacyl-CoA dehydrogenase trifunctional multienzyme complex subunit beta
HIF	hypoxia-inducible factor
HLI	hindlimb ischemia
HuR	human antigen R
IRE	iron regulatory element
KD	knock-down
KO	knock-out
miRNA	microRNA
mRNA	messenger RNA

MSI1	Musashi RNA-binding protein 1
MSI2	Musashi RNA binding protein 2
MTP	mitochondrial trifunctional protein
OA	oleic acid
Oncomir	oncogenic miRNA
PACT	protein activator of PKR
PAGE	polyacrylamide gel electrophoresis
PD	Parkinson's disease
piRNA	piwi-interacting RNA
pre-miR	precursor microRNA
pri-miR	primary microRNA
qRT-PCR	quantitative reverse transcription - polymerase chain reaction
RBM	RNA-binding motif
RBM3	RNA binding motif protein 3
RBP	RNA binding protein
RGG	glycine-rich domain
RISC	RNA-induced silencing complex
RNAi	RNA interference
RP-SMS	RNA pulldown- SILAC mass spectrometry
RRM	RNA recognition motif
RT	room temperature
sgRNA	single guide RNA
shRNA	short hairpin RNA
SILAC	stable isotope labelling of amino acids
siRNA	short interfering RNA
snoRNA	small nucleolar RNA
TSS	transcription start site
TUT/TUTase	terminal uridylyl transferase
UTR	untranslated region

WEMSA	western blot-combined electrophoretic mobility shift assay
WT	wild-type

Introduction

MiRNA Biogenesis, functions and genomic organization

MicroRNAs (miRNAs) are short non-coding RNAs ~22 nt in length that function as important regulators of gene expression[1]. They constitute one of three classes of small silencing RNAs found in animals along with short interfering RNAs (siRNAs) and piwi interacting RNAs (piRNAs) each distinguished by their biogenetic pathway and associated effector proteins[2]. MiRNAs carry out their function within a RNA induced silencing complex (RISC)[3] where they serve as guides directing the RISC towards target messenger RNAs (mRNAs) by binding to partially complementary sequences in their 3'UTR regions. In turn, binding of the RISC leads to either degradation or translational repression of the mRNAs[4,5].

The first miRNA, *lin-4,* was identified as a regulator of protein Lin-14 in the developmental stages of *C. elegans* in 1993[6,7]. For several years this was believed to be the sole example of a rare phenomenon, exclusive to nematodes. However in 2000 a second miRNA, *let-7,* was described and importantly, found to be conserved across the animal kingdom[8,9]. Studies quickly followed showing that these two molecules where in fact members of a much larger family of RNAs, containing hundreds of highly conserved members and representing a common regulatory mechanism[10–12]. Currently, there are 2654 human and 1978 murine mature miRNAs annotated in the online database *miRBase*[13]*.* These regulate the expression of a large number of protein coding and non-coding genes, with approximately 60% of mRNAs predicted

to contain miRNA target sites[14]. MiRNAs have been found to be involved in virtually every cellular process and are essential in development, differentiation and homeostasis[1,2,15]. A majority of miRNAs are expressed in tissue-specific and temporal specific patterns[16] and many diseases are associated with their disregulation including cancer, neurodegenerative diseases, metabolic diseases and cardiovascular diseases[17–21]. Their importance is further highlighted by murine loss-of-function studies, in which disruption of miRNA genes produces mouse phenotypes with various developmental, cellular, physiological and behavioural defects which affect viability and can lead to the development of severe health conditions[15]. Furthermore, deletions of miRNA processing enzymes DROSHA and DICER in mouse embryos have proven lethal[22,23].

MiRNA biogenesis pathway

Canonical MiRNA biogenesis

Canonical miRNA biogenesis requires two sequential cleavages mediated by RNase III type endonucleases DROSHA and DICER[24,25] (Figure 1). RNAse III endonucleases show specificity for double stranded RNA and generate characteristic products with 5' monophosphate groups and two-nucleotide 3' overhangs[26], which are important for recognition by the miRNA biogenesis machinery[27]. MiRNAs are first transcribed as long primary transcripts (pri-miRs) which are variable in length and can often contain multiple mature miRNAs which are found clustered in the genome and transcribed as a single polycistronic unit[24]. Pri-miRs can either be transcribed from independent promoters, or can be found within transcripts of both protein-coding and non-coding sequences[2]. Most pri-miRs are transcribed by RNA Polymerase II (Pol II)[28,29], however viral miRNAs processed through atypical mechanisms have been shown to be transcribed by RNA Polymerase III (Pol III)[30,31].

Embedded in pri-miRs are RNA stem-loop structures that are recognized and cleaved by DROSHA in the nucleus[25]. In order to function DROSHA requires interaction with a second protein; DGCR8 (DiGeorge syndrome chromosomal region 8). These proteins form the core of a heterotrimeric complex known as the microprocessor, composed of two DGCR8 units and one DROSHA subunit and which can also include various co-factors[27,32–36]. Aside from its established role in miRNA biogenesis, the microprocessor can also bind and regulate a variety of cellular RNAs including mRNAs,

long non-coding RNAs and RNAs derived from retrotransposons[37–40]. Additionally, DGCR8 is able to associate with other nucleases and as such is able to mediate small nucleolar RNA (snoRNA)- cleavage in a DROSHA-independent manner[41].

Within the microprocessor, DROSHA cleaves the pri-miR contained RNA stem loops ~11bp from the base of the stem and in doing so determines the final mature miRNA sequences as this cleavage also fixes the site for the subsequent cleavage by DICER[42]. Several structure and sequence features of pri-miRs distinguish them from other hairpin containing transcripts and enhance their recognition and processing by the microprocessor. Structurally, pri-miRs are comprised of a ~35 bp imperfect stem structure with an apical loop and unpaired segments at the base[42,43]. Additionally, various sequence features positively influence microprocessor recognition including a mismatched 'GHG' motif positioned mid-stem, a basal 'UG', an apical 'UGUG' and a 'CNNC' motif ~17 nt downstream of the DROSHA cleavage site[43,44]. This first cleavage step frequently occurs co-transcriptionally and co-ordinately with splicing[45–47].

The stem-loop structures liberated after microprocessor cleavage are known as precursor miRNAs (pre-miRs) and are of ~70nt in length. Pre-miRNAs are recognized and transported out of the nucleus by the RAN-GTP dependent karyopherin, Exportin-5[48] (Figure 2). In the cytoplasm, pre-miRs are recognized and cleaved by DICER[49,50] which removes both the terminal base pairs and the apical loop, producing ~22 nt miRNA duplexes. This activity is parallel to the role that DICER has in siRNA maturation, where its activity was first described[50].

Once formed, the miRNA duplex is incorporated into a protein of the argonaute family (AGO) to form the RISC, which is the effector complex responsible for gene silencing[3]. Loading of the duplex occurs with the assistance of HSC70/HSP90 chaperones, which use ATP to mediate a conformational change of AGO proteins into a high-energy open state that allows for the entry of bulky miRNA duplexes[51]. Subsequently, AGO unwinds the miRNA duplex and ejects the passenger strand in an ATP-independent manner, thus forming the mature RISC complex[52]. RISC loading is an asymmetric process, with one strand being preferentially incorporated into the

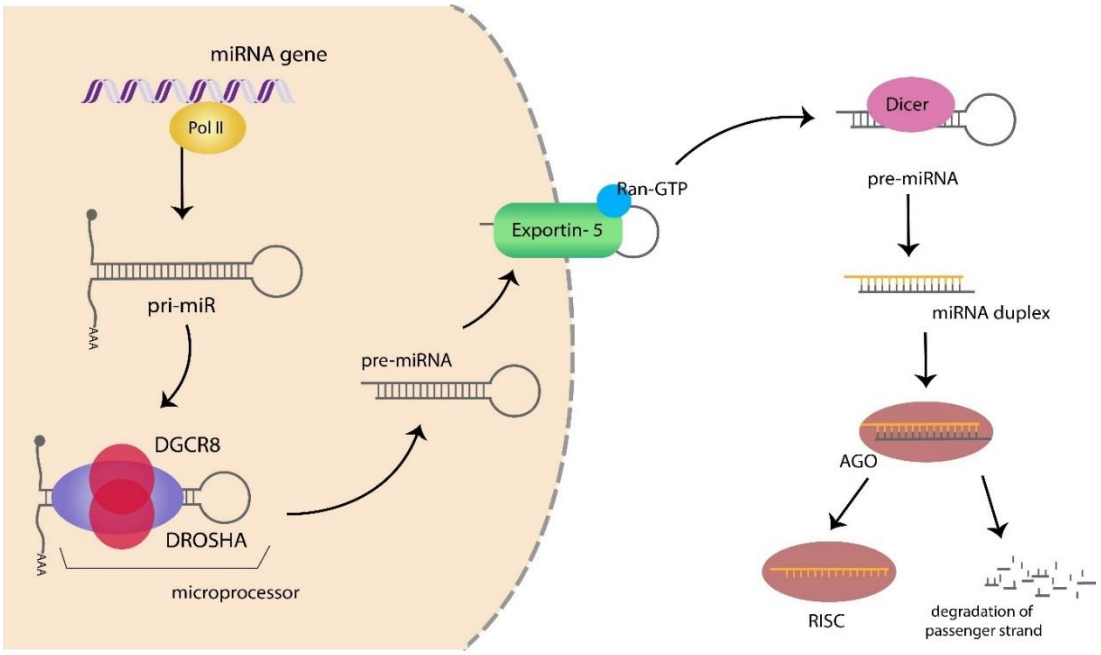

RISC. This is determined by the thermodynamic stability at either end of the miRNA duplex, however this mechanism is not exact and potential for the incorporation of either strand exists[2].

Figure 1 Canonical biogenesis of miRNAs. *Most miRNAs are transcribed by Pol II into long primary transcripts that are capped and polyadenylated. Pri-miRs contain stem-loop structures that in the nucleus are recognized and cleaved by the microprocessor complex into ~70 nt pre-miRNAs. These are then exported out into the cytoplasm by Exportin-5–Ran-GTP. In the cytoplasm pre-miR undergo a second cleavage by Dicer, generating 22nt miRNA duplexes. These duplexes are loaded into an AGO protein where the mature strand remains in complex with AGO, forming the RISC, whilst the passenger strand is ejected and degraded.*

Non-canonical biogenesis of miRNAs

As well as the canonical two-step pathway, alternative mechanisms of miRNA biogenesis independent of either DROSHA or DICER have been elucidated[15] (Figure 2). The first of these involves miRNAs derived from spliced and debranched short introns known as 'mirtrons'[53,54]. Mirtrons are generated independently from DROSHA and are instead processed by the spliceosome into non-linear intermediates subsequently resolved by the lariat debranching enzyme to adopt a hairpin conformation with a traditional 3' 2 nt overhang[53,54]. These hairpins can then enter the canonical pathway at the nuclear export step functioning as Exportin-5 and DICER substrates[54] (Figure 2 B).

A second class of DROSHA-independent noncanonical miRNAs arise from endogenous short hairpin RNAs (shRNAs) directly transcribed by Pol II[55,56]. In this case the first nucleotide of the pre-miR corresponds to the transcription start site (TSS)[56], whilst the exact mechanism of 3' end selection remains unknown but is likely to be coupled to transcription termination[56]. The pre-miR hairpins produced in this way are capped at the 5' end, which has important consequences as it impedes loading of the 5' mature miRNA into the RISC meaning silencing occurs exclusively through the 3' strand[55,56]. Additionally, the nuclear export of capped precursors is mediated by Exportin-1 rather than Exportin-5[56] (Figure 2 C).

DICER has also been implicated in the DROSHA-independent processing of miRNAs from other non-coding RNAs[57]. Examples of this include miR-1983 which arises from a hairpin that partially overlaps with a tRNA[55] and miR-1839 which is cleaved from

the small nucleolar RNA (snoRNA) ACA-45[58]. Several reports have expanded on the latter, noting various examples of molecules with dual snoRNA and miRNA functions, uncovering a more complex relationship between different types of non-coding RNAs[59–62] (Figure 2D). Additionally, DICER is involved in generating viral encoded miRNAs through atypical mechanisms[30,63].

Whilst all these examples are DICER-dependent, miR-451 is a well characterized erythropoietic miRNA that requires DROSHA, but not DICER[64,65]. In this case, the pre-miR-541 produced by DROSHA has a very small stem, and a mature miRNA sequences that extends over the terminal loop[65]. This impedes cleavage by Dicer, and miR-451 is instead cleaved directly by RISC component AGO2 followed by 3' end trimming[64,65] (Figure 2 E).

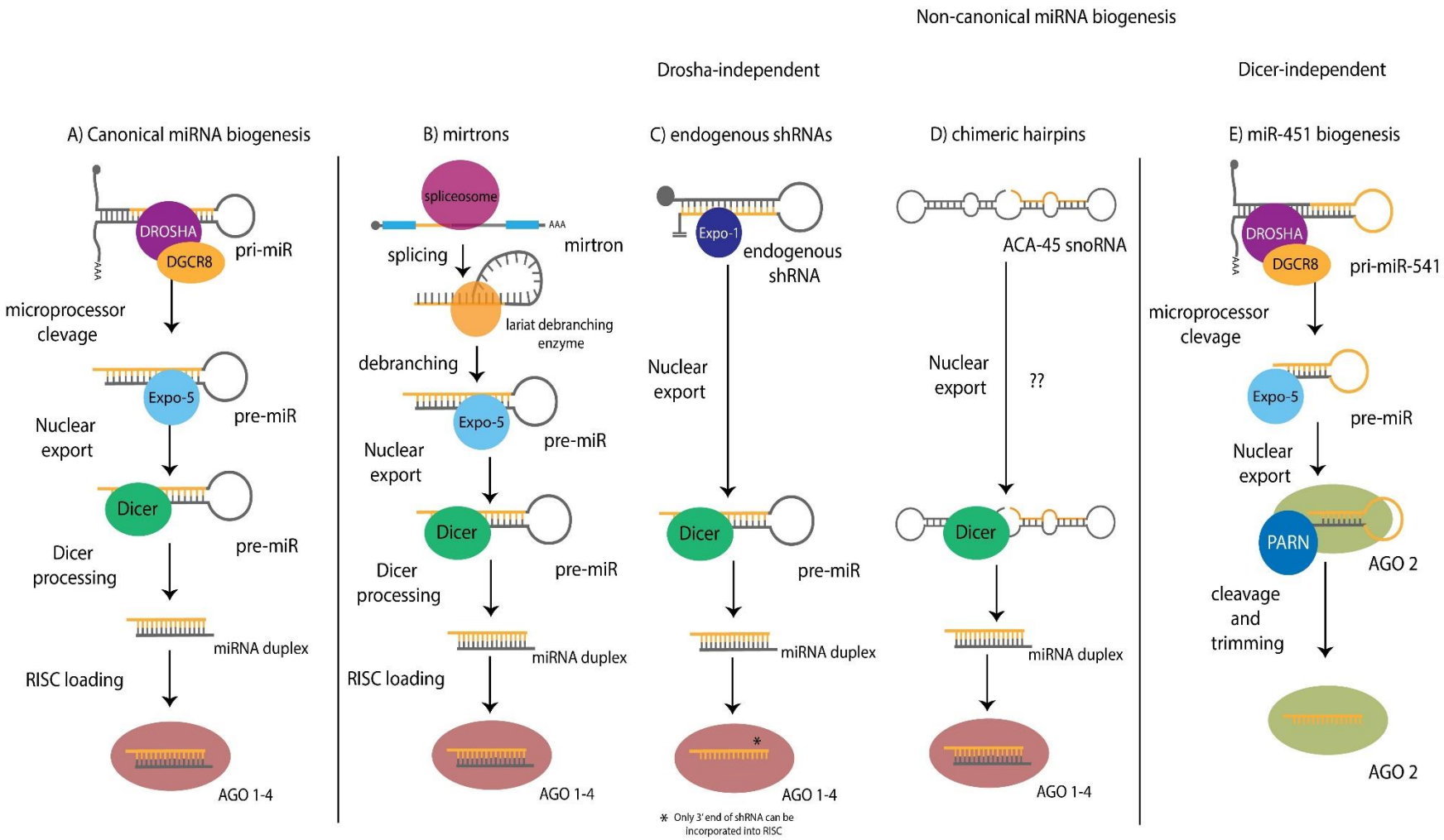
Non-canonical miRNA biogenesis
Drosha-independent
Dicer-independent
A) Canonical miRNA biogenesis
B) mirtrons
C) endogenous shRNAs
D) chimeric hairpins
E) miR-451 biogenesis
DROSHA
DGCR8
pri-miR
microprocessor clevage
Expo-5
pre-miR
Nuclear export
Dicer
Dicer processing
miRNA duplex
RISC loading
AGO 1-4
spliceosome
AAA
mirtron
splicing
lariat debranching enzyme
debranching
Expo-1
endogenous shRNA
ACA-45 snoRNA
??
pri-miR-541
PARN
AGO 2
cleavage and trimming
* Only 3' end of shRNA can be incorporated into RISC

Figure 2 Non-canonical biogenesis of miRNAs. Schematic comparing canonical and non-canonical regulation of miRNAs. A) Canonical biogenesis of miRNA biogenesis; pri-miRs in the nucleus are recognized and cleaved by the microprocessor, subsequently they are transported into the cytoplasm by exportin-5 where they are recognized and cleaved by Dicer into mature miRNA duplexes. These are then loaded into AGO 1-4 to form the mature RISC. B-D) non-canonical DROSHA independent biogenesis of miRNAs. B) mirtrons are processed by the spliceosome into non-linear intermediates that are resolved into hairpins by the lariat debranching enzyme, these then join the canonical pathway as Dicer substrates. C) Endogenous shRNAs are transcribed directly by Pol II and transported to the cytoplasm by Exportin-1 where they are processed by Dicer. Because they are capped at the 5' only the 3' strand can function within the RISC. D) miRNAs can be processed directly by dicer from chimeric transcripts encoding snoRNAs or tRNAs. E) Dicer independent miRNA biogenesis; miRNAs such as miR-541 where the mature miRNA sequence extends over the apical loop cannot be processed by Dicer, instead they are directly loaded and cleaved by AGO2 (the only AGO protein with catalytic activity). They are subsequently trimmed at the 3' end by PARN to form the mature RISC.

MiRNA regulatory mechanisms and cellular functions

Mechanisms of action of the RISC

The core silencing component of the RISC consists of a miRNA bound to a member of the argonaute family protein (AGO); the miRNA functions as a guide whilst the AGO protein is the effector[66–68]. In humans there are 4 members of the AGO family, AGO1/2/3/4[69]. These four proteins bind overlapping pools of miRNAs without an apparent preference[66,68], however AGO2 is the only member of the family with conserved catalytic activity. This activity is essential for siRNA-mediated gene silencing as well as for non-canonical biogenesis of a small number of miRNAs[64,65,68,70]. AGO2 can also mediate endonucleolytic cleavage of mRNAs that show extensive binding to miRNAs, this however is a rare occurrence[66,68]. In fact, most miRNA:mRNA interactions are restricted to the 5' end of the miRNA, requiring an uninterrupted stretch of at least 6 but preferably 7 binding nucleotides around positions 2-8 which are sufficient and necessary for regulation; this region is known as the 'seed'[71–73]. Supplementary 3' binding to miRNA positions 14-16 as well as the presence of an adenosine in position 1 can increase binding affinity for the mRNA[4,74,75]. These lenient binding requirements mean that most miRNAs are able to simultaneously regulate hundreds of different mRNAs[5,76–79].

The RISC induces gene silencing both by blocking translation initiation and by destabilisation, deadenylation and subsequent degradation of mRNAs, with degradation of mRNAs accounting for most of miRNA-mediated repression (66-

90%)[5–7,76–78,80–84]. For the latter, the interaction between AGO and proteins of the GW182 family (TNR6 A/B/C in humans) is required[85,86]. GW182 proteins interact with Cytoplasmic Poly(A) binding protein (PABPC) forming a scaffold that recruits deadenylation complexes PAN2-PAN3 and CCR4-NOT[84,87]. Deadenylated mRNAs are then decapped by decapping protein 2 (DCP2) which functions in conjunction with several cofactors, including helicase DDX6[88,89] (Figure 3). Finally, deadenylated and decapped mRNAs are degraded by the main cytoplasmic nuclease, 5'-to-3' exoribonuclease 1 (XRN1)[89]. Helicase DDX6 also interacts with the CCR4-NOT complex, linking deadenylation and decapping activities[88]. The mechanisms through which miRNAs mediate inhibition of translation initiation are less clear but it is thought they involve interference with the activity or assembly of the eukaryotic initiation factor 4F (eIF4F) complex. Additionally, deadenylation and decapping of mRNAs decreases their translation efficiency[84].

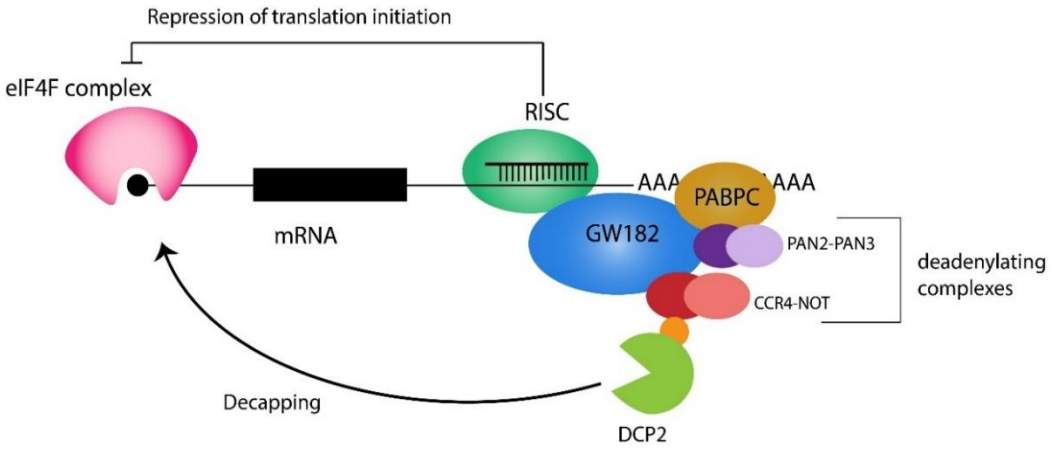

Figure 3 Mechanism of action of the RISC. *Schematic representation of mechanisms of RISC silencing. The RISC directly interferes with the eIF4F initiation complex, in so repressing translation initiation. However, the majority of the silencing effects of the RISC are explained by deadenylation, decapping and degradation of mRNA targets. The RISC interacts with GW182 proteins which also bind PABPC and recruit deadenylating complexes PAN2-PAN3 and CCR4-NOT1. Additionally, GW182 proteins recruit decapping enzyme DCP2. CCR4-NOT1 interacts with cofactor DDX6, through which it can establish a physical interaction to DCP2. Deadenylated and decapped mRNAs will be degraded by cytoplasmic exonuclease XRN1.*

Cellular functions of miRNAs

MiRNAs are implicated in virtually every cellular pathway during development and homeostasis. Strong evolutionary conservation of both miRNAs and their target sites highlights their vast importance, however the repressive effect of a miRNA on a single gene tends to be modest (< 2-fold) and deletion of individual miRNAs can often result in no discernible phenotype[78,90,91]. But whilst miRNAs do not exhibit strong repression of individual targets, they are able to exert their functions on hundreds of targets simultaneously, many of which are expressed either in close spatial or temporal proximity to their regulating miRNA[91]. Additionally, different miRNAs possess overlapping targets and when expressed in the same cell this allows a higher level of target repression whilst generating functional redundancy, dampening the effects of loss of individual miRNAs[90–92]. Taken together, all of this suggests that miRNAs usually function by conferring robustness to gene regulatory networks as well as fine-tuning the levels of co-expressed proteins rather than functioning as molecular switches[90,91,93].

This ability to confer robustness to a gene regulatory network is particularly important during development and differentiation, where miRNAs not only help define but also maintain differentiated cellular states by targeting unwanted transcripts[93]. An example of such is miR-124, which is repressed in neural progenitors with its levels increasing during neurogenesis[91,94–97]. MiR-124 targets multiple non-neural transcripts, including transcripts that are highly expressed in neural progenitors such as laminin-γ1 and integrin-β1[96], as well as Sox9 which preferentially

drives differentiation into glial cells from neural progenitors[96]. In this way, miR-124 ensures the repression of any non-neural transcripts that may still be present during neurogenesis, reinforcing a neuronal gene programme.

An important miRNA family in differentiation is the let-7 family. Let-7 was originally identified as a heterochronic gene in *C. elegans* where it reaches its maximum expression in the last larval stage, and helps regulate the transition to adulthood[8,98]. In mice and humans, the let-7 family consists of 13 mature miRNAs with a conserved seed sequence that originate from 10 different precursors (let-7-a1, -a2, -a3 (human), -b, -c(1), -c2 (mouse), -d, -e, f1, -f2, -g, -i and miR-98)[99]. In mammals, let-7 family members are absent from embryonic stem cells (ESC) as their processing is blocked by pluripotency factor Lin28, however they are broadly expressed across somatic tissues[100–103]. Let-7 miRNAs drive lineage differentiation by silencing many pluripotency-and self-renewal factors including Lin28[104]. This capability was confirmed in mouse *Dgcr8*$^{-/-}$ ESC which are unable to silence self-renewal programmes. Introduction of let-7 into these cells rescues their ability to silence self-renewal[104]. Furthermore, inhibition of let-7 in mouse embryonic fibroblasts (MEF) promoted their de-differentiation. Reciprocally, when ESC-enriched miR-294, miR-295 and miR-291 where introduced together with let-7, they blocked its self-renewal silencing potential by indirectly activating self-renewal genes[104]. This is illustrative of how multiple miRNAs act upon the same pathways, and it is their coordinated action that helps determine cellular outcomes.

As well as helping control neural development, miRNAs regulate adult brain function. Approximately 70% of all miRNAs are expressed in the brain, with half of tissue-enriched/specific miRNAs being found in the brain[105,106]. They are important in neural maintenance, and inactivation of DICER in various brain regions leads to neurodegeneration[107]. In addition, various miRNAs co-ordinately regulate synaptic plasticity by exerting both promoting and inhibitory functions in pathways necessary for synaptogenesis and synaptic maintenance[108].

The ability of miRNAs to confer robustness to gene networks also makes them good at buffering environmental changes, making them important regulators of metabolic homeostasis[21]. They are key regulators of lipid metabolism with several miRNAs including miR-33 and miR-122 regulating the expression of numerous genes involved in lipid synthesis and homeostasis, fatty acid oxidation and cholesterol synthesis and export[109,110]. Additionally, miRNAs also play important roles in glucose metabolism by regulating insulin synthesis, secretion and sensitivity[111–113]. Specifically, miR-375 is enriched in pancreatic β-cells where it has several fundamental roles, influencing insulin expression[114], glucose-dependent insulin secretion[112], and β-cell adaptative proliferation[115]. On the other hand, miR-103 and miR-107 are mediators of hepatic insulin sensitivity through direct regulation of caveolin-1 a critical regulator of the insulin receptor[116].

Their ability to respond to environmental changes also means miRNAs are emerging as important components of the immune response[117]. The innate immune response involves upregulation of various miRNAs, such as miR-155 and miR-146, miR-147,

miR-21 and miR-9, which are transcriptionally regulated by similar factors to inflammatory genes[118–123]. These miRNAs can target pro-inflammatory signalling molecules creating negative feedback loops and ensuring a timely resolution of the inflammatory response[119,124]. Additionally, miR-155 has been shown to fine-tune the levels of multiple immune-related genes including cytokines, chemokines and transcription factors[125]. In contrast, miR-155 has also been shown to positively regulate inflammatory pathways in some situations, contributing to the establishment of a more robust immune response[126]. This again shows the importance of cellular context on miRNA function. Downregulation of miRNAs can also be important in modulating the immune response; activation of interferon response has been shown to alter microprocessor binding to pri-miRs, leading to less efficient processing and reduced mature miRNA levels. This in turn leads to increased levels of IFN-β which again, is key in establishing a robust interferon response[127].

These are just some of the many roles that miRNAs play within cellular regulation, many of which we are awaiting uncovering. These roles can be hard to elucidate as they often operate within complex networks which lead to loss/gain of function studies producing very subtle phenotypes[92]. Furthermore, some miRNAs are not essential under normal conditions, but are necessary in the response to stress[90,92]. An example of this is cardiac-specific miR-208. MiR-208$^{-/-}$ mice have close to normal hearts with no obvious defects, however they do not exhibit cardiac hypertrophy in response to various stresses, as seen in WT mice, meaning miR-208 could have a role in enhancing cardiac function during heart disease[128].

MiRNAs in disease

Because of the multitude of roles that miRNAs play in a cell, it is unsurprising that disregulation of miRNAs is associated with a myriad of pathologies. Changes in miRNA levels have been particularly well documented in different types of cancer. In general, cancer presents a global downregulation of miRNAs[17]. This is attributed to various factors, including genetic loss[129], changes in epigenetic regulation[130], defects in the miRNA biogenesis pathway[131] and dysregulation by aberrantly expressed transcriptions factors such as common oncogene, MYC[132], or tumour suppressor p53[133]. Downregulated levels of DICER have been observed in various tumour types and are associated with poor prognosis[134–136]. Constitutive upregulation of MYC is common in cancer, where it is involved in extensive reprograming of miRNA patterns, inducing widespread repression of miRNAs[132]. On the contrary, most cancers exhibit loss of function of p53, which is a transcriptional activator for a subset of miRNAs that present downregulated levels in various types of tumours[133].

Accompanying global downregulation, select upregulation of oncogenic miRNAs (oncomirs) is also a signature in cancer. For instance, MYC not only causes extensive miRNA downregulation but is responsible for driving expression of the oncogenic miRNA cluster miR-17~92[137]. Overexpression of this cluster is found in various types of cancer and enhances cell proliferation and angiogenesis[17,138–140]. Of the 6 miRNAs in this cluster, miR-19 has the strongest tumorigenic effect by repressing tumour suppressor PTEN, which has roles in inhibiting proliferation and promoting apoptosis[141]. However, miR-17 and miR-20a also contribute to the cluster's oncogenic effects by targeting p21 and inhibiting oncogenic-induced senescence[142],

showing how multiple members of a cluster can potentiate its effects by simultaneously targeting different signalling pathways. MiR-21 is another oncomir found upregulated in most tumour types[143,144]. Mir-21 targets multiple genes involved in tumorigenic processes including important tumour suppressors p53 and PTEN[144]. Furthermore, forced overexpression of miR-21 was sufficient to induce lymphoma in a mice model[145].

Conversely to oncomirs, some miRNAs behave as tumour suppressors. The let-7 family of miRNAs have established roles as tumour suppressors and are frequently downregulated in various cancer types, this is associated with a poor prognosis[146]. This downregulation is driven by the re-expression of LIN28A and LIN28B which are usually confined to early development where they block processing of let-7[147]. Two major targets of let-7 that confer it its tumour suppressor activity are oncogene RAS and chromatin associated protein HMGA2 which functions as a transcriptional regulator, contributing to proliferation and metastasis[146]. Another example of a tumour suppressor miRNA, is miR-7 which inhibits key oncogenic processes in various types of cancer, including cell survival and proliferation and metastasis[148], and is frequently found to be downregulated in glioblastoma[149].

Aside from cancer, changes in expression levels of miRNAs are also associated with metabolic diseases. Several studies have found the upregulation of diverse miRNAs, including miR-143, miR-335 and miR-103/107, in obese mice[116,150–152]. Additionally, studies in both cell lines and murine models have shown levels of specific miRNAs, including miR-34a miR-146, miR-122 and miR-335 to be altered in various diabetic

models[153]. Supporting this, a pancreas-specific deletion of *Dicer1* in mice was shown to produce severe defects in pancreatic development, with insulin-producing β-cells being the most affected[154]. Because of their extensive roles in regulating lipid and glucose metabolism, miRNAs are involved in all stages of non-alcoholic fatty liver disease (NAFLD), with patients exhibiting alterations in the levels of multiple miRNAs[155]. MiR-34a has proven particularly relevant both in patients with NAFLD and type 2 diabetes who show increased levels hepatic of miR-34a[155,156].This effect seems to be at least partly mediated through miR-34a regulation of sirtuin 1 deacetylase (SIRT1) a NAD+ dependent enzyme which is a key regulator of metabolic homeostasis[157].

Cardiovascular disease has also been linked to aberrant miRNA expression[20]. Heart failure is preceded by pathological enlargement of the cardiac muscle, known as hypertrophy, which is underpinned by gene reprogramming and reactivation of fetal cardiac genes[158]. Both upregulation and downregulation of individual miRNAs leads to cardiac hypertrophy and subsequent heart failure through modulation of different pathways[128,159–162]. Amongst these are 2 clustered miRNAs, miR-133 and miR-1, which target various genes involved in cardiac function and which show decreased levels in models of cardiac hypertrophy[160,163–165]. Inhibition of miR-133 induces pronounced hypertrophy[160] and overexpression of either miRNA shows cardioprotective effects and inhibition of hypertrophy[160,164]. Downregulation of another miRNA, miR-25, leads to the re-expression of developmental transcription factor HAND2 which also results in cardiac hypertrophy[159]. On the other hand, elevated levels of miR-25 lead to impaired Ca^{2+} uptake during contractions, via

negative regulation of a calcium transporting ATPase[166,167]. Impaired Ca^{2+} uptake is another hallmark of heart disease, meaning both downregulation and upregulation of miR-25 are associated with heart failure, highlighting the complexity of miRNA regulatory networks in multifactorial diseases. MiRNAs can also have a positive effect in reducing atherosclerosis, by regulating differentiation and proliferation of vascular smooth muscle cells[168] and endothelial cells[169], the two major cell types in veins and arteries. MiRNAs have also been implicated in other cardiac disease associated processes such as cardiac regeneration following injury[170], disruptions of cardiac rhythm[171] and regulation of cardiac fibroblasts[172].

A downregulation of several miRNAs has been observed in patients with Alzheimer's disease (AD) compared to age matched controls[173]. Amongst the targets of these miRNAs are the β-amyloid precursor (APP) and the enzyme that cleaves it, β-Secretase (BACE), generating plaques of β-amyloid as well as cofilin which contributed to the formation of neurofibrillary tangles (NFT)[173–175]. β-amyloid plaques and NFT represent two major characteristics of AD brains. Differences in miRNA profiles have also been observed in multiple sclerosis[176], bipolar disorder[177] and schizophrenia[178,179] were the upregulation of several miRNAs could be attributed to increased pri-miRNA processing associated with increased expression of DICER[178] or microprocessor components[179]. Loss of DICER and DGCR8 has also been associated with loss of dopaminergic neurons in Parkinson's disease (PD)[180]. Additionally, many miRNAs, which target genes linked with PD pathogenesis or neuroinflammatory response, appear dysregulated in PD. In particular, downregulation of brain enriched miR-7 in PD has been observed; miR-7 downregulates the neuroinflammatory

response as well as directly regulating *SNCA* which encodes α-SYN, a protein involved in differentiation and survival of dopaminergic neurons[180].

Evolution of miRNAs

Basic RNAi machinery consisting of a Dicer-like and an Ago-like protein is found in all kingdoms within the eukaryotic domain, suggesting it has been present since the last eukaryotic common ancestor[181]. Whilst this machinery has been lost in specific lineages, other eukaryotes have built from that basic pathway acquiring additional regulatory mechanisms that led to miRNAs[182]. MiRNAs have also been detected in various kinds of DNA viruses, with over 400 viral miRNAs annotated[31,183,184].These miRNAs represent viral transcripts that have evolved to be able to serve as substrates for the cellular miRNA processing machinery, and can regulate both host and viral targets[31,185].

Although both plants and animals share widespread regulation by miRNAs, there are important differences between them suggesting that their miRNA pathways have evolved independently[186]. Stem-loop precursors in plants tend to be both longer and more variable in structure than animal precursors[187] and are processed by Dicer in the nucleus whilst animal DICER processing is restricted to the cytoplasm[188]. Additionally, plant miRNAs tend to show extensive and near-perfect complementarity to their mRNA targets[189,190], as well as relying primarily on target cleavage as their mechanism of action both of which are rare in animals[4,191,192].

Within the metazoan kingdom a core of 30 miRNAs have been identified across bilaterians and were likely present in the last ancestor to all Bilateria[193]. These represent a first burst of ‘evolutionary innovation’ where there was a faster than

usual increase in the generation of new miRNA families[194,195]. Two other such bursts have subsequently taken place, the first at the base of the vertebrate lineage and a second at the lineage leading to eutherians[194–196]. This expansion of the miRNA repertoire is an ongoing process, exemplified by the presence of lineage specific miRNAs in rodents and primates[195,197,198]. A direct correlation has been repeatedly found between the number of miRNA families and morphological complexity suggesting miRNAs could be an important factor in the emergence of more complex organisms[193–197].

Along with the continuous addition of miRNAs to the genome, high conservation of sequence and rare secondary loss are three distinguishing characteristics of miRNA evolution[194,196,197]. The acquisition of novel miRNA families occurs through various mechanisms including duplication events, *de novo* generation and evolution of intronic sequences[194]. Non-local duplications arise either from genome wide duplications or from transposable elements[194,199], meanwhile tandem duplications occur locally and are especially common in miRNA clusters. The abundance of hairpins as secondary RNA structures also facilitates the generation of *de novo* miRNAs[194,197]. These structures are not likely to arise with all the characteristics required for precise DROSHA and DICER processing but rather undergo gradual evolution into a true miRNA structure[197]. As such, intermediates lacking some of these characteristics have been identified in the human genome[200]. Many miRNAs, especially younger ones, are found in introns of protein coding genes. This is thought to be evolutionarily advantageous as it bypasses the need for evolution of a promoter

unit[195,201]. The same holds true for miRNA clusters, as they are usually transcribed as a single polycistronic unit[201].

MiRNAs also shape the evolution of their target mRNAs both by conservation and non-conservation of target sequences in their 3' UTRs. Genes that are expressed in the same tissue as a miRNA, but in a different temporal pattern show high conservation of complementary sequences in their 3' UTRs[91,202]. Contrarily, mRNAs that are expressed at the same time and place as a miRNA selectively avoid complementary sequences, generating what are known as "anti-targets"[91]. This selective avoidance has also had an impact on 3'UTR length with housekeeping genes showing shorter UTR's with less possibilities for target miRNA sequences[91].

MiRNA organisation in the genome

MiRNAs are found both in an intragenic and intergenic context. Intragenic miRNAs are those mapped to regions corresponding to previously annotated genes[203] and they represent over half of annotated human miRNAs[204–206]. These can be further classified into intronic and exonic miRNAs, with approximately 90% of intragenic miRNAs found in introns[204,207] and over 80% of intragenic miRNAs are found in the same strand as their host genes[204–206]. Most exonic miRNAs are confined to non-coding 3' and 5' regions[204]. With a few exceptions, intragenic miRNAs are mostly co-expressed with their host genes and are under their transcriptional control[207–209]. On the contrary, intergenic miRNAs are independent transcription units with their own promoters and core transcriptional elements, which share the same characteristics as those of protein-coding genes[210,211] (Figure 4). They possess clearly delimitated transcription start and termination sites[211]. MiRNAs are often found in clusters[10–12]; approximately 30% of mouse and 20% of human miRNAs are found less than 10kb away from another miRNA[212].

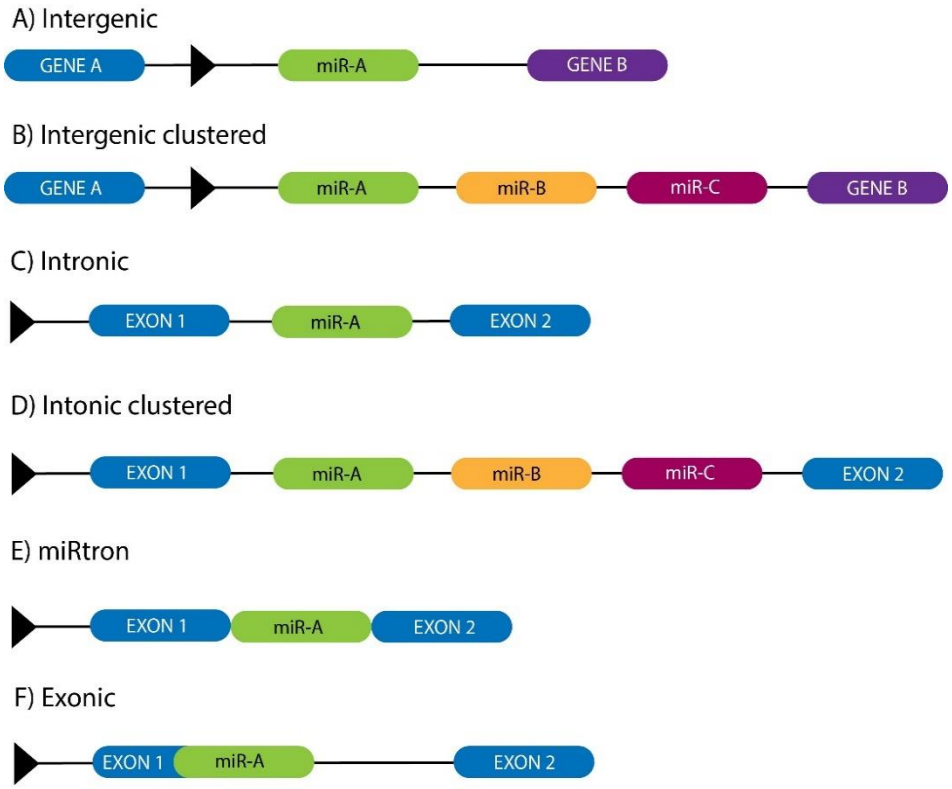

Figure 4 Genomic organization of miRNAs. *Diagram showing different organization of miRNAs within the genome. Black arrows represent promoter sites. A-B) Intergenic miRNAs are found between two genes and are under transcriptional control of their own promoter. C-D) Both individual and clustered miRNAs can be found in introns of protein coding genes and non-coding genes. The miRNAs are usually under the transcriptional control of their host genes. E) MiRtrons span the entire length of an intron and are processed by the splicing machinery. F) MiRNAs can also be found in exons of protein coding genes and non-coding genes, usually confined to non-coding 3' and 5' regions.*

MiRNA clusters

MiRNA clusters range in size from two miRNAs to several dozen miRNAs. They can be classified into homogeneous or heterogenous clusters depending on whether or not they contain miRNAs from the same family, which share their seed sequences[213]. More than half of annotated clusters contain multiple miRNA families[214,215]. MiRNA clusters are usually transcribed as single polycistronic units[24,211]. While this leads to miRNAs from the same cluster usually having shared expression patterns, this is not always the case due to post-transcriptional regulation of individual miRNAs[212,216].

MiRNA clusters arise by a variety of mechanisms including tandem duplication, *de novo* hairpin formation within an existing transcript and dispersal of locally duplicated miRNAs into existing clusters[212,217,218]. Duplicated miRNAs often undergo sequence divergence leading to novel regulatory targets, with changes to a single nucleotide being sufficient to alter a miRNAs target pool[105,106].

MiRNAs in the same cluster often have overlapping gene targets, increasing the level of repression they can exert on a single gene or pathway. Furthermore, they tend to co-regulate genes in the same protein complexes or functional pathways, increasing connectivity within regulatory networks[212,214,215,219]. For instance miRNA cluster miR-141~200c represses four separate components of a protein complex involving ZEB1/CtBP1 that acts as a translational repressor during differentiation[219], whilst miRNAs in murine cluster miR-183~96~182 target four different members of the insulin signalling pathway[220].

The potential of various miRNAs within a cluster to repress the same mRNAs as well as co-operatively targeting various components in a regulatory network has led to them having important roles in differentiation and development[213]. Examples include miRNA cluster miR-17~92 which is highly expressed in embryonic cell and a hemizygous deletion of which can lead to skeletal development defects such as microcephaly, short stature and digital abnormalities[221,222]. Additionally, this cluster is also important in myocardial development as several of its members target important cardiac progenitor genes[223]. MiRNA cluster miR-143/145 is enriched during cardiogenesis, with both miRNAs co-operatively regulating differentiation of vascular smooth muscle cells by targeting various factors that promote a less differentiated, more proliferative state[224]. Multiple clusters can also be involved in co-ordinated regulation, two functionally overlapping clusters, miR-34b/c and miR-499, target over 200 genes related with cell fate control, brain development and cytoskeleton organisation which makes them essential in brain development, spermatogenesis and formation of motile cilia[225].

The widespread regulatory functions of miRNA clusters, also means their disregulation is often associated with a variety of diseases, the most studied being cancer[213]. Both oncogenic and tumour suppressing miRNA clusters are often located in fragile genomic locations where there are likely to undergo amplifications, deletions and translocations[213]. For example, amplification and overexpression of oncogenic miRNA cluster miR-17~92 is associated with several types of tumours. Targets of this cluster are enriched in cell differentiation, cell cycle and apoptosis pathways and increased expression of this cluster translates into higher proliferation

and inhibition of cell death[226–228]. Likewise, increased expression of miRNA cluster miR-182~96~183 promotes tumorigenesis in medulloblastoma, as the combined effects of these three miRNAs influence multiple biological processes concerning cellular maintenance, survival and migration[229]. In a contrary manner, deletion or downregulation of miRNA cluster miR-15-a/miR-16-1 is also found in numerous types of tumour, as these miRNAs are tumour suppressors which target proteins involved in cellular proliferation and oncogenesis[230–232]. Similarly miRNA cluster miR-497~195 is frequently silenced in hepatocellular carcinoma, with its targets being enriched for cell-cycle regulators[233].

Besides its well established oncogenic potential, miR-17~92 cluster is also associated with age-related heart failure with various members targeting proteins involved in extracellular matrix remodelling[234]. MiRNA cluster miR-182~96~183 whose targets include several transcription factors that control T and B cell homeostasis and tolerance[235], was identified to be upregulated on various lupus-prone mice models. MiRNA cluster miR-132/212 is downregulated since the earliest stages of Alzheimer's disease, and is implicated in processes such as inflammation, synaptic function, structure and plasticity, and neural migration and morphology[236,237]. Downregulation of cluster miR-15/107 is also associated with Alzheimer's disease as well as schizophrenia[238].

MiRNA cluster 14q32

The largest known mammalian miRNA cluster is found on chromosome 14q32 in humans (12F1 in mice) and contains 54 miRNAs[239], and is highly conserved across

eutherian mammals[240]. These miRNAs are within the imprinted *DLK1-DIO3* genomic region, and are expressed exclusively from the maternal allele[239,241]. This imprinted region contains paternally expressed genes DLK1, RTL1 and DIO3 and maternally expressed genes *MEG3* (murine *Gtl2*), *MEG8*(*RIAN*) and antisense *RTL1* (*Rtl1as*). Additionally, the 14q32 region is rich in non-coding RNAs, hosting several long non-coding RNAs (lncRNA) and snoRNAs[241,242] (Figure 5). MiRNAs clustered in this region, are transcribed as a single polycistronic transcript, which is under transcriptional regulation of transcription factor MEF2A[243,244].

MiRNA cluster 14q32 is enriched in the brain and has important functions in brain development, with 14q32 miRNAs involved in dendritic growth, synaptic plasticity and differentiation and migration of neural progenitors[243,245–248]. MiRNAs in the 14q32 cluster have also been linked to diverse pathologies including, diabetes[249], schizophrenia[250], cardiovascular disease[251] and cancer[252–257].

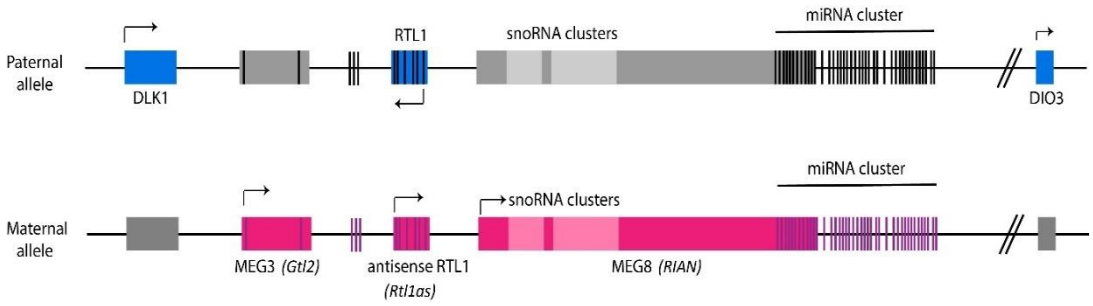

Figure 5 DLK1-DIO3 imprinted genomic region. *Genes in blue and pink are transcribed from the paternal and maternal alleles respectively. Arrows above/below the genes show the direction of transcription. Vertical lines represent miRNAs in the region; these are all transcribed from the maternal allele as indicated by the purple colouring. The lighter shade of pink/grey represent the regions corresponding to snoRNA clusters, transcribed from the maternal allele.*

Despite the miRNA 14q32 cluster being transcribed as a single unit, altered expression levels of either specific subsets or individual mature miRNAs in this cluster are associated with diverse cellular processes and pathologies. For example, miR-134, miR-154, miR-299, miR-323, miR-337 and miR-370 are increased in developing lungs compared to adult lungs, but not of other miRNAs in the cluster[258]. Similarly, while miR-134 is poorly expressed in neural progenitors and upregulated in postmitotic neurons, miR-369, miR-496 and miR-543 show higher expression in neural progentitors[248]. In cancer, distinct miRNAs form this cluster form part of miRNA signatures associated with different tumour subtypes[259–265]. For instance, individual 14q32 miRNAs are found in miRNA signatures associated with the estrogen receptor (ER), progesterone receptor (PR) and HER2/Neu (HER) status of breast tumours, namely miR-377 is associated PR positive tumours, miR-376 with HER positive tumours and miR-342 is predictive of ER positive tumours whilst miR-399 is predictive of ER negative tumours[264].

Another group (led by our collaborator Yael Nossent) highlighted the importance of miRNAs in the 14q32 cluster in neovascularization[251]. Reverse target prediction using 197 genes involved in both angiogenesis and arteriogeniesis showed an enrichment for target sites of 27 miRNAs in this cluster. The cluster was further studied through microarray analysis in a murine hindlimb ischemia (HLI) model which showed an upregulation of over half the miRNAs in the cluster after induction of HLI[251].

Regulation of miRNA biogenesis

Transcriptional regulation

Given their widespread regulatory roles as well as their strict temporal and spatial-specific expression, miRNA biogenesis is tightly regulated at every step of their biogenetic pathway[266,267]. Transcriptional regulation marks the first stage of miRNA biogenesis control (Figure 6 A). Although some virally encoded miRNAs have been shown to be processed by Pol III[30,31], most pri-miRs are transcribed by Pol II, producing transcripts that are both capped and polyadenylated[28,29]. Promoters for these Pol II transcribed miRNAs are similar to mRNA encoding promoters[209] and as such are subject to regulation by the same host of Pol II regulatory factors[268]. MiRNAs found within the introns of protein-coding genes (intronic miRNAs) can either possess their own promoter or be co-ordinately expressed with their host genes, in which case they are subject to the same transcriptional regulation as them[208,209,269]. Additionally, miRNAs can target their own host mRNAs in autoregulatory loops[93,270,271].

Transcription factors are important in establishing tissue-specific expression patterns for miRNAs. For instance, myogenic transcription factor, MyoD, binds to regions upstream of muscle specific miRNAs miR-1, miR-133 and miR-206 inducing their expression during myogenesis[272,273]. In a contrary manner, transcription factor REST inhibits the expression of brain specific miR-124 in non-neural and neural progenitors, and downregulation of REST during neural differentiation allows the

expression of miR-124 which targets many non-neural transcripts, facilitating the establishment of a neural identity[274].

Because of their regulatory role, miRNAs often form feedback loops with transcription factors. For example, miR-133b is positively regulated by transcription factor PITX3 which in turn contains miR-133b target sites in its 3'UTR region, forming a negative feedback loop during differentiation of dopaminergic neurons[275]. Similar regulatory loops are formed by RUNX1/miR-27a during megakaryocytic differentiation[276] and c-MYB/miR-15a during hematopoiesis[277].

Alteration of miRNAs patterns in cancer often has roots in transcriptional regulation and several examples exist of miRNAs under the regulation of known oncogenes and tumour suppressors. For instance, tumour suppressor protein p53 has been shown to positively regulate members of the miR-34 family influencing apoptosis and cell-cycle arrest[278]. Transcription factor and oncogene c-MYC is an important regulator of miRNA biogenesis with a predominantly repressive role in global miRNA expression[132] whilst upregulating select miRNAs such as the pro-tumorigenic miR-17~92 cluster[137] and miR-9[279].

Epigenetic regulation also influences expression of many miRNAs whose promoters are subject to DNA methylation[280], these patterns are often found altered in oncogenesis[281]. Global silencing of miRNAs via CpG island hypermethylation has emerged as a hallmark of cancer[282–284], contributing to proliferation and metastasis[281,282]. Consistently with miRNA expression patterns in cancer[17] particular instances of hypomethylation also exist, for example in the promoter of let-7a which-

induces its expression and leads to increased proliferation in lung adenocarcinomas[284].

Post-transcriptional regulation of miRNAs

Regulation of DROSHA processing

Together with transcriptional regulation, post-transcriptional regulation of miRNAs is observed at various stages of their biogenetic pathway. The first of these steps involves the cleavage of pri-miRs by DROSHA, acting within the microprocessor complex. Processing efficiency by the microprocessor can be highly variable between miRNAs and can be important in determining mature miRNA levels[285,286]. Furthermore, primary miRNA transcripts can be several kilobases in length containing multiple mature miRNAs[24,208] and miRNAs in these polycistronic clusters show differential processing allowing control of individual miRNA levels[45,287,288]. Here, secondary structure of pri-miRs can be an important factor in determining accumulation of mature miRNAs[287,288].

Regulation of pri-miR processing can occur via interaction of modulating proteins with either core microprocessor components or its many identified co-factors that bind to pri-miR directly[32,36]. Two of these co-factors, RNA DEAD-box helicases p68 (DDX5) and p72 (DDX17), can themselves regulate the processing of a subset of pri-miRs[32,36,289], as well as interacting with a variety of regulatory factors co-ordinating a response to internal and external signals. For example, p68 promotes pri-miR-21 processing in response to signalling by TGF-β and BMP family growth factors through

the SMAD pathway, an important process in vascular homeostasis[290]. On the other hand, the Hippo signalling pathway regulates microprocessor activity via the interaction of transcriptional coactivator YAP with p72, limiting its availability to associate with the microprocessor[291]. The Hippo pathway controls organ size through regulation of cell proliferation and survival and is often dysregulated in solid tumours, contributing to a global downregulation of miRNAs in cancer[291]. In a similar way, induction of p53 results in the upregulation of a subset of miRNAs in a p68/p72 dependent manner and without a change in their pri-miR levels[289] (Figure 6 C). This is in contrast to the transcriptional regulation of miR-34, showcasing a dual role for p53 in miRNA biogenesis[289]. Another important tumour suppressor, BRCA1 also increases processing of a subset of miRNAs normally downregulated in cancer through interaction with both DROSHA and p68[292].

Regulatory proteins can also interact directly with pri-miRNAs to either promote or repress their processing (Figure 6 B). One way to do this is by impeding the interaction between the pri-miRs and the microprocessor, as is the case of the NF90/NF45 protein complex which is able to suppress DROSHA processing of several pri-miRNAs by binding to them and blocking their access to the microprocessor[293–295]. RBPs can also affect the structure and stability of the pri-miRs they interact with, for instance proteins HuR and MSI2 form a complex on the terminal loop of miR-7-1, a brain-enriched miRNA, causing stabilization of the stem and subsequent repression of DROSHA processing[296]. This regulatory mechanism is vital in establishing the tissue specificity of miR-7 and its importance is highlighted by the observed dysregulation of miR-7 in glioblastomas[297]. It is important to note that regulation of miRNA

precursors very often occurs through terminal loops of miRNAs which tend to be highly conserved[298].

Proteins can have contrary effects on the regulation of different miRNAs. For example, hnRNPA1 can bind to the terminal loop of pri-mir-18a, a miRNA in the 17~92 cluster, causing relaxation of the stem structure that enhances its processing by DROSHA[298,299]. However, when hnRNPA1 binds to the terminal loop of pri-let-7-a1 it has the opposite effect; blocking DROSHA processing through competition with splicing factor KRSP which in turn acts as a positive regulator for both DROSHA and DICER processing of a subset of miRNAs[300,301] (Figure 6 B). This further illustrates how one protein can have multiple roles in RNA biogenesis.

Regulation of Dicer processing

After Exportin-5 mediated transport of pre-miRs, the second cleavage step occurs in the cytoplasm and is catalysed by DICER[49,50]. Pre-miR hairpins have a 3' 2nt overhang and 5' monophosphate group produced by DROSHA which are important for recognition and processing by DICER[25,26,302], therefore modifications to both ends of the precursor regulate DICER function (Figure 6 D). On one hand, due to single nucleotide bulges in the stem, a small group of miRNAs including miR-105 and many let-7 family members only have a 1nt overhang at their 3' end[303]. This difference is enough to significantly hinder DICER processing and thus these miRNAs are subject to regulation by terminal uridylyl transferases (TUTases) TUT7/4/2 which mono-uridylate their 3' ends restoring the 2nt overhang and increasing their processing by DICER[303]. Conversely, RNA methyl-transferase BCDIN3D can methylate the 5'

monophosphate group of pre-miRNAs, blocking recognition by DICER and hindering their processing[304].

Similar to the co-factors associated with the microprocessor which assist and regulate DROSHA processing, DICER has two partner proteins, the HIV-1 TAR RNA binding protein (TRBP) and protein activator of PKR (PACT)[305–307]. Whilst in *Drosophila,* the homolog to TRBP (Loquacious) is essential for pre-miR processing this is not the case in humans[266]. Still, TRBP and PACT have been shown to alter the processing rates of certain pre-miRs as well as fine-tuning their length and potentially influencing strand selection[308–312].

As with DROSHA regulatory proteins can interact with pre-miRs through their terminal loop. Examples of this include RBM3 which enhances pre-miR association and processing by DICER[313] and MBNL1 which competes with negative regulator LIN28A for binding to pre-miR-1 leading to its upregulation[314] (Figure 6 E). Because of the conserved structure, the interactions that occur via the terminal loops of miRNA progenitor transcripts often take place with both pri- and pre-miRs affecting both DROSHA and DICER processing steps. Such is the case of previously mentioned KSRP[301] as well as TAR-DNA binding protein 43 (TDP-43) which forms part of both microprocessor and DICER complexes and increases their affinity for miRNA precursors as TDP-43 also binds both pri- and pre-miRs[315]. This higher affinity leads to increased processing of a specific set of miRNAs, which has repercussions in neural outgrowth[315]. In a contrary manner Y-box-binding protein 1 (YB-1) can bind to the terminal loop of pri- and pre-miR-29b but unlike TDP-43 this interaction blocks

recruitment of both DICER and the microprocessor leading to a downregulation of mature miR-29-b[316]. This downregulation of miR-29b can lead to unwanted cell proliferation in glioblastoma multiforme[316].

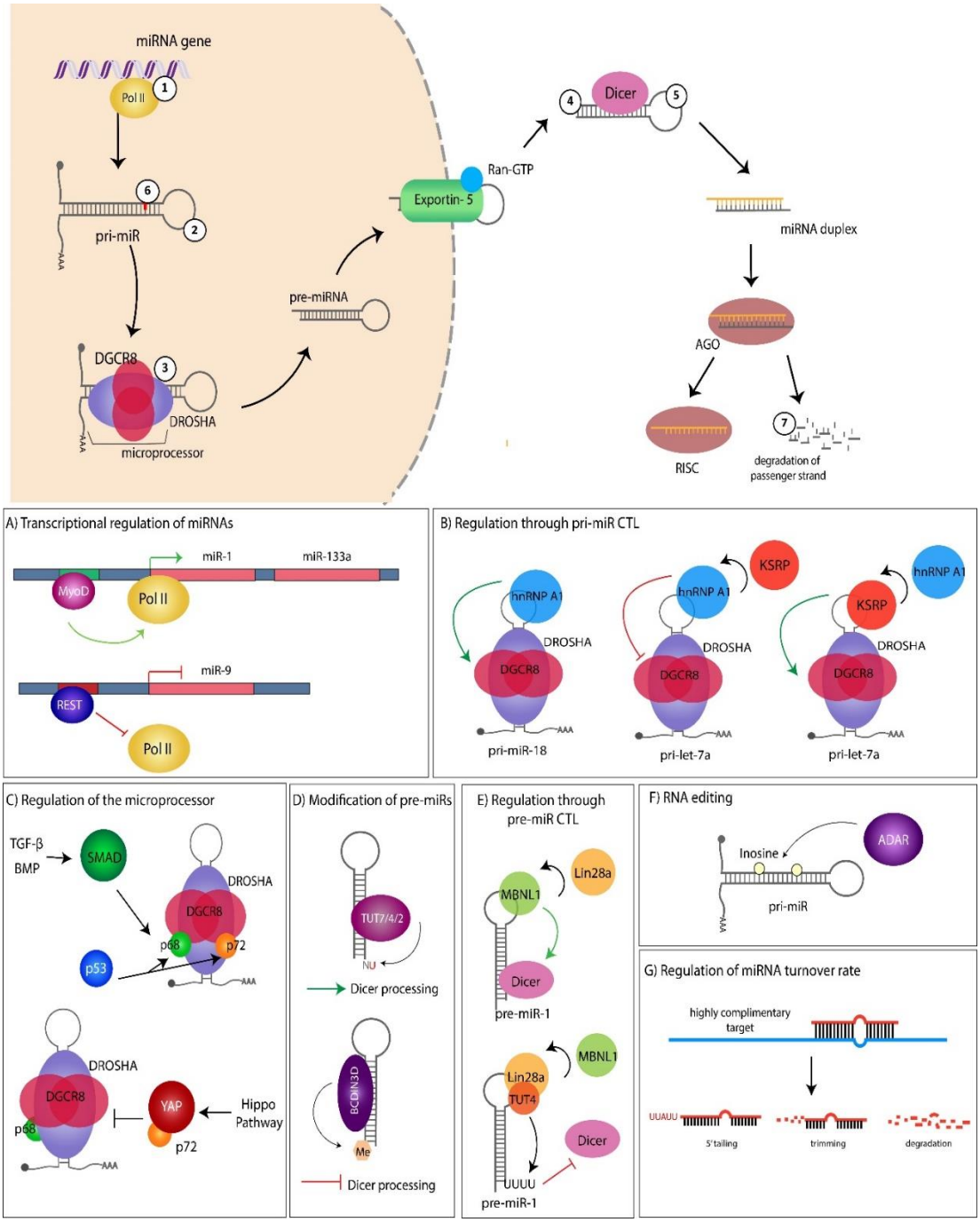
miRNA gene
Pol II
1
pri-miR
6
2
DGCR8
3
DROSHA
microprocessor
pre-miRNA
Exportin- 5
Ran-GTP
4
Dicer
5
miRNA duplex
AGO
RISC
7
degradation of
passenger strand
A) Transcriptional regulation of miRNAs
miR-1
miR-133a
MyoD
Pol II
miR-9
REST
Pol II
B) Regulation through pri-miR CTL
hnRNP A1
DROSHA
DGCR8
pri-miR-18
KSRP
hnRNP A1
DROSHA
DGCR8
pri-let-7a
KSRP
hnRNP A1
DROSHA
DGCR8
pri-let-7a
C) Regulation of the microprocessor
TGF-β
BMP
SMAD
DROSHA
DGCR8
p68
p72
p53
DROSHA
DGCR8
p68
YAP
p72
Hippo
Pathway
D) Modification of pre-miRs
TUT7/4/2
NU
Dicer processing
BCDIN3D
Me
Dicer processing
E) Regulation through
pre-miR CTL
Lin28a
MBNL1
Dicer
pre-miR-1
MBNL1
Lin28a
TUT4
Dicer
UUUU
pre-miR-1
F) RNA editing
Inosine
ADAR
pri-miR
G) Regulation of miRNA turnover rate
highly complimentary
target
UUAUU
5'tailing
trimming
degradation

Figure 6 Regulation of miRNA biogenesis. Schematic representation of mechanisms regulating miRNA biogenesis. The top panel indicates the stages of the miRNA biogenesis pathway that are regulated by different mechanism, the encircled numbers correspond to the panels in the bottom. 1) Transcriptional regulation of miRNA biogenesis; most miRNAs are transcribed by Pol II and as such subject to regulation by Pol II regulatory factors, these can exert positive regulation such as MyoD on the miR-1 cluster, or negative regulation such as REST on miR-9. 2) Regulation by factors binding pri-miRs CTL; different factors binding to the same pri-miR CTL can have opposite effects on DROSHA processing depending on context. For example, hnRNP A1 is a negative regulator of pri-let-7a processing and is a competitor of positive regulator KSRP. The same protein can also have opposite effects on the processing of different pri-miRs as is the case of hnRNP A1, which contrary to its negative effects on pri-let-7a processing enhances processing of pri-miR-18. 3) Regulation of the microprocessor; proteins that interact with the microprocessor core or its cofactors can negatively or positively impact the processing of pri-miRs. Helicases p68 and p72 are microprocessor cofactors that can regulate a subset of miRNAs, additionally SMAD and p53 positively regulate pri-miR processing through interaction with these cofactors. On the contrary, transcriptional coactivator YAP sequesters p72 hindering microprocessor activity. 4) Modification of pre-miRs; 5' monophosphate groups and 3' 2nt overhangs are necessary for Dicer recognition of pre-miRs, BCDIN3D can methylate the monophosphate group of certain pre-miRs preventing Dicer recognition and processing. Conversely, TUTase4/7/2 can facilitate the processing of pre-miRs that lack the 2 nt overhang through their mono-uridylation. 5) Regulation by factors binding pre-miRs CTL; similarly, to pri-miRs, regulatory factors interact with pre-miR terminal loops affecting miRNAs positively or negatively, for example positive regulator MBNL1 competes for binding of pre-miR-1 with Lin28a which negatively regulates pre-miR-1 biogenesis through a uridylation dependent mechanism 6) RNA editing; conversion of adenine to inosine by ADARs can affect both DROSHA and Dicer processing as well as altering the seed sequence, generating a new pool of miRNA targets. 7) Regulation of miRNA turnover rate; miRNAs tend to be stable with a half-life of several hours to several days however mechanisms exist to accelerate their degradation. For instance, highly complementary targets lead to rapid miRNA degradation through tailing and trimming.

Lin28 regulation of let-7 biogenesis

One of the best characterized examples of miRNA biogenesis regulation, acting at both DROSHA and DICER processing steps, is the regulation of the let-7 miRNA family by LIN-28. Members of the let-7 family are important regulators of developmental timing[8] with known tumour suppressor roles[268,317,318] frequently found dysregulated in certain types of cancer[99,319]. During development, pri-let-7 levels remain constant, but mature let-7 is absent in mouse and human embryonic stem cells, increasing its levels upon differentiation[106,320,321]. This is due to pot-transcriptional regulation by Lin28. Lin28 is an important pluripotency factor, found to be one of four factors sufficient for reprogramming induced pluripotent stem cells[322]. Contrary to let-7, Lin28a is widely expressed in undifferentiated cells, where it inhibits maturation of let-7 and as differentiation progresses expression of Lin28 is lost allowing for a rise in levels of mature let-7[323].

In mammals, there are two LIN28 homologs, LIN28A and LIN28B[324]. These present some differences in their regulation of let-7; both LIN28A and LIN28B are able to bind a conserved motif (GGAG) in the terminal loop of let-7 precursors which directly blocks DROSHA[100,101] and DICER[102,325,326] processing. However, the main mechanism action of LIN28A (but not LIN28B) involves the recruitment of a terminal uridylyl transferase, either TUT4 or TUT7, following its association with pre-let-7[327,328]. TUT4/7 catalyses the addition of a poly(U) tail to the 3' end of pre-let-7 which impedes cleavage by DICER and serves as a marker for degradation by the 3'-5' exoribonuclease DIS3L2[329,330] (Figure 7). Additionally, our group has shown that E3

ubiquitin ligase TRIM25 is required as a cofactor in the LIN28A/TUT4 regulatory pathway providing an example of a newly characterized RNA binding protein[331] .

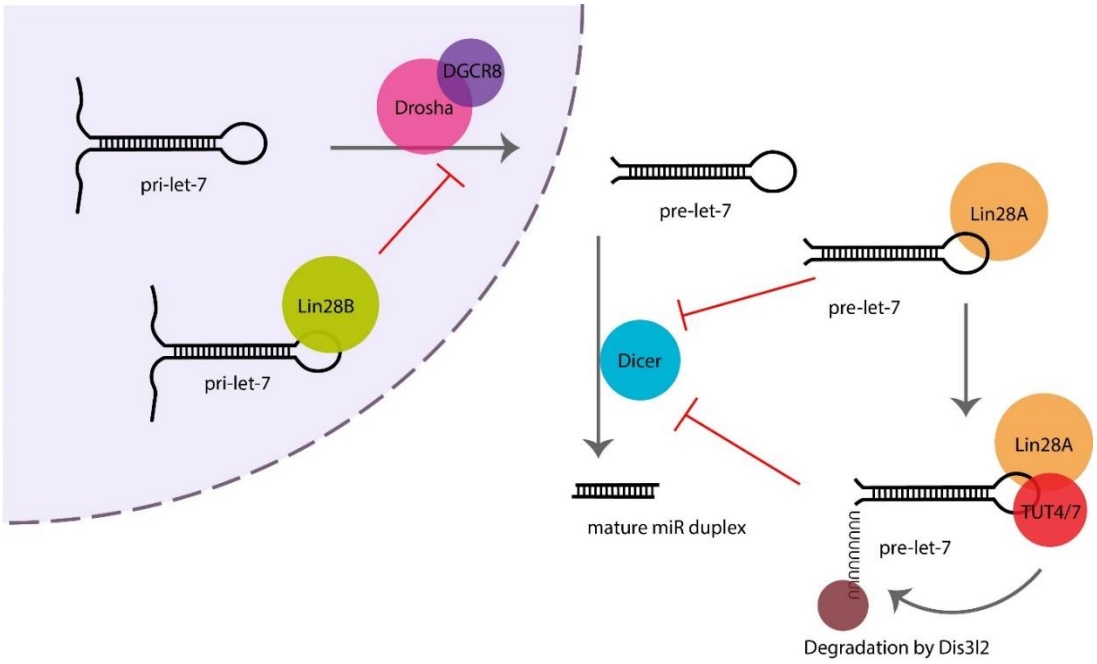

Figure 7 LIN28 regulation of pre-let-7. Schematic representation of the regulation of pre-let-7 processing by Lin28. Lin28b mainly acts in the nucleus blocking Drosha processing. Lin28a mostly localizes to the cytoplasm where it directly blocks Dicer processing. Additionally, Lin28a mediates the recruitment of TUT4/7 which leads to uridylation of pre-let-7 3' end and subsequent degradation by exonuclease Dis3l2.

Other mechanisms of miRNA regulation

RNA editing, carried out by adenosine deaminases acting on RNA (ADARs), is another form of regulation of miRNA biogenesis. ADARs convert adenosines in editing sites into inosine, modifying the stability and structure of miRNAs and hindering or promoting their processing by DROSHA and DICER[332–335]. Furthermore, if the site of RNA editing lies within the mature miRNA sequence an A→I conversion results in a new set of targets being regulated[217,218,220]. RNA editing can be tissue specific and is particularly widespread in the brain, helping establish expression patterns of

miRNAs[205,208,209]. ADARs are also able to regulate both DROSHA and DICER processing steps in an editing-independent manner[333,339,340] (Figure 6 F).

Finally, regulating the turnover rate of mature miRNAs is another way to control their levels. In general, miRNAs are inherently stable molecules that can persist in the cell for several hours or even days[341,342]. However, persistence of miRNAs in the cell can also be subject to active regulation, either by accelerated degradation or stabilization of mature miRNAs. One way to influence miRNA stability is through adenylation. Hepatic miRNA, miR-122, is frequently adenylated by GLD-2 polymerase which stabilizes it[343]. In contrast, during infection, a virally encoded polymerase ,VP55, also adenylates host miRNAs facilitating their degradation[344]. This shows that stability of miRNAs is dependent on their context. Rapid degradation of miRNAs has also been described for other cellular processes including cell-cycle progression, growth-factor stimulation and neuronal activity[345]. Furthermore, highly complementary mRNA targets can induce degradation of miRNAs through a tailing and trimming mechanism that is at least partially dependent on TUT1 and DIS3L2[342,346,347] (Figure 6 G).

Interplay between miRNA regulation and cellular metabolism

Metabolic enzymes as novel RNA binding proteins

Most of the proteins so far identified as regulators of miRNA biogenesis are well-known players in RNA metabolism with well characterized RNA-binding motifs. However, in the last few years proteome-wide studies have led to the discovery of many novel RNA binding proteins without traditional RNA-binding motifs[348–351]. One group of proteins whose regulatory roles have traditionally been overlooked but are now emerging both as RNA-binding proteins and regulators of cellular processes are metabolic enzymes[348–352]. Throughout the last three decades, studies have increasingly identified metabolic enzymes as RNA binding proteins[352–354]. Metabolic enzymes show tissue specificity as their expression profiles vary depending on cellular identity[352]. Additionally, the levels of these proteins are altered in periods of fasting and in response to day/night cycles via nuclear hormone receptor signalling pathways[355–358]. This means enzymes could provide a link between gene regulation and environmental cues. Enzymes that exhibit secondary functions, not related to their catalytic activities, are sometimes called 'moonlighting enzymes'[359].

Targets for these enzymes are diverse with some of them, such as thymidylate synthase (TS), catalase and dihydrofolate reductase (DHFR) binding their own mRNAs and forming autoregulatory loops[353]. Meanwhile, enolase 1 (ENO1) and serine hydroxy-methyltransferase 2 (SHMT2) each bind different sets of hundreds of

mRNAs, the difference between their targets showing they have some degree of binding specificity[351].

The RNA-binding activity of moonlighting enzymes can be controlled via the availability of metabolites. The best understood example of a protein switching between its catalytic and RNA-binding activities in response to metabolic cues is cytosolic aconitase/iron regulatory protein 1 (IRP1)[360–362]. When cells have high iron supplies, IRP1 is coupled with a Fe-S cluster which confers it aconitase activity, catalysing the conversion of citrate into isocitrate. However, in iron-depleted cells IRP1 does not possess this catalytic cluster and so functions as an active RNA-binding protein[363]. Active IRP1 binds to iron regulatory elements (IREs) controlling the expression of genes related to iron metabolism, for instance it simultaneously inhibits the translation of ferritin mRNA and the degradation of transferrin receptor mRNA by binding to IREs in their UTRs[361].

For some moonlighting enzymes, metabolite availability regulates their RNA-binding activity through direct competition. This is the case of several enzymes including glyceraldehyde 3-phosphate dehydrogenase (GAPDH), lactate dehydrogenase (LDH), alcohol dehydrogenase (ADH) and phosphoglycerate kinase (PGK) which require mono- or di-nucleotides as coenzymes[235,242,243]. For these enzymes, RNA-binding occurs through their structurally conserved (di)nucleotide binding domain (known as a Rossmann fold) such that coenzyme binding inhibits their RNA-binding activity[354,364,365]. RNA-binding enzymes containing Rossmann folds have a preference for AU rich-elements (ARE)[364] which are important in regulating mRNA decay and

rates of translation and are frequently found in lymphokine, cytokine and proto-oncogene mRNAs[366,367]. An additional switch-mechanism for GAPDH functions in T-cell activation which is dependent on the transition from oxidative phosphorylation to aerobic glycolysis has also been described[368]. When T-cells are utilizing oxidative phosphorylation GAPDH is free to bind and ARE in the 3'UTR of IFN-γ repressing its translation. However, when T-cells become active they switch to glycolysis and GAPDH becomes engaged in the glycolytic pathway leading to the upregulation of IFN-γ and subsequent cytokine production.

Not all enzymes show mutually exclusive catalytic and RNA-binding functions. AUH is an RNA-binding protein with enoyl-CoA hydratase activity, it catalyses the conversion of HMG-CoA to 3-MG-CoA in leucine catabolism[369,370]. Like (di)nucleotide binding enzymes AUH binds AREs, however it does not possess a Rossmann fold or any traditional RNA-binding motifs[369,371]. Instead, a region of 20 amino-acids containing evenly spaced Lys residues forming a "Lysine comb" is sufficient for RNA-binding. This region is distinct from the catalytic site permitting RNA-bound enzyme to be active[369]. AUH is a mitochondrial enzyme localized to the inner membrane via its interaction with mitochondrial ribosomes[372]. Here, it modulates mitochondrial translation in addition to metabolizing leucine providing a link between mitochondrial metabolism and gene regulation[372].

Other mitochondrial metabolic enzymes also have shown RNA-binding capability[354]. Hydroxysteroid 17-Beta Dehydrogenase 10 (HSD17B10) is a multifunctional enzyme that oxidises various fatty-acid, alcohol, and steroid substrates and additionally

functions as part of RNAse P, a complex required for maturation of mitochondrial transcripts[373,374]. Trifunctional-enzyme subunit β (HADHB) is required for oxidation of fatty acids but can also bind renin mRNA, decreasing its stability[375]. Similarly, isocitrate dehydrogenase (IDH) binds to eight major mitochondrial mRNAs[376], with this binding inhibiting its enzymatic activity allosterically[377].

Many identified moonlighting metabolic enzymes still await *in vivo* validation as well as elucidation of the function and physiological relevance of their RNA-binding activities. So far, research has mostly been focused on the interaction of metabolic enzymes with mRNAs however it is tempting to consider that these proteins could also be interacting with another network of important gene regulators; miRNAs. We are still uncovering novel participants in miRNA regulatory pathways and with the increasing elucidation of their regulatory roles, metabolic enzymes are good candidates especially when we consider miRNAs are key participants in metabolic homeostasis[21].

Regulation of RNA binding activity by cellular metabolites

RNA-binding activity of moonlighting enzymes is commonly regulated by cellular metabolites that function as their substrates or co-factors either through direct competition or allosterically[352]. However, cellular metabolites have the potential to regulate RNA-binding activity of proteins other than their natural enzymes. This regulation can happen indirectly, by influencing post translational modifications. Protein acetylation is dependent on the cellular availability of acetyl-coA, a metabolite which is also necessary for the synthesis of various molecules[378]. Many

proteins including both metabolic enzymes and traditional RBPs undergo acetylation, and acetylation of RNA-binding proteins can influence their RNA-binding potential[352,378–381].

Metabolites regulation can also happen directly, for example the RNA-binding activity of translation regulator Mushashi-1 (MSI1) is allosterically regulated by oleic acid (OA), an 18 carbon ω-9 mono-unsaturated fatty acid[340]. OA binds to the RNA-binding domain of MSI1, changing the environment surrounding amino acids critical for RNA-binding. Other 18-22 carbon *cis* ω-9 mono-unsaturated fatty acids can inhibit MSI1 binding, however closely related elaidic acid, which is also a ω-9 mono-unsaturated fatty acid but with a *trans* bond cannot. MSI1 in turn, regulates the expression of stearoyl-coA desaturase, an enzyme which catalyses the conversion of saturated fatty acids into mono-unsaturated fatty acids. In this way MSI1 acts as a metabolite sensor, regulating the expression of metabolic enzymes in response to availability of specific metabolites[382].

Aims

The biogenesis of miRNAs is constantly regulated in response to the cellular and extracellular environments, allowing for their controlled production in temporal and spatial specific manners. This regulation is the result of multiple interacting factors that act on all stages of the miRNA biogenesis pathway to fine-tune the levels of mature miRNAs. There are still many unknown components in these regulatory networks and as our knowledge of RNA binding proteins expands, novel mechanisms of miRNA biogenesis will continue to emerge.

This study focused on unravelling the mechanisms and factors behind the post-transcriptional regulation of miRNAs. The experiments were carried out to elucidate the details of miRNA biogenesis regulation in three specific contexts with the following aims:

1. Post-transcriptional regulation of miRNA cluster 14q32;

- Identifying protein factors binding to 14q32 miRNA precursors differentially regulated during ischemia.
- Validating proteins identified as binding to 14q32 pre-miRNAs
- Exploring the expression of these proteins in a murine hindlimb ischemia model
- Determining the effects of altering the levels of these proteins in a NIH-3T3 serum starvation model

2. Post-transcriptional regulation of miRNA biogenesis by Lin28a during neurogenesis

- Determining the Lin28a domains involved in its binding to pre-let-7-a-1 and pre-miR-9
- Exploring the regulatory effect of constitutive expression of Lin28a on other miRNAs during neurogenesis

3. Inhibitory effect of oleic acid on regulation of miRNA biogenesis by RBPs.

- Evaluating the effect of oleic acid (OA) and elaidic acid (EA) on pre-miR-7/protein complexes
- Determining the effect of OA and EA on *in vitro* processing of pri-miR-7
- Determine the effect of OA on levels of miR-7 in cell culture.

Materials and methods

Cell culture

P19, HeLa (ATCC) and NIH-3T3 (ECACC) cells where grown under standard conditions (37°C and 5% CO_2) in DMEM growth media (GIBCO) supplemented with 10% Foetal Bovine Serum (GIBCO) unless otherwise indicated. Cells were passaged at 80% confluence using TrypLE express (GIBCO).

P19 cell lines with stable expression of Lin28a-GFP or GFP-only were gifts from Dr. Eric Moss (Rutgers School of Biomedical and Health Sciences, formerly The University of Medicine and Dentistry, New Jersey, USA). P19 cell lines stably expressing untagged Lin28a were previously generated in our research group using the Flp-in system (Thermo Fisher Scientific)[383].

Cellular serum starvation of NIH-3T3 cells

For starvation experiments NIH-3T3 passaged cells were first allowed to grow for 24 hours in fully complemented media. Following 24 hours, cells were washed twice with non-complemented media following which with either fully complemented DMEM media (10% foetal bovine serum) or media without complementation (0.5% foetal bovine serum) was added. Cells where then grown for an additional 24 hours before experiments were carried out.

Preparation of total protein extracts from cell lines

Cells were carefully washed twice with PBS. After removing PBS cells were scraped in appropriate volume of **Roeder D** (350µl for a p100 dish, 50µl for a 6-welled plate) and

collected in a microfuge tube. Samples were vortexed and then sonicated in an ice water bath twice for 5 minutes in 30 second cycles. After sonication tubes were centrifuged for 10 minutes at 10,000 rpm, 4 °C. Supernatant was collected and samples were quantified using the Nanodrop 2000 (Thermo Fisher Scientific).

Pre-miR in vitro transcription

Template DNA was generated by amplifying RNA of interest with primers that included a T7 promoter sequence (TAATACGACTCACTATAGG). *In vitro* transcription reactions were set up in a 25µl volume which included 10µl of DNA template PCR product, 1.25µl of 20mM rNTPs (Roche), 0.5µl of RNaseOUT (Invitrogen) and 1µl of T7 RNA polymerase (NxGen T7 RNA Polymerase, Lucigen supplied at 50,000 U/mL) and 10µl of reagent buffer (Lucigen). Reactions where incubated for 90 minutes in a 37°C water bath after which 2µl of TURBO DNase was added (Ambion, supplied at 2 U/µl) and reactions were incubated a further 10 minutes at 37°C. RNA was then precipitated by adding 1/10 3M NaAc and 3x volume 100% ethanol and incubating 1 hour on dry ice. Pellets were washed and resuspended in 25µl water to which 25µl of **UEO running buffer** was added. Samples were boiled for 10 minutes at 90°C before running on a pre-warmed 10% PAGE/UREA denaturing gel. Gels were stained using **RNA staining solution**, bands were cut out and incubated o/n in 300µl of **RNA elution buffer**. The following day RNA was precipitated by adding 900 µl 100% ethanol and incubating 1h on dry ice. RNA was then washed in 70% ethanol and resuspended in 200 µl water.

Western blot analysis

Protein samples were resolved by standard SDS-PAGE electrophoresis using NuPAGE Bis-Tris gels run in 1X NuPAGE MOPS SDS running buffer supplemented with 1:000 NuPAGE antioxidant (Invitrogen). Polyacrylamide concentration was 10% in all cases except when resolving protein extracts overexpressing Lin28a truncations, where 4%-12% gradient gels were used. Gels were transferred for onto a nitrocellulose membrane (0.45µm pore, GE healthcare). The membrane was blocked overnight at 4°C in 1:10 western blocking reagent (Roche) diluted in **Tris-buffered saline** (TBS) with 0.1% Tween 20 (TBS-T). The following day membrane was incubated for 1 hour with selected antibody diluted in 1:20 western blocking reagent (Roche) in TBS-T. Blots were washed three times for 10 minutes with TBS-T and were then incubated for 1 hour with corresponding secondary antibody diluted in 1:20 western blocking reagent (Roche) in TBS-T.

Secondary antibodies were conjugated to horseradish peroxidase (HRP) and were detected with the SuperSignal West Pico detection reagent (Thermo Scientific). The membranes were stripped using ReBlot Plus Strong Antibody Stripping Solution (Chemicon) equilibrated in water, blocked in 1:10 western blocking solution in TBST, and re-probed as described above.

Quantification of western blot assays

Western blots were quantified using ImageJ analysis software (1.48v, NIH) and ImageStudio (LI-COR Biosciences). Normalization controls are indicated in individual figure legends.

RNA pulldown assay

In vitro transcribed RNA was prepared for coupling to the beads by activation with m-sodium periodate. m-Sodium periodate will specifically oxidize hydroxyl-groups present in adjacent carbons in RNA forming two aldehyde groups. These aldehyde groups will readily react with hydrazide modifications in the agarose beads forming stable linkages. The following activation reaction was set up in a 1.5mL screw cap tube; 6.7µl of 3M NaAc, 10µl of 0.1M m-sodium periodate and 1000 pmol of in vitro transcribed RNA in a final volume of 200µl. This reaction was incubated while rocking for 1h at room temperature (RT) protected from light.

RNA was precipitated for 30 minutes on dry ice by addition of 15µl 3M NaAc and 600µl 100%. RNA was centrifuged for 20 minutes at full speed at 4 °C, washed in 1ml 70% ethanol by spinning 3 min at full speed and resuspended in 500µl 100 mM NaOAc.

Agarose beads (Adipic acid di-hydrazide-Agarose, Sigma-Aldrich) were prepared for coupling by washing thrice with 100mM NaOAc. 200µl prepared beads were added to the 500µ activated RNA and the coupling reaction was left protected from light, rocking overnight at 4 °C. The following day unbound RNA was washed out by a 30 min incubation with 700µl 4M KCl at RT. Beads were collected by centrifugation at 3000 rpm for 2 min. Coupled beads were then washed twice with 1ml 2M KCl and 3 times with 1ml **Buffer G.** Beads were then incubated with protein extracts for 30 minutes at 37°C whilst shaking at 400 rpm in the following reaction; 250µl protein extract (1000µg), 9.75µl 100mM MgCl2, 32.5µl 0.5 M CIP, 3.25µl ATP, 0.5µl

RNaseOUT (Invitrogen) in a volume of 650µl. Reactions were washed three times with buffer G centrifuging for 3 min at 1000 rpm each time.

Proteins were then eluted in 39µl H2O, 15µl NuPAGE sample buffer (Invitrogen) and 6µl NuPAGE sample reducing agent (Invitrogen) by boiling at 70°C for 10 minutes while shaking. Beads were sedimented by spinning 1 minute at top speed. Supernatant was then used for gel electrophoresis and analysed either by SILAC mass spectrometry or western blot.

RNA pulldown followed by SILAC mass-spectrometry (RP-SMS)

SILAC labelling

For labelling, cells were grown in SILAC 'heavy' and 'light' media for six passages (R6K4 'heavy' and R0K0 'light', *DC Biosciences*), supplemented with 10% foetal bovine serum, except for starvation conditions where they were supplemented with 0.5% foetal bovine serum. To verify incorporation of heavy isotopes was evaluated by performing Liquid Chromatography with tandem mass spectrometry (LC-MS/MS) using an orbitrap mass spectrometer. For this, protein extracts diluted in 1X NuPAGE sample buffer and 1X NuPAGE reducing agent (Invitrogen) were run in an SDS-polyacrylamide gel, running in 1X NuPAGE MOPS SDS running buffer supplemented with 1:000 NuPAGE antioxidant (Invitrogen). Gel was stained with GelCode Blue safe protein stain (Thermo fisher scientific) and using a razor blade a 0.5-cm piece of gel was cut from the centre of the lane. In-gel digestion and peptide purification were then carried out as described below. To determine efficiency of heavy label incorporation into peptides randomly selected peptides were examined manually.

In-gel digestion

Isolated gel fragments were cut into small 1mm x 1mm pieces. Gel pieces were transferred into a microfuge tube and incubated 5 minutes at RT with 200µl of 50mM ammonium bicarbonate (ABC). ABC was removed and replaced with 200µl acetonitrile (100%) and samples were incubated a further 5 minutes. These two steps were repeated until the solution was no longer blue. Sufficient 10mM DTT to cover the gel pieces was added and the samples were incubated for 30 mins at 37°C. Liquid was removed and 200µl of acetonitrile were added for 5 min.

In the dark, acetonitrile was removed and enough 55 mM iodoacetamide (IAA) to cover the gel pieces was added. IAA was removed, ABC was added for 5 min, then acetonitrile was added for 5 min. **Trypsin buffer** was prepared on ice and added to cover the gel pieces. These were incubated on ice for 15 minutes. More trypsin buffer was added to cover the gel pieces and incubate at 37 °C for 30 min. **Acetonitrile/ABC solution** was added to cover the gel pieces, which were then left at 37 °C overnight.

A 1:1 volume of 0.1% trifluoracetic acid (TFA) was added to samples which were then left for 20 min. pH was adjusted to 1-3 with 10% (TFA).

A C18 stage tip (Sigma Supelco) was activated by pushing 20µl methanol through the tip. The tip was then conditioned by pushing 40µl of 0.1% TFA through the tip. Sample was loaded unto the tip by spinning. To wash the sample, 60µl of 0.1% TFA were pushed through the tip. Tips were kept at -20 °C until loaded onto a mass spectrometer

Mass spectrometry analysis of pulldown samples

Mass spectrometry was carried out with the help of Dr. Christos Spanos at the WCCB Proteomics Facility. Supernatants recovered from the beads after pulldown were run in an SDS-polyacrylamide gel using 1X NuPAGE MOPS SDS running buffer supplemented with 1:000 NuPAGE antioxidant (Invitrogen), such that the dye migrated 1 cm into the gel. Gel was then stained with GelCode Blue Safe protein Stain (Thermo fisher scientific). Bands were cut out using a razor blade and in-gel digestion proceeded as described above. LC-MS/MS analysis was performed using a Velos LTQ-Orbitrap mass spectrometer. MaxQuant software platform was used to analyse the raw mass-spectrometry data to determine the ratio of the heavy-labelled and light-labelled peptides.

Hindlimb Ischemia Model

All *in vivo* experiments on a murine model were conducted by Yael Nossent's group at the Leiden University Medical Centre and approved by the Committee on Animal Welfare of the Leiden University Medical Centre (Leiden, the Netherlands; approval reference numbers 09163 and 10243). This study was conducted in accordance with the Directive 2010/63/EU of the European Parliament. Unilateral hindlimb ischemia was induced in healthy adult male C57BL6 mice by single ligation of the left femoral artery[251,384]. C57BL/6 mice (n = 4 per time point) were sacrificed at several time points (day 0 [before ligation of the femoral artery] and days 1, 3, 7, 10, 14, and 28 after hindlimb ischemia induction)[385]. Upon sacrifice, the adductor muscles were harvested and either snap-frozen on dry ice or fixed in 4% paraformaldehyde.

Preparation of total protein extracts from adductor muscle

Total protein was isolated from adductor muscle tissue of mice on days 0, 1, and 3 after induction of ischemia. Tissue samples were homogenized in 1 ml of TRIzol reagent (Invitrogen) using the QIAGEN TissueLyser II. 5mm stainless steel beads were used and samples underwent 2 x 60 sec pulses at 30 Hz. After homogenization of the sample, 200µl of chloroform was added to the samples. Tubes were shaken vigorously and left to stand for 2 minutes. Samples were then centrifuged at 13,000 rpm for 15 min, 4°C. The upper clear aqueous phase was recovered and set aside for RNA isolation. The interphase was removed and discarded, and 1 ml of cold acidified acetone/methanol was added to the remaining organic phase. The samples were mixed and left overnight at -20°C. The next day samples were centrifuged at 6000 rpm for 15 min at 4°C. Pellets were washed twice in 95% ethanol and air dried. Samples were resuspended in **optimized lysis buffer K**, incubating overnight at 50°C.

Immunohistochemical Staining

Experiments were conducted by Yael Nossent's group in Leiden University Medical Centre. Formaldehyde-fixed adductor muscles were paraffin-embedded, and 5-µm-thick cross-sections of muscles were stained to visualize the expression of RBPs. Cross sections of adductor muscles were re-hydrated, and endogenous peroxidase activity was blocked. Antigen retrieval was performed with citrate buffer (pH 6.0) at 100°C for 10 min. Muscles were stained with rabbit polyclonal anti-HADHB (Novus Biologicals, NBP1-82609, 1:1,000) or goat polyclonal anti-CIRBP (Abcam, ab106230,

1:400) to visualize HADHB and CIRBP, respectively, and counterstained using haematoxylin.

Microarray analysis in hindlimb ischemia model

Array analysis was performed by Yael Nossent's group on total RNA extracted from adductor muscle tissue from days 0, 1, 3, and 7 after induction of hindlimb ischemia. For array analysis, MouseWG-6 v2.0 Expression BeadChips (Illumina), which contain more than 45 200 transcripts, were used. Expression levels were log2-transformed, and quantile normalized. Transcripts showing background intensity (log2 expression of <6.75) both at baseline and after induction of HLI, were removed from the analysis.

RNA extraction from cell lines

Cells grown in 6 well plates were carefully washed twice with PBS and subsequently homogenized by pipetting in an 1ml of TRIzol reagent (Invitrogen) and transferred to a microfuge tube. After a 5 min incubation at RT 200µl of chloroform was added, tubes were shaken vigorously and left to stand for 2 min. Samples were then centrifuged at 13,000 rpm for 15 min, 4°C. The upper clear aqueous phase was transferred to a new tube and 500µl of isopropanol were added, after mixing tubes were left to stand 10 min at RT. Samples were centrifuged again at 13,000 rpm for 15 min, 4°C. The resulting pellet was washed with 1ml cold 70% ethanol. The pellet was briefly dried and subsequently dissolved in required volume of water, incubating 10 minutes at 55°C. Samples were quantified using the Nanodrop 2000 (Thermo Fisher Scientific).

Pre-miRNA fractionation

For isolation of pre-miRNA containing fractions, total RNA was isolated as above and was briefly run on 10% denaturing PAGE-UREA gel until tracking dyes had separated. The fraction of the gel containing RNAs from 50 nt to 100 nt was cut out using a razor blade and incubated o/n in 300µl of **RNA elution buffer**. The following day RNA was precipitated by adding 900 µl 100% ethanol and incubating 1h on dry ice. RNA was then washed in 70% ethanol and resuspended in water.

Quantification of miRNA levels by qRT-PCR

MiRNA quantification was carried out as instructed using miScript Reverse transcription and SYBR® green PCR kits (QIAGEN). Total RNA was isolated as described above and 400ng were used per reverse transcription reaction. The cDNA was further diluted 1:3 and 2µl were used per qPCR reaction. Specific forward primers were used in this assay, these corresponded to the sense strand of the mature miRNA sequence. The reverse primer used is the miScript Universal Primer (miScript). All reactions were carried out with a technical duplicate and normalized against miRNA-16.For quantification of pre-miR levels the same kits and protocols were used following fractionation as described above. In this case only 50ng were used per transcription reaction.

Detection of miRNA precursor species in adductor muscle of mice in a hindlimb ischemia model were carried out by Yael Nossent with quantification performed using TaqMan microRNA, pre-miRNA and pri-miRNA assays (Applied Biosystems)

according to the manufacturer's protocol. Relative qPCR was performed on the Viia7 system and normalized to snRNA-U6.

Generation of knockout cell lines using CRISPR/Cas9

Introduction of guide RNAs into Cas-9 containing plasmid px458

Target CRISPR sites in HADHB and CIRBP were identified using Sanger's WTSI Genome Editing tool (https://www.sanger.ac.uk/htgt/wge/). Sequences targeting exon 1 of CIRBP an exon 3 of HADHB were selected. For cloning into the sgRNA scaffold in Cas9 containing plasmid px4598 oligonucleotides for selected CRISPR target sequences were synthesized in the form:

5' – CACCGNNNNNNNNNNNNNNNNNN – 3'
3' – CNNNNNNNNNNNNNNNNNNNCAAA – 5'

Oligonucleotides were set up in an annealing reaction as follows; 1µl of Oligo 1 (100µM), 1µl of Oligo 2 (100µM), 1µl 10X T4 ligation buffer (NEB), 6.5µl H_2O, 0.5µl T4 PNK (NEB). The reaction was incubated in a thermocycler set for 30 min at 37 °C, 5 min at 95 °C and then ramp down to 25 °C at 5°C/min.

Digestion of px458 plasmid was performed for 1 hour at 37 °C with BbsI restriction enzyme in the following reaction; 1µg plasmid, 1µl BbsI, 2µl 10X digestion buffer, x µl of H_2O for 20µl final volume. Digested products were then run in a 1% agarose gel in 1X TBE buffer and gel purified using QIAquick gel extraction kit (QIAGEN) according to manufacturer's instructions. Following purification of digested vector and annealing of oligonucleotides, a ligation reaction was set up as follows; 50ng of BbsI digested plasmid, 1µl annealed oligonucleotides (diluted 1:200), 5µl 2X ligation buffer

(NEB), 1µl T4 ligase (NEB), x µl of H_2O for a final volume of 10µl. The reaction was incubated 1hour at 37 °C. The ligation was then transformed into competent bacteria and purified as described below.

FACS flow cytometry of transfected NIH-3T3 cells

Cell sorting was carried out with the help of Dr. Martin Waterfall at the IIIR/SBS Flow Cytometry Facility using the FACSAria cell sorter (BD Biosciences). NIH-3T3 cells were transfected 24 hours before preparation for sorting with 2µg of px458 plasmid containing desired guide RNAs, following the transfection protocol described below. Immediately before sorting cells transfected cells were trypsinized, centrifuged 5 min at 1500 rpm and resuspended in **basic sorting buffer.** Cells were counted and diluted to a concentration of approximately $15x10^6$/ml. To achieve a single cell suspension and eliminate any clumping, cells were filtered by pipetting though a 40µm nylon mesh (Falcon) into a 50 ml conical tube.

In preparation for collection, 50µl of fully complemented media was added to each well in 96-well plates. After sorting a further 50µl were added to each well using a multichannel pipette. Single cells were sorted into individual wells using channel settings to detect GFP-signal in positively transfected cells. As a sorting control, non-transfected cells were also sorted into individual wells.

After sorting cells were grown until single cells had developed into visible colonies, changing the media every 2-3 days. Once colonies were visible cells were passaged into 24-well plates, which were further divided into duplicate plates. One plate was used for cell maintenance whilst the other was used for genomic analysis.

Isolation of genomic DNA and amplification of target regions

Genomic DNA was isolated using GenElute™ Mammalian Genomic DNA Miniprep Kit (Sigma-Aldrich). Trypsinized cells were centrifuged for 5 min at 1500 rpm and culture media was completely removed. Pellets were resuspended in 200µl of resuspension solution and transferred to a microfuge tube to which 20µl of Proteinase K solution and 200µl of Lysis solution were added. Samples were thoroughly vortexed and incubated at 70 °C for 10 minutes. 200µl of 100% ethanol were added to incubated samples, which were then vortexed and loaded unto a previously equilibrated column using a pipette tip with the end cut to avoid shearing. Samples were centrifuged at 7000 rpm for 1 min and then washed twice with 500µl wash solution, centrifuging first for 1 min at 7000 rpm and then for 3 min at 13,000 rpm. Columns were then transferred to new collection tubes and DNA was eluded in 200µl elution solution by centrifuging at 7000 rpm for 1 min.

Genomic DNA preparations were then used as template to amplify the region surrounding CRISPR target sequences. Primers were designed using Primer3 to

Step		Temperature (°C)	Time	Cycles
Initial Denaturation		98	30 sec	1
Cycling	Denaturation	98	10 sec	30
	Annealing	60	30 sec	
	Extension	72	15 sec	
Final extension		72	10 min	1
Hold		4	-	-

encompass a region between 500-1000 nucleotides surrounding CRISPR targets, ensuring no binding to other genomic regions. PCR amplification reactions were set up as follows; 1µl of genomic DNA, 2.5µl forward primer (10µM), 2.5µl reverse primer (10µM), 10µl 5X Phusion HF Buffer (NEB), 1µl dNTPs (10mM working mix) (Roche),

0.5µl Phusion® High-Fidelity DNA Polymerase (NEB) 32.5µl H_2O. PCR amplification was conducted under the following settings:

After amplification, 10µl of 6X purple loading dye (NEB) were added and PCR products were run on a 1% agarose gel in 1X TBE. Bands were cut and gel purified using QIAquick gel extraction kit (QIAGEN) according to manufacturer's instructions.

Cloning and sequencing of amplified target regions

Purified products were cloned into pJET1.2/blunt cloning vector (Thermo Scientific) for sequencing. Blunt-end cloning reactions were set up as follows; 50ng of purified PCR product, 10µl 2X reaction buffer, 1µl pJET1.2/blunt cloning vector, 1µl T4 DNA ligase, x µl H_2O to a final volume of 20µl. Reactions were incubated at room temperature for 10 min and used directly for transformation using the protocol described below. Reactions were sequenced using both pJET1.2 Forward and Reverse sequencing primers. All sequencing was carried out at Edinburgh Genomics.

Transient transfection of cultured cell lines

For transfections, cells were plated at a confluency of ~80%. Transfections were carried out using lipofectamine 2000 (Invitrogen). For each transfection reaction two 15 ml conical tubes were set up; one tube containing 245µl of OPTI-MEM media (GIBCO) + 5µl of lipofectamine (Invitrogen) and a second tube containing the required concentration of plasmid + the required volume of OPTI-MEM for a final volume of 250µl. The typical concentration of DNA added was 500ng, however this was adjusted according to protein expression levels. Tubes were briefly vortexed and incubated for 5 min at RT. Lipofectamine was then added drop-by-drop into the plasmid containing

tube containing for a final volume of 500µl. This reaction was incubated for 30 min at RT. In the meantime, cells were washed twice with OPTI-MEM media before adding 1.5ml of fresh DMEM media supplemented with 10% FBS. Finally, the lipofectamine and plasmid mixture was added to the cells drop-by-drop. An additional mock reaction was always set up in parallel were lipofectamine was mixed into a tube containing 250µl of OPTI-MEM but no DNA.

Bacterial transformation

A 50µl aliquot of competent DH5α *E.coli* cells was thawed on ice and either 10µl of ligation reaction or 1µl of DNA plasmid were added to the aliquot. Tubes were gently mixed, without vortexing, and incubated for 30 minutes on ice. Tubes were then placed in a heat block, surrounded by water for 90 s at 42 °C and immediately after placed in ice for 90 sec. Subsequently, 800µl of SOC media was added to bacteria and tubes were left shaking for 1h at 37 °C. Whilst bacteria were shaking LB agar plates containing appropriate selection antibiotic were pre-warmed at 37 °C. After 1 hour, 200µl of bacteria were spread on pre-warmed LB agar plates using a shaped glass Pasteur pipette, sterilized with ethanol. Plates were incubated overnight at 37 °C.

The following day, individual colonies were selected and grown in 5ml of LB broth with appropriate selection antibiotic. The next day plasmids were purified using QIAprep spin miniprep kit (QIAGEN) following manufacturer's instructions.

Cloning of Lin28a truncations into T7-expression vector

Lin28a truncations were cloned into an expression vector (g10) which contains a T7-protein tag sequence. For this, Lin28a fragments were amplified using primers which annealed to the desired start and end sites of each Lin28a truncation. Additionally, all forward primers contained an XbaI restriction site and all reverse primers contained a BamHI site which were used for sticky-end cloning. Amplified PCR products were run in a 1% agarose gel and gel purified using QIAquick gel extraction kit (QIAGEN) according to manufacturer's instructions.

Digestion reactions for purified PCR products and g10 expression vector were set up as follows; 500 ng DNA, 1µl XbaI restriction enzyme (NEB), 1µl BamHI restriction enzyme (NEB), 5µl 10X NEBuffer (NEB) and H_2O to 50µl. These were incubated for 1 hour at 37 °C. Digestions were then run in a 1% agarose gel and gel purified using QIAquick gel extraction kit (QIAGEN). Purified and digested products were then ligated using T4 DNA ligase (NEB). 100ng of digested vector were used per ligation reaction; the amount of insert for each reaction was calculated to achieve a 3:1 insert to vector molar ratio. Ligations were set up as follows; 100 ng vector, x ng insert (3:1 molar ratio), 1.5µl 10x T4 DNA ligase buffer (NEB), 0.5µl T4 DNA ligase (NEB) and x µl H_2O for a final volume of 15µl. Ligations were incubated overnight at 4 °C. The following day 10µl of the ligation reaction were directly used for transformation as described in protocols above. Individual colonies were grown in 5 ml of LB broth supplemented with ampicillin and plasmid DNA was purified using QIAprep spin miniprep kit (QIAGEN) following manufacturer's instructions.

Electrophoretic mobility shift assay (EMSA)

32P-αUTP was used for internal labelling of pre-miR probes generated through *in-vitro* transcription. For this, reactions were set up as following; 10 ng of DNA template, 2.5µl 10X T7 reaction buffer (Lucigen), 1.25µl of 20nM GCA rNTP mix (Roche), 1.25µl 1nM UTP (Roche), 0.5µl RNase out (Invitrogen), 1µl T7 RNA polymerase (NxGen T7 RNA Polymerase, Lucigen supplied at 50,000 U/mL) and 2.5µl 32P-αUTP in a final volume of 25µl. Reactions were incubated for 90 minutes at 37 °C and subsequently run in a 10% PAGE-UREA gel and purified as described in the sections above. Purified radiolabelled pre-miRs were then incubated with total HeLa extracts in the absence and presence of increasing concentrations of oleic acid (OA) and elaidic acid (EA) in the following set up; 1µl probe, 150 ng protein extract, 2µl **solution A**, 0.5µl RNaseOUT (Invitrogen), x µl of OA/EA and **Roeder D** for a final volume of 20µl. Reactions were incubated on ice for 1 hour. Following incubation 5µl of native loading buffer (0.02% Xylene Cyanol, 0.02% Bromophenol Blue) was added and samples were separated on a on 6% non-denaturing PAGE by running in 0.5 × TBE at 8 W. The gel was then dried and exposed to a phosphor screen overnight. The gel-exposed phosphor screen was scanned using a Fujifilm FLA 5000 scanner. Image analysis and quantitation were performed using Aida Image analyser V.4.27 software.

Western blot-combined EMSA (WEMSA)

For WEMSA, initial steps were carried out as described above and after samples were separated by PAGE, the proteins were transferred onto a nitrocellulose membrane and western blot proceeded as described in protocols above.

In-vitro processing assays

In vitro processing assays were carried out by in our group by Santosh Kumar. Pri-mi-7-1 and pri-miR-16 were synthesized by *in vitro* transcription using plasmids containing respective sequences as templates and were labelled using 32P α-UTP. Radiolabelled pri-miRs (~ 30,000 cpm) were incubated with 50% HeLa cell extract in either the presence or absence of OA and EA, and processing was performed at 37 °C for 30 min with 0.5 mM ATP, 20 mM creatine phosphate, and 3.2 mM MgCl2. Next, phenol chloroform extraction was performed, followed by precipitation and separation on 8% denaturing PAGE in 1 × TBE.

Buffer list

RNA extraction solution

Sodium Acetate	0.3 M
EDTA	0.5 mM
SDS	0.1% w/v

pH 5.2

Roeder D

Glycerol	50g (39.7 mL)
Potassium Chloride	100mM
EDTA	0.2mM
Tris pH 8.0	100mM

Add 250ul DTT (100mM) + 50ul PMSF (200mM) to filtered 50ml

Buffer G (Gregory 2014)

Tris-HCl pH 7.5	20mM
NaCl	137mM
EDTA	1mM
TritonX-100	1%
Glycerol	10%
MgCl2	1.5mM

Add 500ul DTT (100mM) + 50ul PMSF (200mM) to filtered 50ml

UEO RNA loading buffer

EDTA	20mM
Urea	7M

Bromophenol blue

Xylene cyanole

Acetonitrile/ABC solution

Ammonium bicarbonate	10mM
Acetonitrile	10%

Trypsin Buffer

Trypsin solution: Add 20µl of 0.1% trifluoracetic acid to 20µg trypsin.

Acetonitrile/ABC solution	227µl
Trypsin solution	3µl

Tris-buffered saline (TBS)

Tris-Cl	50mM
NaCl	150mM

pH 7.6

Phosphate-buffered saline (PBS)

Sodium Chloride	137mM
Potassium Chloride	2.7mM
Na2HPO4	100mM
KH2PO4	18mM

pH 7.4

Acidified acetone/methanol

Acetone	50%
Methanol	50%
HCL (10M)	0.05%

Optimized lysis buffer K

EDTA	20mM
NaCl	140mM
Tris	100mM
SDS	5%

TBE 1 X

Tris	0.5M
Boric acid	0.5M
14.88g EDTA	10mM

Add ~2.5g of NaOH pellets per litre to adjust pH to 8.3

RNA staining solution

Stains all stock	10%
Formamide	10%
Isopropanol	50%

Stains-all stock: 0.1% Stains-all (Sigma) w:v in formamide.

Basic sorting buffer

PBS	1X
EDTA	1mM
HEPES pH 7.0	25mM
Fetal Bovine Serum	1%
Antibiotic-Antimycotic	1X

Filter sterilized

RNA elution buffer

NaAc pH5.2	0.3M
EDTA	0.5mM
SDS	0.1%

Solution A

Magnesium Chloride	32mM
ATP	5µM
CIP	0.4M

Antibody list

Antibody	Catalog number	Host species
Anti-CIRBP	Protein tech (10209-2-AP)	Rabbit polyclonal
Anti-DHX9	Protein tech (17721-1-AP)	Rabbit polyclonal
Anti-DIS3L2	Abcam (ab50848)	Rabbit polyclonal
Anti-HADHB	LSBio (LS-B13884-50)	Rabbit polyclonal
Anti-HnRNPA1	Millipore (05-1521)	Mouse monoclonal
Anti-HuR	Millipore (07-468)	Rabbit polyclonal
Anti-Lin28	Abcam (ab46020)	Rabbit polyclonal
Anti-MSI2	Millipore (04-1069)	Rabbit monoclonal
Anti-T7-tag-HRP	Millipore (69048)	Mouse monoclonal
GAPDH	Protein tech (10494-1-AP)	Rabbit polyclonal
Anti-mouse IgG	Cell signalling (7076S)	
Anti-Rabbit IgG	Cell signalling (7074S)	

Primer list

Primer	sequence
HADHB CRISPR gRNA For	CACCCGCATTCCATTTCTGCTGTC
HADHB CRISPR gRNA Rev	AAACGACAGCAGAAATGGAATGCG
CIRBP CRISPR gRNA For	CACCAGCAGGTCTTCTCCAAGTAT
CIRBP CRISPR gRNA Rev	AAACATACTTGGAGAAGACCTGCT
Sequencing primer HADHB KO For	AAAGCTGTCCAGACCAAGTC
Sequencing primer HADHB KO Rev	ATCTCACCAGCCCCAAAGAA
Sequencing primer CIRBP KO For	GGGTGGTGGTTAAGGCAAAC
Sequencing primer CIRBP KO Rev	TGGAAGGACACACATGGACA
Pre-miR-329 T7 For	TAATACGACTCACTATAGGTGTTCGCTTCTGGTACCGGA
Pre-miR-329 Rev	AAAAAGGTTAGCTGGGTGTG
Pre-miR-495 T7 For	TAATACGACTCACTATAGGAAAGAAGTTGCCCATGTTAT
Pre-miR-495 Rev	AAGAAGTGCACCATGTTTGT
Pre-miR-9 T7 For	TAATACGACTCACTATAGGTCTTTGGTTATCTAGCTGTA
Pre-miR-9 Rev	ACTTTCGGTTATCTAGCTTTA
Pre-let-7a T7 For	TAATACGACTCACTATAGGATGTTCTCTTCACTGTGGG
Pre-let-7a Rev	TGCAGACTTTTCTATCACGTTAGG
CIRBP XbaI For	TTTTCTAGAATGGCATCAGATGAAGGCAAG
CIRBP BamHI Rev	AAAGGATCCTTACTCGTTGTGTGTAGCATA
HADHB XbaI For	TTTTCTAGAATGACTACCATCTTGACT
HADHB BamHI Rev	TTTGGATCCTTTGGGGTAAGCTTCCA

*HADHB contains two BamHI sites that where substituted out with silent mutations:
SITE 1: For-ATCCGTCCTTCCTCACTGGA Rev-GCCATTATCTTTGGTAACTGT
SITE 2: For-CCCGAAAGATCAGCTTTTAC Rev-TCCTGGGACACATATATAAA

Lin28a XbaI For	TTTCTAGAATGGGCTCCGTGTCCAACCAGCGTTTG
Lin28a BamHI Rev_190	TTGGATCCTCAGTAGGTTGGCTTTCCCTGTGCACTAGGG
Lin28a XbaI For_24	TTTCTAGAGCGCCGGAGGACGCGGCC
Lin28a BamHI Rev_209	TTGGATCCTCAATTCTGTGCCTCCGGGAGCAGGGTAG
Lin28a BamHI Rev_123	TTGGATCCTCACCGCCTCTCACTCCCAATACAGAATACTCC
Lin28a XbaI For_123	TTTCTAGACGGCCAAAAGGAAAGAGCATGCAG AAGCG
Lin28a BamHI Rev_74	TTGGATCCTCACACAAAGACATCCACTGGGGGG TCGAG
Lin28a XbaI For_156	TTTCTAGACCCCAGCCCAAGAAGTGCCACTTCTG
Pri-miR-329-mmu For	AAGGTCACGTTGGGGAATTA
Pri-miR-329-mmu Rev	ACCACGAAGCCTCCAAGAT
Pre-miR-329-mmu For	TGGTACCGGAAGAGAGGTTTT
Pre-miR-329-mmu Rev	AGGTTAGCTGGGTGTGTTTCA
Pri-miR-494-mmu For	TGCCTTTGTTTGCTTTCTGA
Pri-miR-494-mmu Rev	GTCATCAGGGACAGGGAGTG

Pre-miR-494-mmu For	GGAGAGGTTGTCCGTGTTGT
Pre-miR-494-mmu Rev	AGGTTTCCCGTGTATGTTTCA
Pri-miR-495-mmu For	AGCATCCCTTCACACTCAGG
Pri-miR-495-mmu Rev	GAGCTCTCCAAGGTGAGATTTG
Pre-miR-495-mmu For	GTTGCCCATGTTATTTTTCG
Pre-miR-495-mmu Rev	AGTGCACCATGTTTGTTTCG

ALL miRNA primers for qRT-PCR correspond to their respective mature miRNA sequence

Results

Post-transcriptional regulation of 14q32 cluster microRNAs

Because of the vital and widespread function of miRNAs, their biogenesis is tightly regulated at every step of the pathway, both at the transcriptional and post-transcriptional level[266,267]. Additionally, this is further complicated by the fact that miRNAs are frequently found in clusters, which are transcribed as a single polycistronic unit[10–12]. In humans, the largest of these clusters is cluster 14q32 (12F1 in mice) referring to its position in the genome[239]. This miRNA cluster is found within an imprinted region of the genome that is also host to several lincRNAs and snoRNAs[241,242]. It is expressed throughout the developing embryo, and in adults its expression is enriched in the brain[239,241,243]. It has important functions in neurogenesis including differentiation and proliferation of neural precursors, dendritic development and synaptic formation[243,245–248]. Additionally, its disregulation has been associated with various diseases including cancer, schizophrenia and cardiovascular disorders[249–257]. However, this disregulation of 14q32 miRNAs can be restricted to altered levels of specific subsets or individual miRNAs rather than the cluster as a whole[259–265].

The importance of this cluster in neovascularization was previously highlighted by our collaborators in the Netherlands[251]. The role of this cluster in neovascularization was first identified through reverse target prediction, were various genes involved in both angiogenesis and arteriogeniesis were probed for miRNA target sites. An enrichment of binding sites for 27 miRNAs in the 14q32 cluster was found in these probed genes.

To further study the importance of this cluster in neovascularization a microarray analysis was then performed in a murine hindlimb ischemia model (HLI), were ligation of the femoral artery was carried out to reduce blood flow to adductor muscle resulting in an ischemic tissue. This microarray analysis showed an upregulation of over half the miRNAs in the cluster after the induction of ischemia[251].

Within the group of miRNAs that were upregulated two distinct temporal patterns were seen; early responders first showed increased levels 24 hours after HLI whilst late responders did so after 72 hours. Importantly, the three distinct response patterns, (early-responders, late-responders and non-responders) were independent from the position of the miRNAs within the cluster, suggesting that the difference observed is due to post-transcriptional regulation of the cluster (

Figure 8).

Additionally, gene-silencing oligonucleotides (GSO) were used to further study the effects of select 14q32 miRNAs on blood flow recovery. For this, miRNAs representing each temporal response pattern were selected, namely miR-329 (late responder), miR-494 (early responder) and miR-495 (non-responder). Mice were injected with GSO targeting these miRNAs and the next day HLI was induced. Blood flow recovery was then monitored for the following 17 days. All the treated groups, GSO-329, GSO-494 and GSO-495 showed significantly improved blood flow recovery when compared to GSO-control treated mice[251]. Further experiments showed that GSO-mediated silencing of all three miRNAs resulted in an increase in arteriole diameter and treatment with both GSO-329 and GSO-495 additionally showed an increase in

capillary density. This reflects the involvement of these miRNAs in the regulation of both arteriogeniesis and angiogenesis. Several pro-arteriogenic and pro-angiogenic genes were also confirmed to be upregulated after GSO-mediated silencing of miR-329 and miR-494, including Tlr4, Vegfa, Fgrf2, Mef2a, Arf6 and Efnb2. No targets for miR-495 have been confirmed by GSO-495 silencing thus far, however there is still a large number of putative targets whose change in expression has not been analysed.

These results indicate a direct involvement of these miRNAs in the regulation of neovascularization. However, this is a complex process involving multiple networks of regulating factors, including miRNAs, for which many details are still unknown.

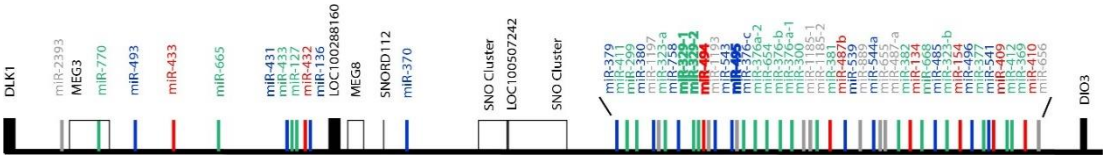

Figure 8 Changes in expression level of 14q32 miRNAs following ischemia. Microarray analysis were performed on murine adductor muscle samples to measure levels of 14q32 miRNAs after induction of hindlimb ischemia. These miRNAs were classified into three temporal upregulation patterns; early responding (green), late responding (red) and non-responding (blue). MiRNAs in grey were not included in the miRNA analysis. MiRNAs in bold were used in later experiments to represent each of the three temporal patterns[251].

Pri-miR, pre-miR and mature miRNA levels of 14q32 miRNAs following ischemia

To further investigate post-transcriptional regulation of miRNAs in this cluster, it was important to determine the levels pri-, pre- and mature miRNA levels for selected 14q32 miRNA in an HLI model. The levels of mature and precursor miR-329, miR-494 and miR-495 in adductor muscle following HLI were measured by qRT-PCR using

specific primers for each pri-miR, pre-miR and mature miRNA species (Figure 9). These miRNAs correspond to those previously selected to represent each distinct temporal pattern and whose inhibition showed a positive effect on blood flow recovery.

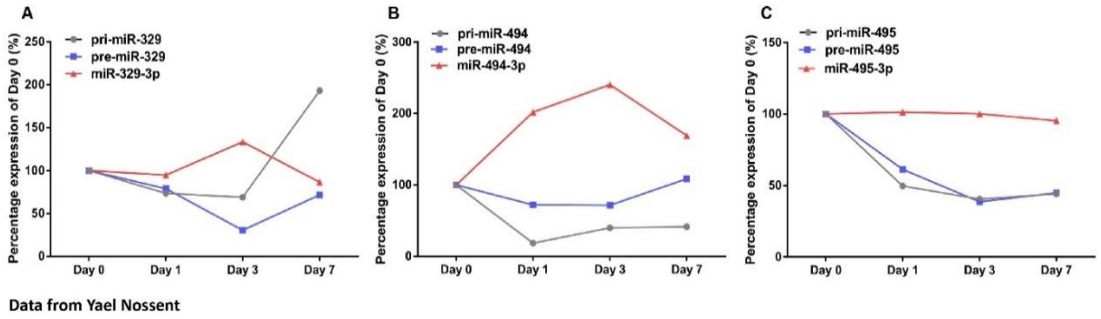

Figure 9 Levels of 14q32 miRNA precursors. Levels of pri- pre- and mature miRNA levels for A) late-responding miR-329 B)early-responding miR-494 and C)non-responding miR-495 were measured by qRT-PCR using specific primers after induction of hindlimb ischemia. N=4 mice per timepoint.

Mature miRNA levels of late-responding miR-329 showed no change 24 h after ischemia, but an increase in levels was observed after 72 hr. Then, there was a return to basal levels by day 7 post-ischemic induction. This expression pattern contrasts with the changes in pre-miR-329 and pri-miR-329 levels. Expression of both pri- and pre-miR-329 slightly decreased 24 hr after induction of HLI, but whilst the levels of pri-miR-329 are then maintained 72 hr after HLI induction before showing a strong increase after 7 days, expression of pre-miR-329 continues to decrease after 72 hr before showing a slight increase at day 7 (Figure 9 A). Mature miRNA levels of early-upregulated miR-494 show an increase 24 hr after ischemia which is further intensified by 72 hr after induction. This trend is then reversed, with lower expression of mature miR-494 at day 7 relative to day 3 post ischemia, although expression is

still higher than base levels. Again, these changes do not correspond to the changes in miR-494 precursor levels. Pri-miR-494 shows a decrease from day 1 that is maintained throughout days 3 and 7, whereas levels of pre-miR-494 show only a slight decrease 24 hr post ischemia (Figure 9 B). Finally, mature miR-495 levels remained unchanged after induction of ischemia, despite a reduction in levels of both pri-miR-495 and pre-miR-495 beginning 24hr after induction of ischemia and continuing at later timepoints (Figure 9 C). In general, while there is a decrease in pre-miR expression levels, increased (miR-494 and miR-329) or sustained (miR-495) expression levels of mature miRNAs were observed. This suggests the possibility of post-transcriptional regulation of these miRNAs at the processing step converting pre-miRs to mature miRNAs.

Identification of novel protein factors binding 14q32 pre-miRs

To further explore the regulation of the pre-miR to mature miRNA processing step of 14q32 miRNAs, a serum starvation model was employed in NIH-3T3 (mouse fibroblast) cells. This is a system often used in the in-vitro study of ischemia and is a simplification of the far more complex processes that occur in ischemia *in vivo.* There are three main contributing factors driving ischemia *in vivo;* nutrient depravation, hypoxia and hypothermia. Serum-starvation mimics the effects of nutrient depravation. Additionally, in whole muscle tissue there is a coexistence of multiple cell-types, one of which is fibroblasts. Serum-starvation of NIH-3T3 fibroblasts therefore allows to study effects on miRNA regulation that are also expected to occur in an *in vivo* ischemic model. Using this simplified model allows for controlled

conditions that are reproducible and production of sufficient material for experiments carried out.

Using this starvation model, protein factors capable of differentially binding to the upregulated pre-miR-329 and unresponsive pre-miR-495 were sought. To identify interacting RBPs, RNA pulldown assays followed by stable isotope labelling of amino acids (SILAC)-mass spectrometry (RP-SMS) were carried out. SILAC was carried out utilizing the incorporation into NIH-3T3 cells of non-radioactive 'heavy' [Arg^{13}]/[Lys^{13}] isotopes which can be distinguished from naturally occurring 'light' [Arg^{12}]/[Lys^{12}] isotopes, allowing for the quantification of relative abundance of proteins using mass spectrometry. Here, *light* NIH-3T3 cells were grown in media fully complemented with 10% fetal bovine serum (non-starved) while *heavy* cells were grown in media complemented with 0.5% fetal bovine serum (starved). Total extracts of both heavy and light cells were then combined and incubated with agarose beads chemically coupled to either pre-miR-329 or pre-miR-495 (Figure 10). Proteins that showed differential binding upon starvation represent putative factors for post-transcriptional regulation of 14q32 miRNAs.

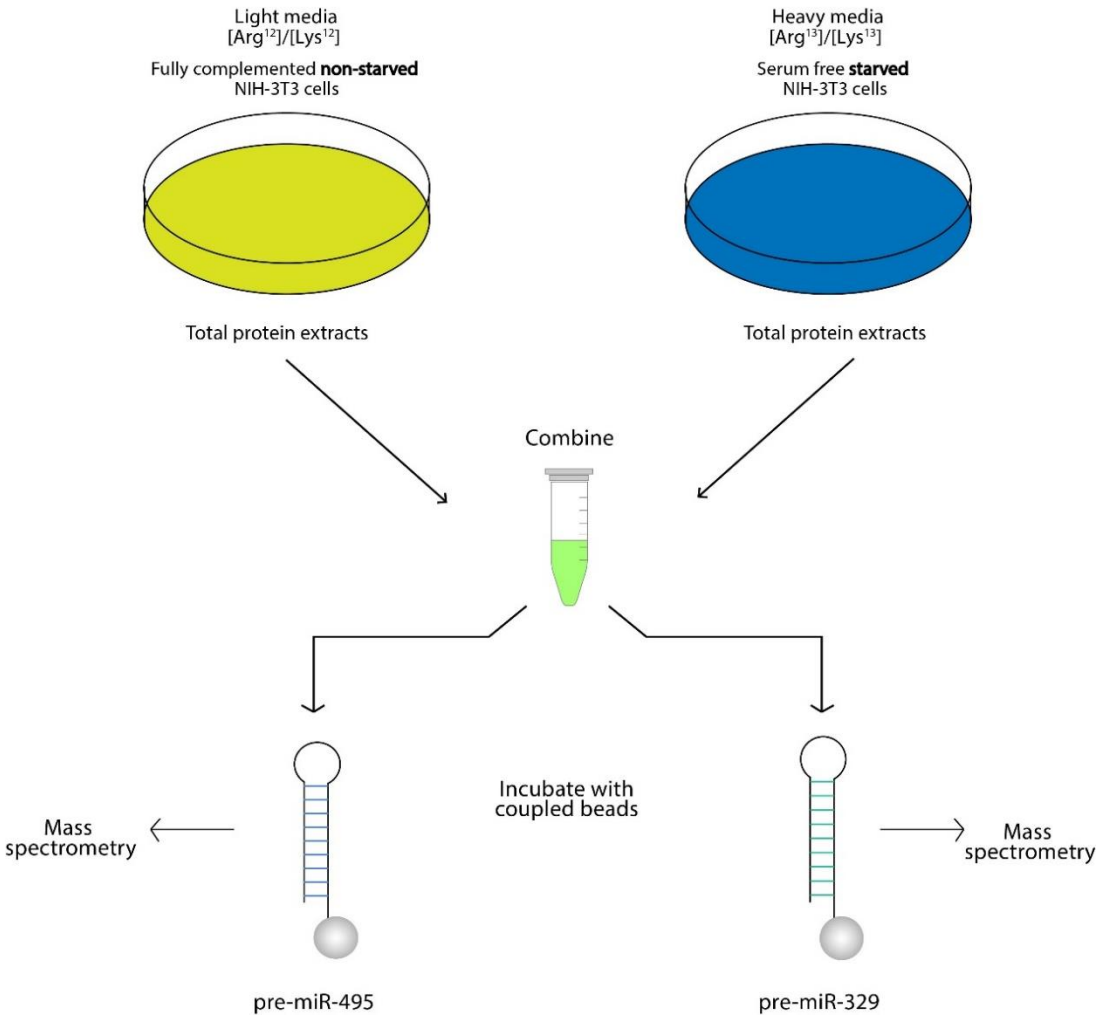

Figure 10 RNA pulldown followed by SILAC-mass spectrometry. *Diagram representing methodology used to identify protein factors binding to 14q32 pre-miRs, pre-miR-329 and pre-miR-495 in a cellular starvation model.*

A total of 104 and 111 proteins showed decreased or increased binding of at least 50%, respectively, to either pre-miR-329 or pre-miR-495 upon starvation (Figure 11). Of these proteins, only a subset showed differential binding upon starvation to both pre-miRs, with 20 proteins showing decreased binding and 35 proteins showing increased binding to both pre-miR-329 and pre-miR-495. These binding patterns indicate the potential for pre-miR-329 and pre-miR-495 to be co-regulated by certain

protein factors whilst possibly also being individually regulated by another set of proteins.

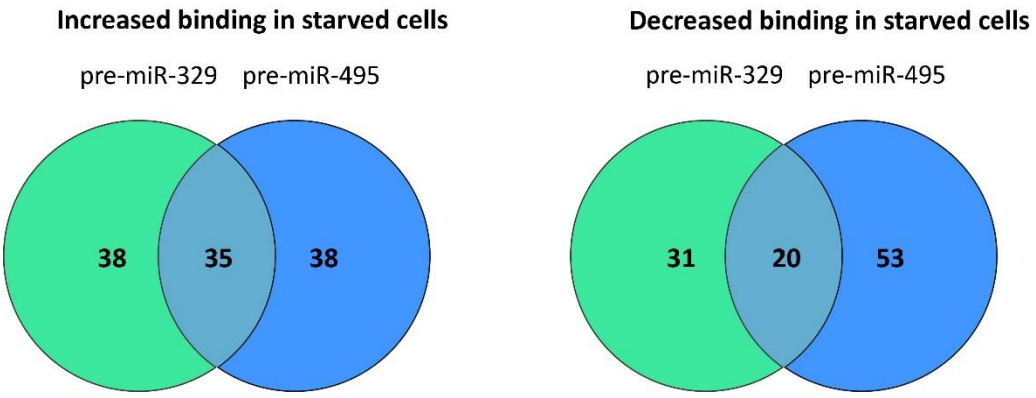

Figure 11 Proteins showing decreased and increased binding upon serum starvation. *Proteins identified by RNA pulldown followed by SILAC-mass spectrometry as binding pre-miR-329, pre-miR-495 or both pre-miRs differentially upon starvation.*

Validation of proteins showing differential binding to pre-miRs upon starvation

To continue gaining insight into the regulation of these pre-miRs, eight proteins identified by RP-SMS were selected for validation by RNA pulldown followed by western Blot analysis. The focus on these eight proteins was based on them showing differential binding upon starvation to either pre-miR-329, pre-miR-495 or both miRNAs as well as them having been reported to bind RNA in genome wide studies without having established roles in miRNA biogenesis. The selected proteins are summarized in Table 1.

For this experiment NIH-3T3 cells were grown in either starved or non-starved conditions and total cell extracts were then individually incubated with beads coupled to pre-miR-329 or pre-miR-495. Proteins that bound to the coupled beads were then analysed by western blot using specific antibodies against the selected

proteins. In all experiments, RNA-helicase DHX9, an abundant protein with high RNA-binding affinity, was used as a positive RNA-binding control.

Protein name	Canonical roles	Changes in binding upon starvation	Ratio Non-Starved/Starved (pre-miR-329)	Ratio Non-Starved/Starved (pre-miR-329)
Cytoskeleton associated protein 4 (**CKAP4**)	Endoplasmic reticulum (ER) transmembrane protein which helps maintain ER structure by anchoring rough ER to microtubules[386].	Increased binding to both pre-miR-329 and pre-miR495.	0.348	0.356
Cold-induced RNA binding protein (**CIRBP**)	Cellular stress response protein which binds and stabilizes specific mRNAs under stress conditions[387,388].	Increased binding to both pre-miR-329 and pre-miR495.	0.328	0.408
Putative RNA-binding protein 15 (**RBM15**)	Various functions; involved in regulation of alternative splicing[389], adaptor protein within the methyltransferase writer complex[390] and is required for XIST-mediated silencing[391].	Increased binding to pre-miR-329 and decreased binding to pre-miR-495 upon starvation.	0.508	0.436
F-box-like/WD repeat-containing protein TBL1XR1 (**TBL1R**)	Nuclear protein that functions as part of various transcriptional repressor and activator complexes[392].	Only binds to pre-miR-329 with decreased binding upon starvation	2.240	---
Trifunctional enzyme subunit beta (**HADHB**)	One of two subunits of mitochondrial trifunctional protein, which catalyses the last three steps of β-fatty acid oxidation. This subunit contains the 3-ketoacyl-coA-thiolase activity[393].	Increased binding to both pre-miR-329 and pre-miR495.	0.437	0.360

Protein disulphide-isomerase (**P4HB/PDI**)	Multifunctional protein that catalyses disulphide bond formation and isomerization and additionally functions as a chaperone[394].	Increased binding to both pre-miR-329 and pre-miR495.	0.558	0.469
RNA binding protein 28 (**RBM28**)	Component of the spliceosomal ribonucleoprotein complexes[395].	Only binds to pre-miR-329 with decreased binding upon starvation	1.897	---
Pyruvate kinase PKM (**PKM1**)	Glycolytic enzyme that catalyses the conversion of phosphoenolpyruvate and ADP into ATP and pyruvate[396].	Increased binding to both pre-miR-329 and pre-miR495.	0.434	0.445

Table 1 Selected proteins for validation following RP-SMS

The binding of two of the selected proteins, Cold-Induced RNA Binding Protein (CIRBP) and Hydroxyacyl-CoA-dehydrogenase trifunctional enzyme subunit beta (HADHB), to pre-miR-329 and pre-miR-495 was successfully validated by RNA pulldown followed by western Blot (Figure 12). Unfortunately, validation of the other selected proteins was unsuccessful; no specific signal was detected either in the total extract input or the pulled down fraction using antibodies against CKAP4, PDI or PKMI whilst the signal for RBM28 was very faint in the input and virtually undetectable in the pulled down fractions (data not shown). A signal for RBM15 could be detected in the input but was not detected in the pulled down proteins, similarly TBLR1 was also detected in the input but the signal in the pulldown fractions was inconsistent and did not correspond to the changes in binding expected from RP-SMS. Further experiments therefore focused on CIRBP and HADHB, however it is important to note that the lack of validation does not rule out the possibility that other proteins detected by RP-SMS could be binding to 14q32 miRNA precursors and regulating their processing.

HADHB is one of two subunits that constitute the mitochondrial trifunctional protein (MTP), along with HADHA. The MTP is a multienzyme complex found in the inner mitochondrial membrane that catalyses the last three steps of the β-oxidation of fatty acids, the metabolic pathway that breaks down fatty acids to produce energy[397,398]. This complex is an octamer consisting of four α-subunits (HADHA) which contain 2,3-enoyl-coA hydratase and 3-hydroxyacyl-coA dehydrogenase activity and four β-subunits (HADHB) which exhibits 3-ketoacyl-coA thiolase activity[399]. HADHB exhibits a classical thiolase fold which consists of two domains comprised of a 5-

stranded β-sheet sandwiched between two α-helixes on either side and a third loop domain, it assembles into a tight homodimer[399,400].

Aside from its canonical role in β-oxidation of fatty acids, HADHB has been shown to bind to bind to the 3'UTR of renin mRNA (*REN),* destabilizing it[375,401]. In those studies, HADHB was shown to be present in the nucleus and cytoplasm in addition to is expected mitochondrial localization[375,401].

CIRBP is a stress-response protein originally identified as being upregulated in response to mild cold-shock[402], but whose expression has since been shown to increase in response to various stresses including UV radiation[403] and hypoxia[404]. Upregulation of CIRBP is regulated at various stages including transcription, translation and splicing[405–407]. CIRBP consists of two domains, an N-terminal RNA recognition motif (RMM) and a C-terminal glycine-rich domain (RGG)[356]. Under normal conditions CIRBP is a nuclear protein, however upon stress it is translocated to the cytoplasm in a mechanism mediated by methylation of its glycine rich domain[408,409]. CIRBP is regulated by an additional post-transcriptional modification, phosphorylation by protein kinase GSK3β, which was shown to increase the RNA binding capacity of CIRBP by 2-fold[410].

CIRBP mediates the post-transcriptional upregulation of specific stress-induced targets involved in various cellular pathways including proliferation[411], translation regulation[412], survival[413,414] and DNA repair[415]. Upon stress, CIRBP binds to the 3'UTR of target mRNAs, stabilizing them and consequently leading to their enhanced translation[412,415,416]. Additionally, CIRBP was shown to increase rate of translation at

the initiation stage[410] and influence gene expression through poly-adenylation of its targets[417]. Countering its positive regulatory functions, upon stress CIRBP can migrate to stress granules were it functions as a translational repressor[408]. Additionally CIRBP can directly interact with protein kinase and cell-cycle regulator DYRK1B, promoting cell-cycle progression[418,419]. The multiple roles and modes of regulation of CIRBP allow it to be a versatile protein that can respond in multiple ways to a variety of cellular stresses.

Western blot analysis of RNA pulldowns with starved and non-starved 3T3-NIH cells generally showed an increase in both HADHB and CIRBP binding to pre-miR-329 and pre-miR-495 upon starvation (Figure 12-13). This increase was particularly evident in the binding of HADHB to pre-miR-329, where HADHB displayed little to no binding under non-starvation conditions but showed an increase upon starvation. Similarly, HADHB also exhibited increased binding to pre-miR-495 upon starvation, however this increase was more modest and, in contrast to pre-miR-329, some binding is also observed under non-starved conditions (Figure 12-13).

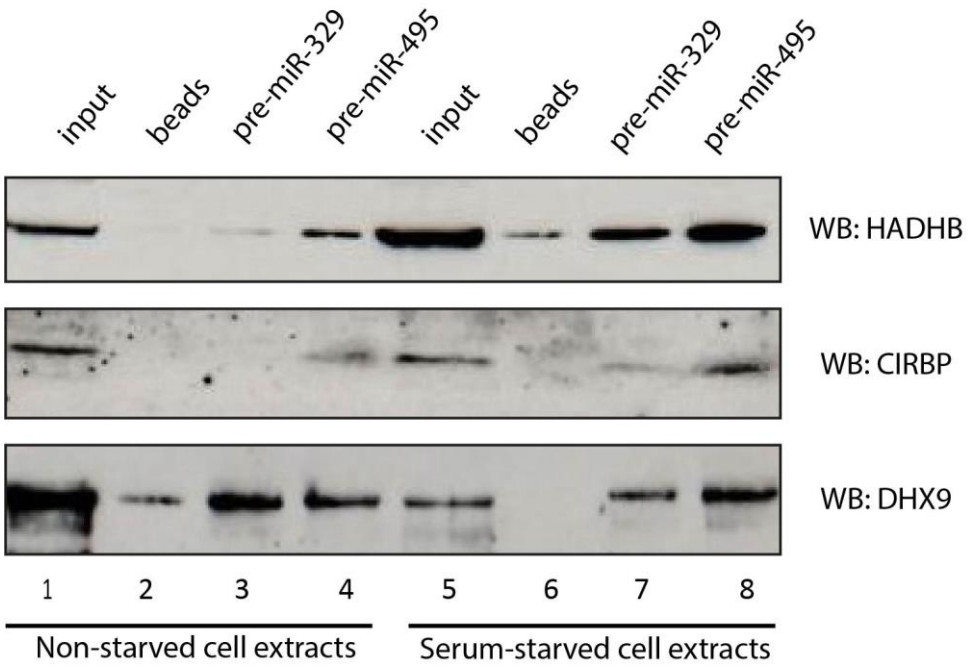

Figure 12 Validation of CIRBP and HADHB binding to 14q32 pre-miRs. *Western blot analysis following RNA pulldown. Total extracts from cells grown in fully-complemented media (lanes 1-4) or serum-free media (lanes 5-8) were incubated with agarose beads coupled to pre-miR-329 (lanes 3,7) or pre-miR-495 (lanes 4,8). Bound protein fractions were recovered, run on a gel, transferred and blotted against antibodies indicated in the left side of the panel. DHX9 serves as a binding control. Lanes 1 and 5 correspond to the loaded extract and lanes 2 and 6 correspond to the extract incubated with uncoupled beads. DHX9 serves as a positive binding control.*

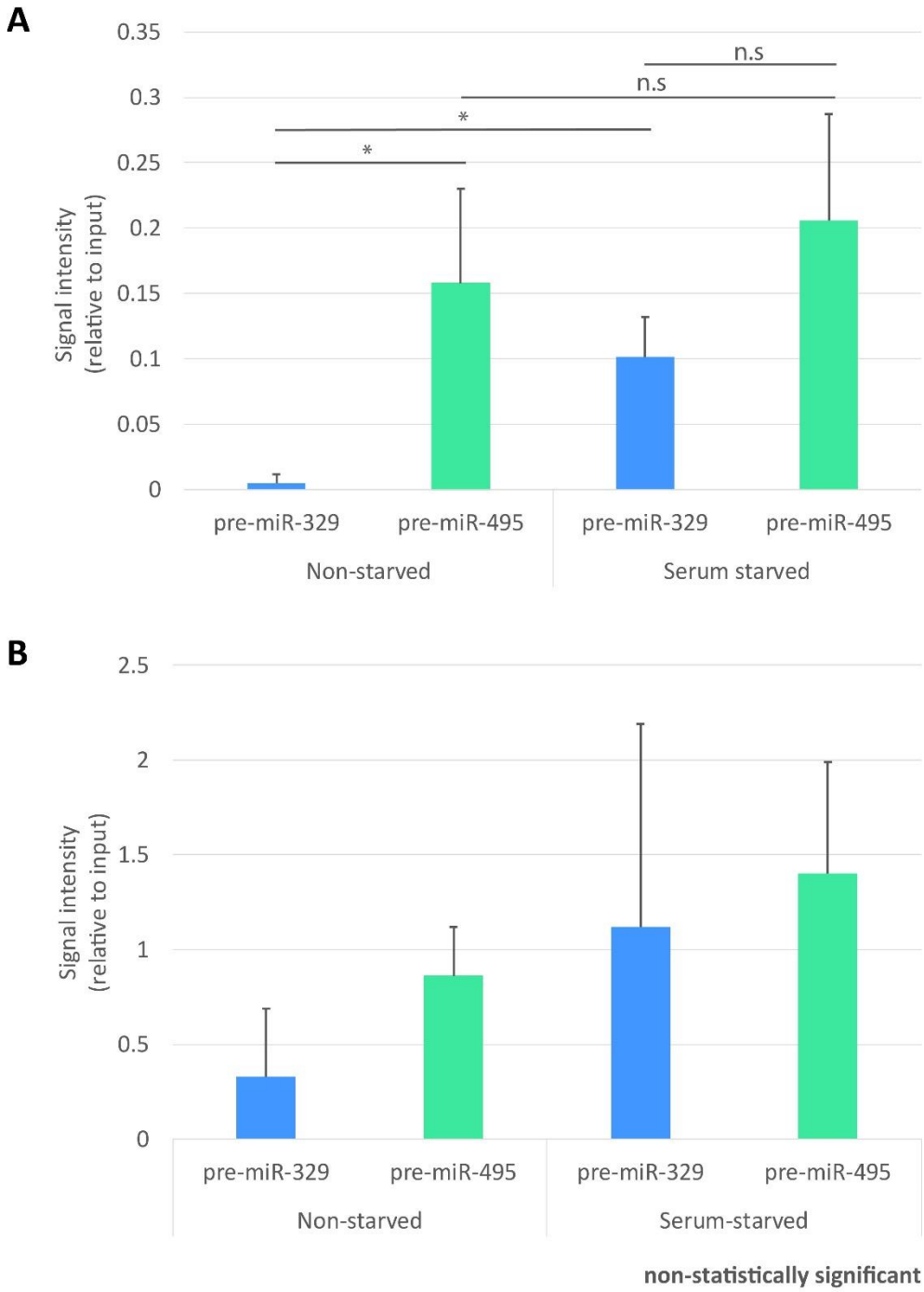

Figure 13 Quantification of HADHB and CIRBP binding in RNA pulldown assays. *Densitometry analysis of western blot showing HADHB (A) and CIRBP (B) binding to pre-miR-329 and pre-miR -495 in RNA pulldown assays. These results represent three independent experiments. *=p<0.05*

Expression of HADHB and CIRBP *in vivo*

After validating binding of CIRBP and HADHB to pre-miR-329 and pre-miR-495 in RNA pulldown assays it was of interest to explore the changes in levels of these proteins *in vivo,* looking at the expression of both HADHB and CIRBP in adductor muscle after induction of HLI. Expression of both HADHB and CIRBP in adductor muscle of mice one day after ischemia was confirmed via immunohistochemistry, both proteins were found dispersed throughout the cells (Figure 14). Localization of both proteins in the cytoplasm is consistent with their potential to bind pre-miRs *in vivo*.

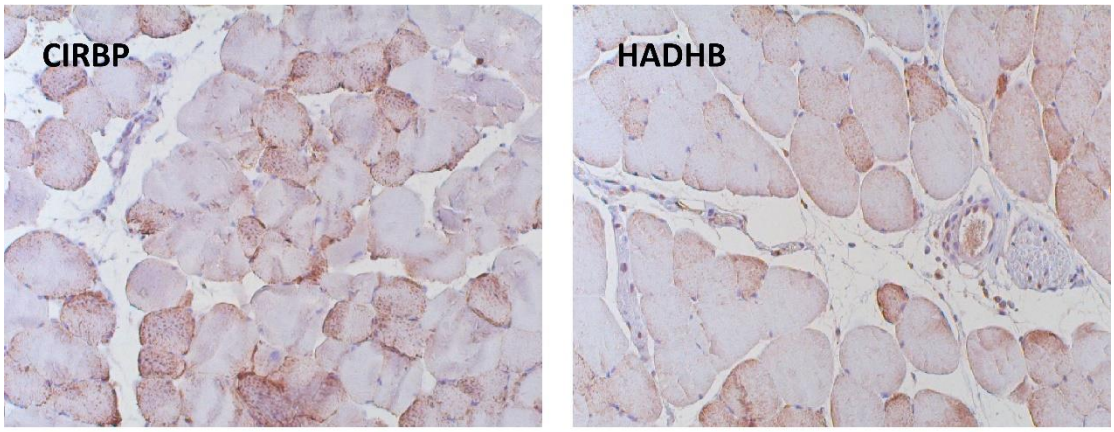

Data from Yael Nossent

Figure 14 Presence of HADHB and CIRBP in adductor muscle following induction of ischemia. Immunochemical staining of adductor muscle tissue samples of mice one day after induction of HLI. Antibodies against CIRBP and HADHB were used, as indicated in the upper left corner of the panels. Antibody staining is seen in a brown hue, whilst nuclei are observed in blue.

Expression levels of *HADHB* and *CIRBP* mRNAs were obtained from microarray analysis of adductor muscle tissue at several timepoints after induction of HLI. An increase in mRNA levels of CIRBP was observed from 24 hours after induction of ischemia which continued until 72 hours post-ischemia were CIRBP mRNA reached maximum expression. HADHB mRNA expression showed an increase only after 72

hours before returning to base levels by day 7 post-ischemia. This increase at day 3 corresponds to the time point were largest changes in levels of mature miR-329 as well as both pre-miR-329 and pre-miR-495 were observed. To confirm that changes in mRNA levels corresponded to an increase in protein levels, western blot analyses were carried out using total protein extracts of adductor muscle tissue at 24 and 72 hours after ischemia (Figure 15). An increase in HADHB protein levels after induction of ischemia was observed at day 3 after HLI induction, but not at day 1, this corresponds to the change observed in mRNA levels. Unfortunately, CIRBP protein levels could not be detected due to a low signal.

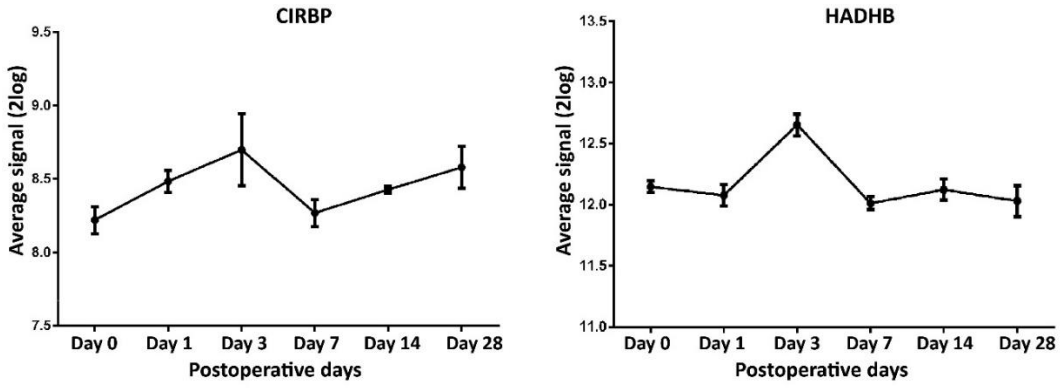

Data from Yael Nossent

Figure 15 Changes in mRNA levels of CIRBP and HADHB following induction of ischemia. Data for the levels of CIRBP and HADHB was obtained from microarray analysis at various timepoints after the induction of HLI. Each datapoint corresponds to the average of 4 mice.

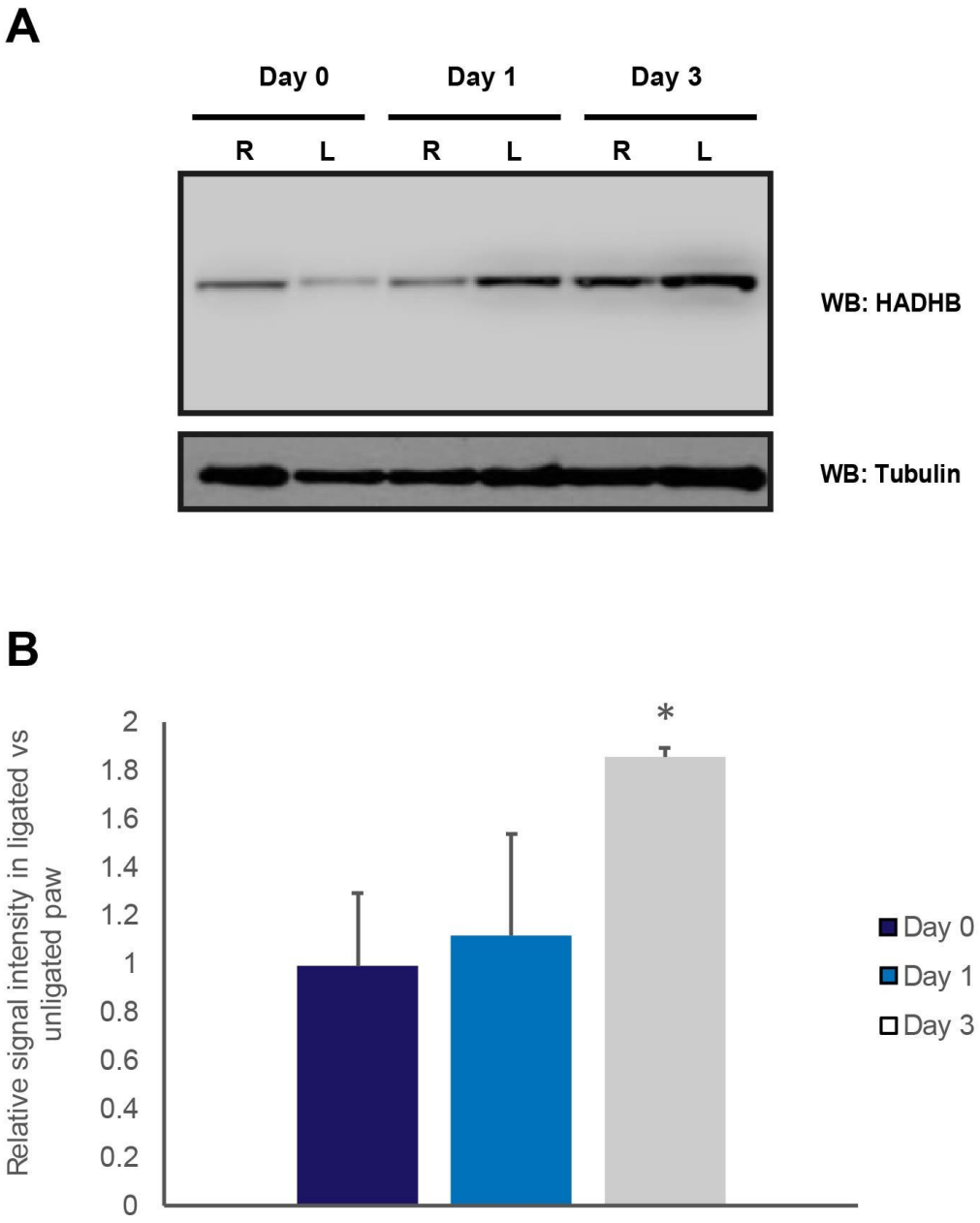

Figure 16 Levels of HADHB protein in adductor muscle following induction of ischemia. *Total protein was extracted from the adductor muscle samples from mice at days 0, 1 and 3 after induction of hindlimb ischemia. For each time point samples from the right (R) un-ligated paw and left (L) ligated paw were compared. Total protein was analysed by western blot (A) with antibodies against HADHB and tubulin as a protein loading control. Densitometry analysis of western blot signal was then performed (B) with HADHB protein levels normalized to tubulin. Ratios of the ligated vs un-ligated paw are presented. One-sample T-test was used to analyse the results, *=p<0.05.*

Overexpression of HADHB and CIRBP in cellular cultures

After the potential for physiological relevance *in vivo* was established, the next question concerned the effects of altering the levels of HADHB and CIRBP proteins in NIH-3T3 cells. Initially, HADHB and CIRBP proteins were cloned into an expression vector containing a T7-tag and subsequently overexpressed in NIH-3T3 cells (Figure 17). Levels of mature miR-329 and miR-495 were then measured by qRT-PCR and compared to mock-transfected cells. MiR-423, a widely expressed and stable miRNA not found in in cluster 14q32 was included as a control[420–423]. Overexpression of either protein had no effect on the protein levels of either miR-329 or miR-495 (Figure 18).

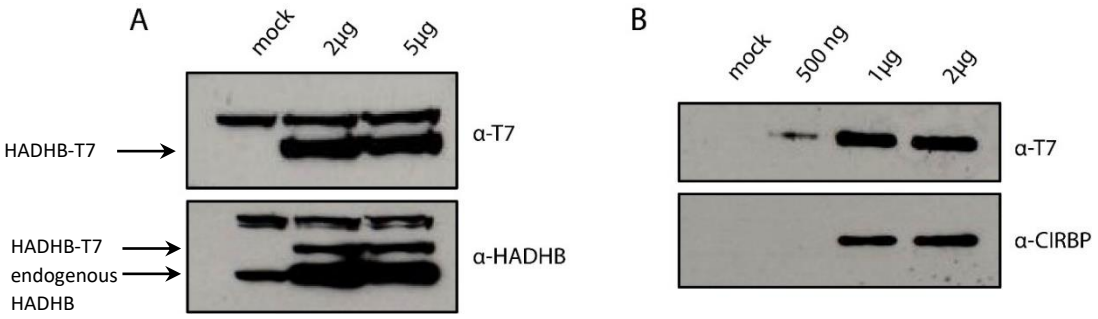

Figure 17 Western Blot showing overexpression of HADHB and CIRBP. Total protein extracts of cells transfected with either T7-CIRBP or T7-HADHB expression vectors in increasing concentrations (as indicated above the panels) and mock-transfected cells were blotted against CIRBP and HADHB, as well as T7-antibody.

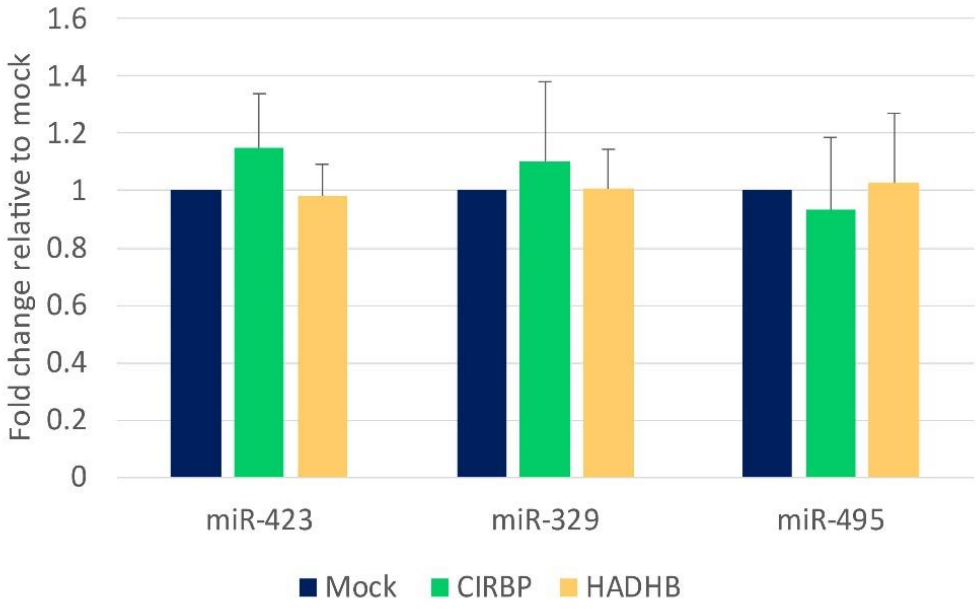

Figure 18 Changes in levels of miR-329 and miR-495 upon overexpression of CIRBP and HADHB. *CIRBP and HADHB were transfected into NIH-3T3 cells. Levels of miR-329 and miR-495 were measured by qRT-PCR and compared in mock transfected cells and CIRBP/HADHB transfected cells. Measurements were normalized to miR-16, miR-423 was used as a control miRNA. One-sample T-test showed no significant difference between mock transfected and CIRBP/HADHB transfected cells.*

Generation of HADHB KO cell lines by CRISPR/CAS9

A more comprehensive approach to analysing changes in miR-329 and miR-495 levels in response to changes in expression levels of RNA binding protein HADHB and CIRBP involved the generation of knock-out (KO) cell lines using the CRISPR/Cas9 system (Figure 19). To do this one guide RNA targeting exon 1 of CIRBP and exon 3 of HADHB were selected and cloned into a spCas9 nuclease expressing vector which also contains a GFP marker (px458). NIH-3T3 cells were then transfected with these expression plasmids and after 24 hours positively transfected cells were individually selected by fluorescence-activated cell sorting (FACS) flow cytometry, utilising the fluorescent signal from the GFP marker. Selected cells were grown into individual colonies which were screened for mutations in *HADHB* or *CIRBP* genes by amplifying the region surrounding the target sequence and inserting it into a vector with regions aligning to sequencing primers. Ten 96-well plates were sorted for each targeted protein, however only around 40 wells grew into single colonies that could be screened. Finally, depletion of proteins in colonies with identified DNA deletions was confirmed by western blot (Figure 19).

Whilst some of the colonies screened for deletions in *CIRBP* showed mutations in one copy of the gene, no colonies with complete depletion of CIRBP were generated. Two individual clones with total depletion of the *HADHB* gene were successfully generated, these cells were labelled AQ and Z as reference. The region surrounding the targeted sequence in the *HADHB* gene was amplified and sequenced, and for each of these clones two distinct mutations were identified (Figure 20). All the mutations

identified for both clones either correspond to frame-shift mutations or span an intron-exon junction. To confirm these mutations translated to a complete depletion of protein levels total protein extract of colonies AQ and Z were compared in a western blot against decreasing amounts of NIH-3T3 protein extracts (Figure 21). No signal was detected in either of the *HADHB* KO clones when probed with HADHB antibodies.

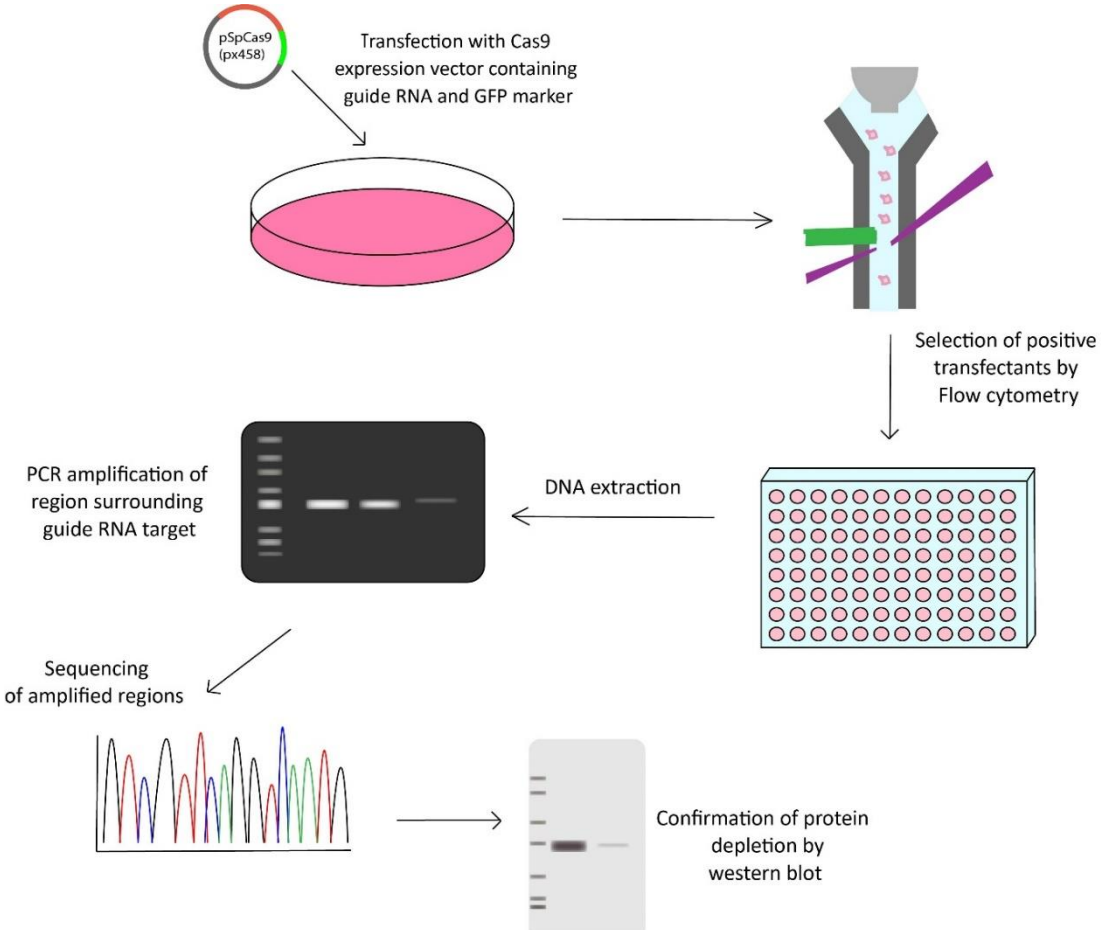

Figure 19 Generation of knock-out cell lines using CRISPR/Cas9 system. *Schematic representation of methodology used in the generation of HADHB and CIRBP knockout cells. 3T3-NIH cells were transfected with plasmid px458, a Cas9 expressing vector with a GFP marker cassette into which guide RNAs where integrated. After 24 hours positively transfected cells were sorted into individual colonies by flow cytometry. Genomic DNA was extracted from all colonies that grew, and the region surrounding the guide RNA target was amplified. These amplification products were extracted and cloned into a sequencing vector. Protein levels were verified for colonies in which disruptions of the gene were identified by sequencing.*

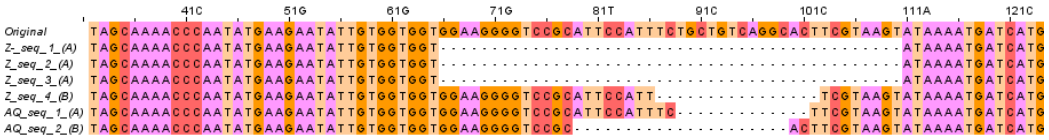

Figure 20 Sequence alignment of CRISPR-Cas9 target region in HADHB knockout clones. Alignment of the sequences corresponding to the region surrounding the CRISPR-Cas9 target sequence from genomic DNA of HADHB KO clones AQ and Z. All sequences correspond to either a frame shift mutation or an exon-intron junction

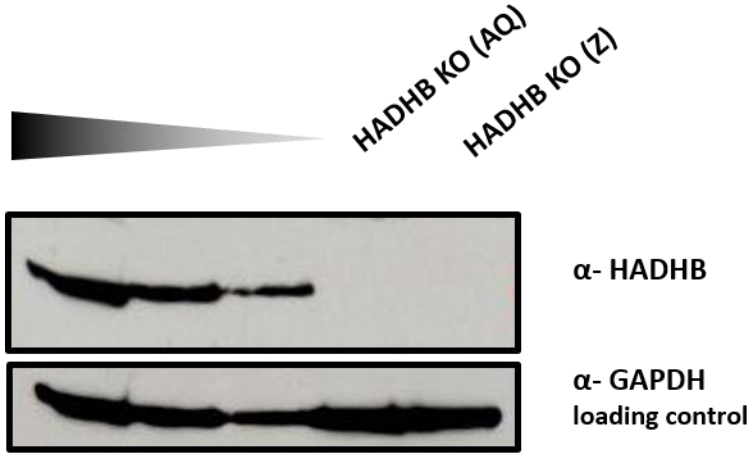

Figure 21 Depletion of HADHB protein levels in knockout clones. Western blot analysis of HADHB levels in total protein extracts of knockout clones AQ and Z. Extracts were run alongside decreasing quantities of NIH-3T3 WT protein extract. Housekeeping gene GAPDH is used as a loading control.

Levels of mature miR-329 and miR-495 in *HADHB* KO cell-lines

Once depletion of HADHB had been confirmed, the impact of this depletion on the levels of mature miR-329 and miR-495 was examined. For this, qRT-PCR analysis was used to compare the levels of these miRNAs in the WT an KO cell lines. In both *HADHB* KO cell lines, a decrease of over 80% compared to WT NIH-3T3 cells was observed for both mature miR-329 and miR-495 (Figure 22). As a control, levels of mature miR-423 were also measured in both WT and KO cells. Importantly, no changes were observed in levels of miR-423, this is an indication that the effects of *HADHB* depletion are specific and not due to a global reduction in miRNA biogenesis.

Levels of pre-miR-329 and pre-miR-495 in KO-cell lines

To determine if the change in mature miR-329 and miR-495 levels was in fact due to changes in post-transcriptional regulation of the pre-miR to mature miRNA processing step it was important to look at the levels of pre-miR-329 and pre-miR-495 in the KO cell lines. Levels of pre-miR-329, pre-miR-495 and pre-miR-423 were analysed in *HADHB* clones AQ and Z (Figure 23). Unlike mature miRNA levels, pre-miR-329 and pre-miR-495 levels remained constant. This corroborates that there is in fact a change in mature pre-miR-329 and pre-miR-495 processing as similar levels of pre-miRs result in much lower levels of mature miRNAs. These results are consistent with *in vivo* observations, where an increase in HADHB levels correlates

with an increase in miR-329 levels and a steady level of miR-495 levels despite a decrease in pre-miR-329 and pre-miR-495.

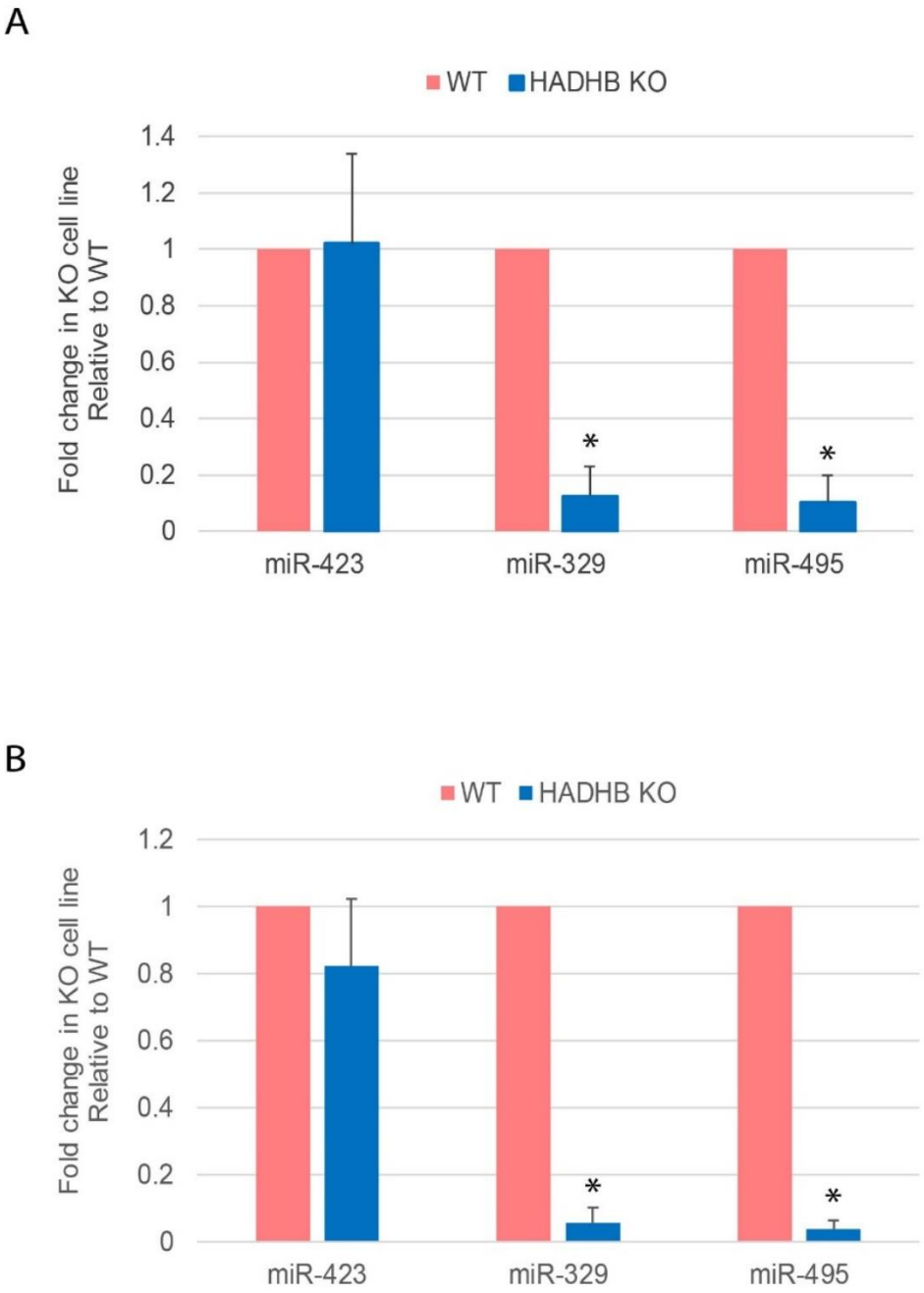

Figure 22 Levels of mature miR-329 and miR-495 in HADHB knockout clones. *Levels of mature miR-329 and miR-495 were measured in WT and KO cell lines in the two HADHB clones; AQ (A) and Z (B). All measurements were normalized against miR-16 and miR-423 was used as a control miRNA. Statistical significance was determined using One-sample T-test where *=p<0.05*

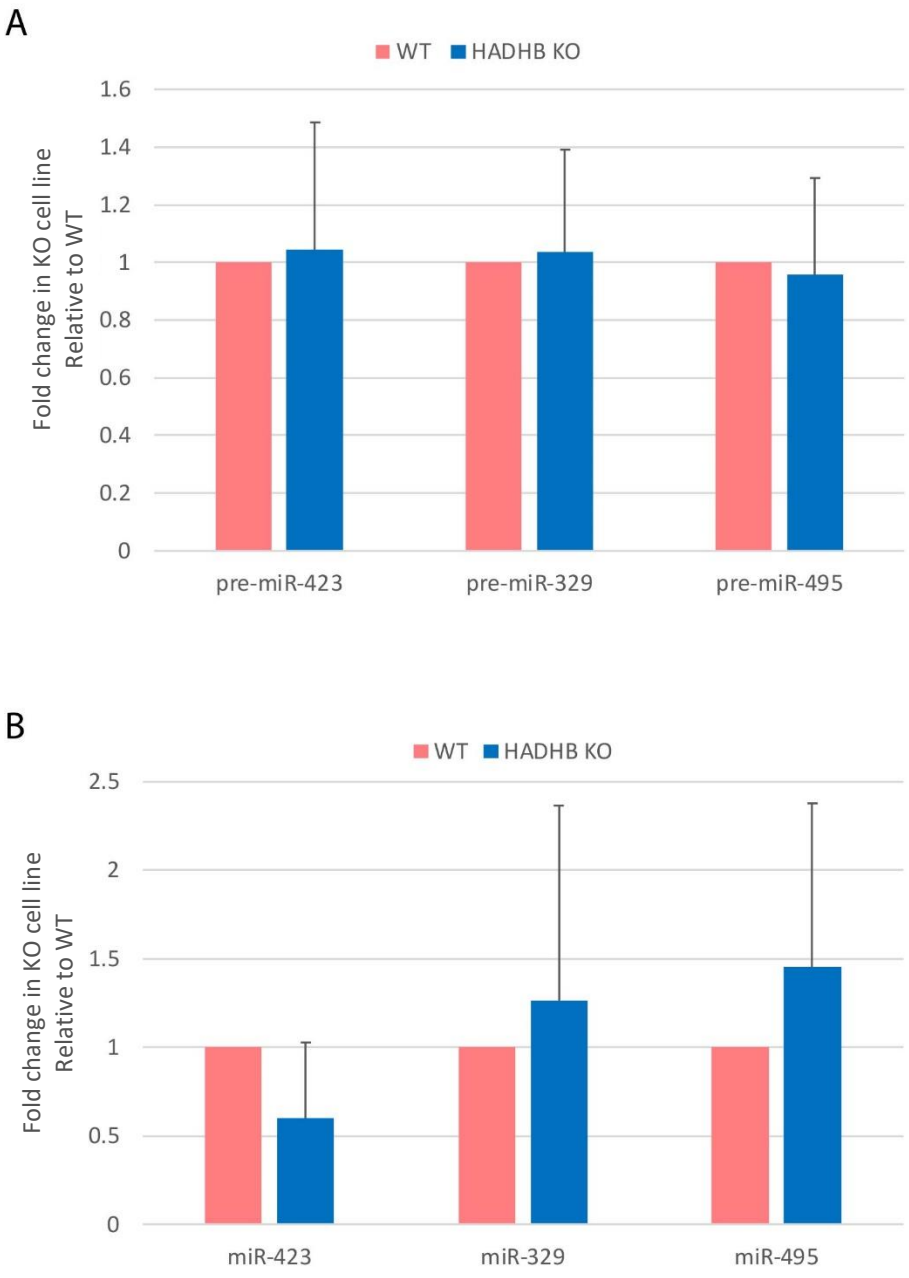

Figure 23 Levels of pre-miR-329 and pre-miR-495 in HADHB knockout clones*. Levels of pre-miR-329 and pre-miR-495 were measured in WT and KO cell lines in the two HADHB clones; AQ (A) and Z (B). All measurements were normalized against pre-miR-16 and pre-miR-423 was used as an external control. Statistical analysis using one-sample T-test showed no significant differences.*

Following these results, it was attempted to see whether the expression of mature miR-329 and miR-495 in HADHB KO cell lines could be restored upon the re-

expression of HADHB. For this, T7-tagged HADHB was transiently expressed in HADHB KO cells by transfection of an expression vector. Mature miRNA levels were measured 48 hours after transfection, however no effect on the levels of mature miR-329 and miR-495 was observed (Figure 24). Similarly, no effects were seen at 24 and 72 hours (Data not shown). It is possible that this time frame is not sufficient for recovery of HADHB activity and that longer expression times are needed for the rescue of mature miRNA levels. Other possibilities include that exogenous HADHB is not undergoing post-translational modifications necessary for it to carry out its RNA-binding activities or that it's localization within the cell is not reflecting that of the endogenous protein. To address this, the following steps would be to establish a stable re-integration of HADHB.

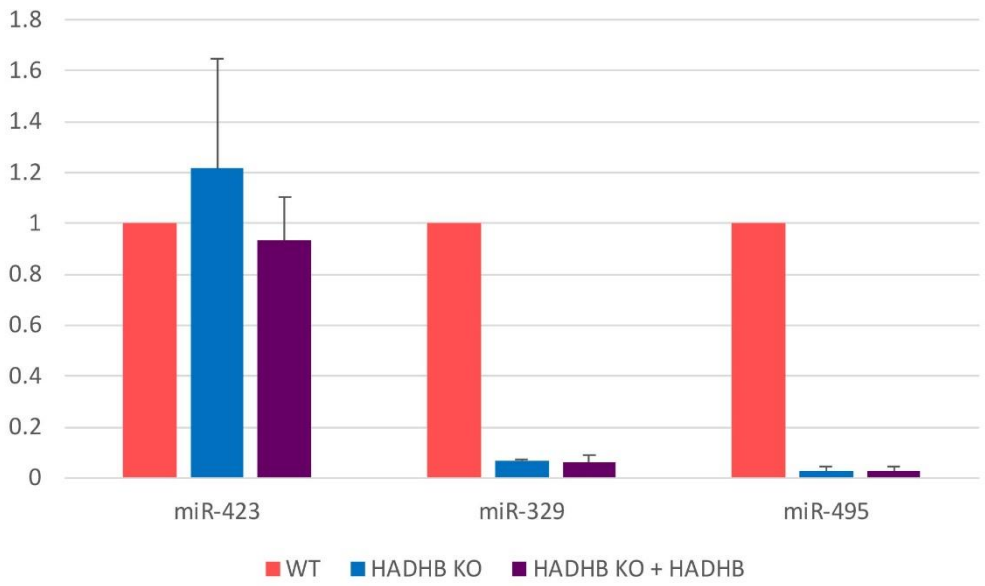

Figure 24 Mature miR-329 and miR-495 levels after re-expression of HADHB in KO cell lines. *HADHB was transiently expressed in HADHB KO cell lines. Mature miRNA levels were measured 48 hours after transfection and compared to the levels of WT and HADHB KO cell lines. All values are normalized to miR-16 and miR-423 was used as an external control.*

Discussion

Despite miRNAs of the 14q32 cluster being dysregulated in multiple pathologies, knowledge regarding post-transcriptional regulation of the cluster is lacking. Previous experiments identified the upregulation of over half the miRNAs in this cluster upon induction of hindlimb ischemia[251]. This upregulation occurred in three distinct temporal patterns that were independent of the position of the miRNAs within the cluster. The different changes in levels of individual miRNAs despite the transcription of the cluster as a single polycistronic unit suggested post-transcriptional regulation during the biogenesis of 14q32 miRNAs. Further analysis indicated the processing step from pre-miR to mature miRNA of selected miRNAs was likely be subjected to regulation by unknown factors.

Here, identification of these protein factors was sought through RP-SMS, focusing on the regulation of pre-miR-329 and pre-miR-495, precursors of two miRNAs from the 14q32 cluster that are important in the response to ischemia. In this study we used serum-starvation to identify factors binding to and regulating pre-miR-329 and pre-miR-495 processing in NIH-3T3 cells. Because *in vivo* ischemia is a much more complex process in the future it would be important to also study the effects of hypothermia and hypoxia in both this cell line and other cell types that are present in whole muscle tissue.

In the serum-starvation model used here, HADHB and CIRBP were identified as binding differentially to pre-miR-329 and pre-miR-495, with both proteins showing

increased binding to these pre-miRs upon serum starvation (Figure 12-13). Furthermore, deletion of HADHB in NIH-3T3 cells resulted in a reduction of over 80% in the levels of mature miR-329 and miR-495 but did not alter the levels of pre-miR-329 and pre-miR-495 (Figure 22-23). Taken together this suggests that these proteins have a role in regulating the processing of pre-miR-329 and pre-miR-495. A decrease in pre-miRNA processing often leads to accumulation of pre-miRNA as well as a reduction in mature miRNA levels, however this was not observed in this study. This could be due to rapid turnover of unprocessed pre-miRNA species, but further exploration of transcription and degradation rates would be necessary to corroborate this.

Although a strong reduction in miRNA levels was seen upon deletion of HADHB, overexpression of HADHB and CIRBP had no effect on mature miR-329 and miR-495. This could be due to various reasons. For example, it is possible that endogenous levels of these proteins are already sufficient for maximizing their interaction to pre-miR-329 and pre-miR-495 or that these proteins might require interaction with other protein factors that are limiting the upregulation of these miRNAs. Another possibility is that endogenous proteins undergo post-transcriptional modifications necessary for their binding to pre-miR-329 and pre-miR-495 that are lacking from overexpressed HADHB and CIRBP.

CIRBP and HADHB were part of a large group of proteins that were identified to bind differentially to these pre-miRs upon starvation (Figure 11), however they were the only proteins successfully validated in this study via RNA pulldown followed by

western Blot. This prompted them to be the focus of subsequent studies, but this does not invalidate the initial SILAC-mass spectrometry findings and the information obtained from this experiment can be used in the future as potential research avenues.

Importantly, both HADHB and CIRBP were shown to be expressed in adductor muscle *in vivo,* dispersed throughout the cell. Specifically, both proteins were present in cytoplasm, where Dicer cleaves pre-miRs into miRNA duplexes meaning that the spatial context of these proteins would permit them to bind to pre-miRs (Figure 14). Because immunohistochemistry was only carried out at one time point after ischemia it is not possible to ascertain whether these proteins showed a change in localization after ischemic induction, which would be interesting to explore further in the future.

Additionally, the mRNA levels of both *HADHB* and *CIRBP* show an increase upon induction of HLI which reaches a maximum at Day 3 (Figure 15). In the case of HADHB, the same was observed at the protein level (Figure 16). Again, this is temporally consistent with the largest increase in mature miR-329 levels and simultaneous decrease in pre-miR-329 and pre-miR-495 levels.

Understanding how the upregulation of these proteins is mediated in response of ischemia is of interest moving forward. Expression of CIRBP has previously been reported to increase in response to hypoxia[404], one of the major consequences of ischemia. Interestingly, this upregulation is independent of hypoxia inducible factor 1 (HIF1), the main regulator of the ischemic response[404,424]. Several mechanisms have been proposed to mediate increased CIRBP expression in response to stress,

including more efficient splicing of CIRBP pre-mRNA in response to mild hypothermia and changes in the abundance of three major CIRBP transcripts in response to temperature, each with different transcriptional start sites and varying 5' UTR lengths[406,407].

A further study identified an element in the CIRBP 5'UTR that functions as a mild-cold response element (MCER) and which can be bound by transcription factor Sp1, whose levels in the nucleus were increased at 32 °C compared to 37 °C[405]. Sp1 is a transcriptional factor that regulates the expression of thousands of genes. It is considered to be a basal transcriptional factor and is ubiquitously expressed[425]. However, interaction with a wide repertoire of transcriptional regulators as well as modulation by post-transcriptional modifications means that the activity of Sp1 can be altered in response to various cellular contexts[425,426]. Sp1 has been shown to be upregulated in response to ischemia[427] and the activation of various genes under conditions of serum-starvation and hypoxia has been shown to be dependent on Sp1[428–433]. Interestingly, HADHB is also under the transcriptional control of Sp1[398]. Taken together, it's tempting to speculate a potential role of Sp1 in mediating the increase of CIRBP and HADHB levels in response to hypoxia and in the future, this would be interesting to explore further.

Apart from the increase in protein levels, cytoplasmic translocation of CIRBP and HADHB is likely to be an important factor in them binding pre-miR-329 and pre-miR-495, as it is in the cytoplasm where Dicer mediates the processing of pre-miRs into miRNA duplexes. HADHB is a mitochondrial protein, where it carries out its

canonical role in fatty-acid oxidation. However, both here and in other studies presence of HADHB in the cytoplasm has been reported[375,401]; the mechanisms regulating HADHB localization are unknown and would be interesting to study moving forward. CIRBP is considered a nuclear protein under normal conditions, but has been shown to translocate to cytoplasm upon a variety of stresses[408,415,434]. Nuclear export is dependent on methylation of arginine residues in the RGG domain of CIRBP, which seem to be dependent on protein arginine methyl-transferase 1 (PRMT1)[408,435]. Interestingly, PRMT1 levels have been shown to increase upon the induction of ischemia[436]. In the future it would be interesting to explore the effects of PRMT inhibitors on the localization of CIRBP, and whether this has a subsequent effect on levels of 14q32 miRNAs.

Methylation is not the only post-translational modification known to affect the activity of CIRBP, phosphorylation of the RGG domain by Glycogen synthase kinase 3 β (GSK3β) is able to increase the RNA-binding activity of CIRBP twofold[410]. Activity of GSK3β can vary in response to hypoxia, with both inhibition and activation being observed in different cell types[437–439]. The activation of GSK3β presents another possible factor affecting the regulation of CIRBP in ischemia and understanding its potential effects could open up various potential therapeutic targets in the future.

CIRBP had an evolutionarily conserved homolog, RNA-binding motif protein 3 (RBM3)[440]. Like CIRBP, RBM3 is upregulated in response to a variety of stresses and is involved in the stabilization and increased translation of mRNAs in multiple cellular pathways. Whilst both proteins are widely expressed their localization can vary with

differences at tissue and cell-type level as well as subcellular localization. For example, in testis CIRBP is predominantly expressed in germ cells whilst RBM3 is found in Sertoli cells and whilst under normal conditions both proteins show a mostly nuclear localization RBM3 shows enhanced cytoplasmic presence in the brain whilst CIRBP shows greater cytoplasmic localization in spermatids[440]. Information on how upregulation of RBM3 is achieved is lacking in comparison to CIRBP.

Interestingly, RBM3 has been associated with regulation of miRNA biogenesis[313,441]. In one study, miRNA arrays showed that 60% of miRNAs detectable in a neural cell line were downregulated upon knockdown of RBM3 whilst there were no changes in pri-miR levels, indicating the involvement of RBM3 in post-transcriptional regulation of miRNA biogenesis. RBM3 was found to associate with pre-miRs and promote their processing by dicer[313]. Considering their homology, this suggests CIRBP could be playing an equivalent role. In this study miR-329 and miR-495 were not amongst the RBM3-upregulated miRNAs, this could be due to the subtle differences in RBM3 and CIRBP structure or more likely because of the difference in cell type and cellular context. It would be interesting to further explore the relationship between CIRBP and RBM3 regulation of miRNA biogenesis, whether they share miRNA targets and whether they indeed employ the same mechanism. A second study found an opposite effect of RBM3 levels where RBM3 knockdown increased the levels of miR-142 and miR-143. These miRNAs are upregulated in fever-like temperatures (40 °C) were their expression shows opposite patterns to RBM3 levels[441]. This shows that RBM3 has the potential to decrease miRNA levels, and it would be of interest to explore the possibility of negative regulation on miRNA levels by CIRBP.

HADHB is one of two subunits that form the mitochondrial trifunctional protein, responsible for the oxidation of fatty acids, the other subunit being HADHA. Interestingly, HADHA was identified in a study as interacting partner of Dicer[442]. In the study, immunoprecipitations were carried out to identify novel Dicer interacting partners, and along with TRBP and PACT, HADHA was pulled down. Furthermore, over-expression of HADHA resulted in lower levels of specific pre-miRNAs ,including pre-miR-126, accompanied by an increase in mature miR-126. Knockdown experiments with HADHA specific siRNAs showed the opposite effect; higher levels of pre-miR-126 and a 50% reduction in miR-126 levels[442]. These results suggest that the association of HADHA with Dicer enhances processing of specific pre-miR to mature miRNAs. This increase in pre-miR to mature processing is equivalent to the role proposed for HADHB in this study. HADHA has not been found to associate with RNA, and no mechanism has been proposed for its role in regulating miRNA biogenesis. Being interacting partners, it is likely that HADHB would be able to bind Dicer-associated HADHA. This would provide a mechanism in which the interaction of HADHB and HADHA brings pre-miRs into proximity with Dicer, potentially enhancing their processing. It is something that should be explored further, and it would be helpful to understand whether silencing of HADHA abolishes the regulatory effects of HADHB on miRNA biogenesis and vice versa.

Another potential path for exploring the role of HADHB in miRNA regulation is the effects of its inhibitor, trimetazidine. Trimetazidine, an anti-anginal drug with cardioprotective effects during ischemia, and an inhibitor of HADHB[443,444]. The mechanism behind its cardioprotective functions was first suggested to be a

metabolic shift from fatty-acid oxidation to glucose oxidation[443,445], however this has been disputed with a study finding it had no effect on the turnover of specific substrates or inhibition of β-fatty acid oxidation[446]. Additionally, new side effects have recently been reported[445]. Because of controversial results on the effect of trimetazidine on HADHB function, exploring the effect of trimetazidine on miRNA biogenesis would be an interesting avenue to explore and could even lend insight into potential side effects of the drug.

While in this study CIRBP and HADHB were identified binding to pre-miR-329 and pre-miR-495, their roles in the regulation of miRNA biogenesis are likely to extend to other miRNAs both part of the 14q32 cluster and outside of it. It is important to understand how far reaching the regulatory roles of CIRBP and HADHB are; small RNA sequencing of KO and WT cell lines would be a key step in identifying the extent of their effects on miRNA levels and would be a good next step moving forward. Several miRNAs outside of the 14q32 cluster are responsive to hypoxic/ischemic conditions, including miR-21, miR-210, miR-424, miR-100, miR-15/16 and miR-132/212[447–449]. Additionally, various miRNAs including some hypoxic-responsive miRNAs have shown anti-angiogenic effects, these include miR-15/16, miR-21, miR-100, miR-34a, miR-124, miR-29, miR-206, miR-26 and members of the miR-17~92a cluster[447,448,450]. There is likely to be several mechanisms regulating the changes in expression of these miRNAs, but it is possible that some of them are dependent either on CIRBP or HADHB.

Beyond this, it is possible that CIRBP and HADHB can influence miRNA levels in other cellular contexts. Whilst changes in expression or localization of HADHB in response to external stimuli aren't well documented, it is known that CIRBP is responsive to a variety of cellular stresses and analysing how these changes reflect in miRNA profiles is an interesting avenue to explore. Recently, CIRBP has begun to emerge as a potential oncogene[451,452]. It was found overexpressed in several human tumours, including 33% of colon tumours and 45% of breast tumours[452]. CIRBP can influence multiple aspects of cancer, leading to increased proliferation, decreased apoptosis, avoidance of senescence, downregulation of p53 and upregulation of telomerase activity. It is a potential marker for poor prognosis in adenomas and its downregulation enhances chemeosensitivity[451]. Whilst it is believed that many of these effects are governed through CIRBP targeting cancer-associated mRNAs the possibility of CIRBP-dependent dysregulation of miRNA levels could also be at play, considering that dysregulation of miRNAs in cancer is common. This is an interesting scenario in which to explore the role of CIRBP in miRNA biogenesis.

The identification of CIRBP and HADHB in this study is an important first step in understanding the regulation of 14q32 miRNAs in the response to ischemia. The experimental evidence strongly suggests that these proteins are playing a key role in the processing of pre-miR-329 and pre-miR-495 into mature miR-329 and mature miR-495. Considering the importance of these miRNAs in the ischemic response, understanding their regulation could allow to better influence their levels following ischemia and improving therapeutic effects on neovascularization. However, it is possible that the roles of CIRBP and HADHB in regulating miRNA biogenesis extend

beyond both this cluster and particular cellular context. It is exciting to explore the full extent of their regulatory potential on miRNA biogenesis. Accompanying this, it is of great importance moving forward to elucidate the mechanisms through which these proteins are exerting their effects on miRNA processing, and how these are related to those already described.

Lin28a regulation of miRNAs during neurogenesis

The regulation of let-7 by Lin28a is the best studied example of post-transcriptional regulation of miRNAs. Let-7 was one of the first miRNAs described, initially identified in a screen for heterochronic genes in *C. elegans* where it was found expressed in late larval and adult stages, but not early larval stages[187]. It was then shown to be highly conserved across animal species, conserving its temporal expression pattern[9]. Various miRNAs containing the same let-7 seed sequence are often present in a genome and are referred to as the let-7 family of miRNAs. To distinguish between members of the family a letter and/or number is used. Letters indicate differences in the mature miRNA sequence, outside of the seed, whereas numbers indicate identical mature miRNA sequences originating from different sites in the genome. In mouse and human 9 mature let-7 sequences originating from 12 transcripts are found; let-7-a1, -a2, -a3 (human), -b, -c(1), -c2 (mouse), -d, -e, f1, -f2, -g, -i and miR-98[453].

Let-7 has important conserved roles in development. In *C. elegans* it is necessary for transition from the last larval stage into the adult stage and it is similarly important in the juvenile-to-adult transition in Drosophila[8,454]. In Dgcr8 deficient mouse ES cells, let-7 was able to supress self-renewal by repressing pluripotency factors including *Lin28, Sall4 and N-Myc*[104]. Let-7 was also found to be a barrier in reprogramming of induced pluripotent stem cells (iPSC). A key factor in this impediment was let-7 repression of LIN41/TRIM71 which in turn regulates a broad range of differentiation factors[455]. Let-7 also has specific roles in neurogenesis, promoting neural stem cell

proliferation and differentiation through repression of TLX1, an orphan nuclear receptor that is essential in regulating neural stem cell self-renewal[456,457]. Additionally, let-7 targets IGF2-mRNA binding protein 1 (IMP1), a protein widespread in fetal tissues, but not adult tissues, which can bind to mRNAs of various self-renewal genes leading to their increased expression. Repression of IMP1 by let-7 promotes a developmental switch from highly proliferative neural stem cells to more quiescent adult stem cells[458].

Mature let-7 is absent in mouse and human embryonic stem cells but increases in expression upon differentiation. In contrast, pri-let-7 levels are present in similar amounts in undifferentiated and differentiated cells, indicating let-7 is under negative post-transcriptional regulation in undifferentiated cells[320,321,459]. The protein responsible for inhibiting let-7 processing in undifferentiated cells is pluripotency factor Lin28[100–103]. Lin28 was first characterized in *C. elegans* as an important regulator of developmental timing. It is composed of two RNA-binding domains; a cold-shock domain and a pair of CCHC-type zinc fingers[460]. Lin28 is conserved in mammals where two homologs of Lin28, Lin28a and Lin28b are present[324]. It is abundant in embryonic tissues, embryonic cell lines and human and mouse ES cells after which it is progressively lost during differentiation[461–463]. Furthermore, Lin28a was one of four factors sufficient for reprogramming of induced pluripotent stem cells, along with Oct4, Sox2 and Nanog[322].

Lin28a has let-7 independent roles, regulating translation of a specific subset of mRNAs through binding to conserved motifs and structures in their 3' UTR[464–466].

However, the pluripotency effects of Lin28 are mostly mediated through inhibition of let-7 maturation in undifferentiated cells. As differentiation progresses, Lin28 levels decrease allowing de-repression of let-7[323]. Additionally, both Lin28a and Lin28b are targets of let-7, generating a double-negative feedback loop that functions as a developmental switch[102]. Let-7 has been identified as a tumour suppressor, downregulated in various types of cancer[318,467–470]. Several important oncogenes including *RAS, C-MYC* and *HMGA2* are targets of let-7[268,317–319,471]. In accordance, Lin28a and Lin28b have both been identified as oncogenes, overexpressed in ~15% of primary tumours and cancer cell lines[472]. Expression of both Lin28a/b is activated by binding of oncogene c-Myc and leads to repression of let-7[132,472,473].

Lin28b and Lin28a employ different mechanisms of regulation of let-7 (Figure 7). Lin28a is mainly localized to the cytoplasm, where its main mechanism of inhibition involves it binding to the GGAG motif present in the pre-let-7 CTL[327]. This binding leads to the subsequent recruitment of a terminal uridylyl-transferase (TUT), either TUT4 or TUT7, which catalyses the addition of a poly(U) tail to the 3' of pre-let-7[327,474,475]. This uridylation impedes Dicer cleavage as well as mark pre-let-7 for degradation by 3'-5' exonuclease Dis-3l2[327,329,330]. Additionally, reports suggest Lin28a binding can directly block let-7 processing by Drosha[100,101] and Dicer[102,326]. In contrast, Lin28b functions predominantly in the nucleus, where it binds to pri-let-7 and blocks microprocessor cleavage in a TUT4/7 independent manner[476].

In vivo and *in vitro* studies have found that in addition to pre-let-7, Lin28 can bind to various pre-miRs with a conserved binding motif[464,465,477,478]. However, binding to a

conserved GGAG motif is not sufficient for Lin28a mediated uridylation, as this is dependent on the structure and sequence context surrounding the motif[327,331]. Importantly, it was previously shown in our group that in the case of miR-9, despite a lack of uridylation Lin28a was able to regulate its biogenesis in a uridylation-independent manner[383].

Mir-9 is an evolutionarily conserved miRNA[479]. Studies of miRNA expression profiles have identified it as a brain-enriched miRNA[16,459,480]. MiR-9 has important roles in neural differentiation[481–485]. Like let-7, miR-9 targets TLX inhibiting self-renewal of neural progenitors and promoting differentiation. In turn, TLX represses miR-9 expression, forming a double negative feedback loop[483]. Expression of miR-9 and brain-enriched miR-124 in cultured neural progenitors drive neurogenesis whilst preventing gliogenesis[481]. Additionally, generation of miR-9 deficient mice showed that it orchestrates neurogenesis in the telencephalon by targeting multiple genes involved in neural progenitor proliferation and differentiation[482]. Furthermore, the importance of miR-9 and miR-124 in neural fate determination is illustrated by their ability to transform adult fibroblasts into neurons[484].

MiR-9 is under transcriptional regulation of REST and CREB transcription factors. REST inhibits the expression of miR-9 in undifferentiated cells, whilst dismissal of REST and activation of CREB trigger transcription of miR-9 during differentiation[485]. Previous studies in our group found an expected increase in both pri-miR-9 and mature miR-9 levels during neural differentiation of P19 cells. However, the increase in pri-miR-9 levels was much higher than that of mature miR-9, suggesting that transcriptional

regulation of miR-9 was accompanied by post-transcriptional regulation[383]. Using RP-SMS, Lin28a was identified as binding the miR-9 CTL in undifferentiated cells. Additionally, siRNA mediated depletion of Lin28a led to an increase in miR-9 levels. Importantly, constitutive expression of Lin28a in P19 cells subject to retinoic acid (RA) induced neural differentiation led to a significant reduction in levels of let-7 and miR-9 in late stages of differentiation. However, when GFP-tagged Lin28a was constitutively expressed in the same setting, let-7 levels showed a 4-fold reduction, but miR-9 levels remained unchanged. This indicates these miRNAs are regulated through different mechanisms. Indeed, further *in vitro* processing and uridylation assays showed Lin28a destabilizes miR-9 in a uridylation-independent manner[383].

To better understand these distinct mechanisms of regulation, in this study binding of Lin28a to let-7 and miR-9 was explored in further detail. The inability of GFP-tagged Lin28a to regulate miR-9 processing suggests that different domains of the protein could be involved in binding and it was important to elucidate if this was the case. Furthermore, Lin28a regulation of miR-9 processing by a novel mechanism poses the question of how extensive the role of Lin28a in miRNA biogenesis is. Therefore, the effects of constitutive expression of Lin28a in global miRNA levels were explored.

Differential binding of Lin28 truncated mutant to pre-let-7a-1 and pre-miRNA-9

Structure probing experiments with lead ions and T1 and V1 ribonucleases, carried out in our group, identified different Lin28a binding motifs in pre-let-7a-1 and pre-miR-9 (Figure 25). Lin28a footprinting showed binding to pre-let-7a-1 around well-known AGGG and GGAG motifs, which are known to interact with Lin28 CSD and zinc fingers respectively[326,486–488]. Interestingly, despite possessing a GGAG motif, Lin28a footprinting indicated that the interaction with pre-miR-9 mostly occurred at the GU-rich region in the CTL.

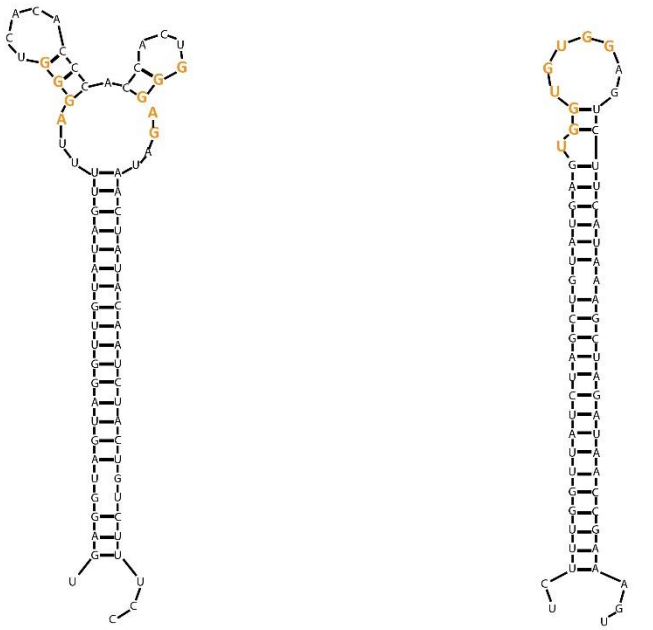

Data from Jakub Nowak

Figure 25 Structure and Lin28a binding motifs of pre-let-7a-1 and pre-miR-9. *Schematic representation of pre-let-7a-1 and pre-miR-9. Lin28a binding motifs identified by footprinting analyisis are marked in bold orange letters.*

In an effort to better understand whether the same Lin28a domains were responsible for both of these interactions, truncated T7-tagged Lin28a constructs with different

configurations of the CSD and zinc fingers were generated for use in RNA pulldown assays (Figure 26). Truncated Lin28a proteins were expressed in HeLa cells.

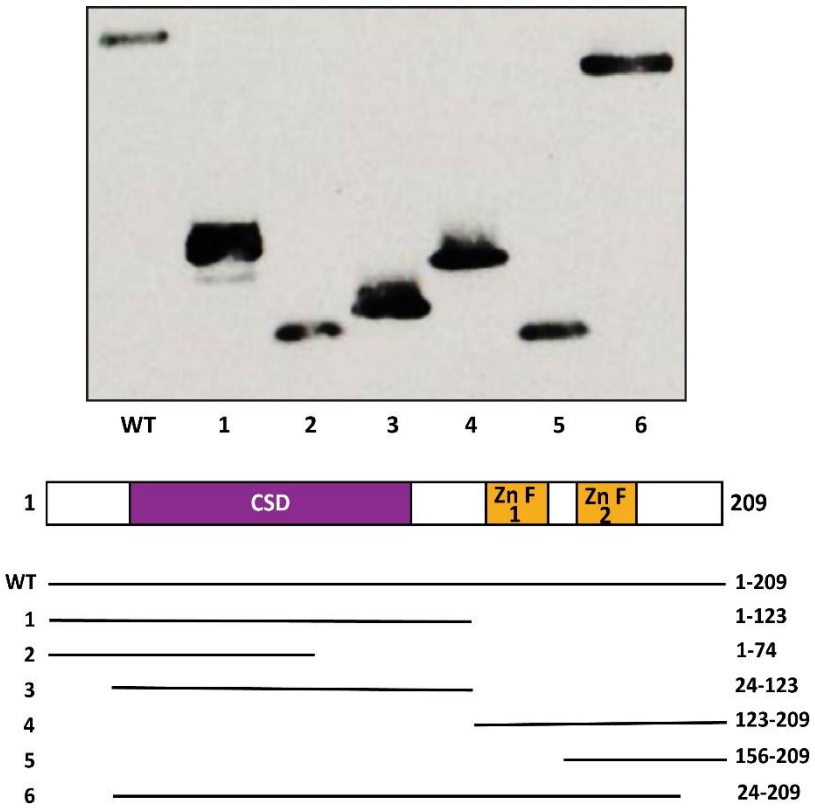

Figure 26 Expression of Lin28a truncations. Western blot showing the expression of T7-tagged Lin28a in HeLa cells. Lane labelled WT represents T7-tagged full length Lin28a. Lanes labelled 1-6 represent Lin28a truncations. These numbers correspond to those in the left of the bottom panel. The bottom panel illustrates the domains contained by individual Lin28a truncations as well as the amino acids encompassed, as indicated to the right of the panel. CSD= cold-shock domain, ZnF= zinc finger domain.

RNA pulldown assays were carried out by incubating beads coupled with either pre-let-7a-1 or pre-miR-9 with total protein extracts from HeLa cells overexpressing each of the Lin28a truncation (Figure 27). Both pre-let-7a-1 and pre-miR-9 were able to pull down full length Lin28a as well as Lin28a with truncated C and N termini but containing both the CSD and the zinc fingers (24-190). This was expected as both pre-

miRs have previously been shown to bind Lin28a. Pre-miR-9 however, was able to pull down Lin28a truncations encompassing the CSD much more efficiently than pre-let-7a-1 (Figure 27). In particular, pre-miR-9 was able to pull down the truncation composed of amino acids 24-123 with a higher efficiency than the full-length protein, 72% of input vs 52% of input. In contrast, pre-let-7a-1 entirely failed to pull down the same fragment. Additionally, pre-let-7a-1 pulled down Lin28a zinc fingers (123-209) twice as efficiently as pre-miR-9. This is consistent with the Lin28a footprint observed in structure probing experiments as the zinc finger domain has been implicated in binding to the GGAG motif[486–488]. Lin28a truncations containing partial CSD (1-74) and a single zinc finger (156-209) also showed slightly stronger binding to pre-miR-9. Taken together these results support the idea that pre-let-7a-1 and pre-miR-9 interact with different Lin28a domains, with the zinc finger domain playing an essential role in pre-let-7a-1 binding whilst both the CSD and zinc finger domain show involvement in pre-miR-9 binding.

Additional experiments in our group confirmed the GGAG motif was not important in Lin28a binding to pre-miR-9. Replacing the GGAG motif with UUUU resulted in a reduction of Lin28a binding to pre-let-7a-1, however this had no effect in Lin28a binding to pre-miR-9. Again, this is consistent with the previous results showing a larger importance of the zinc finger domain in binding to pre-let-7a-1, as this domain is associated with binding to the GGAG motif.

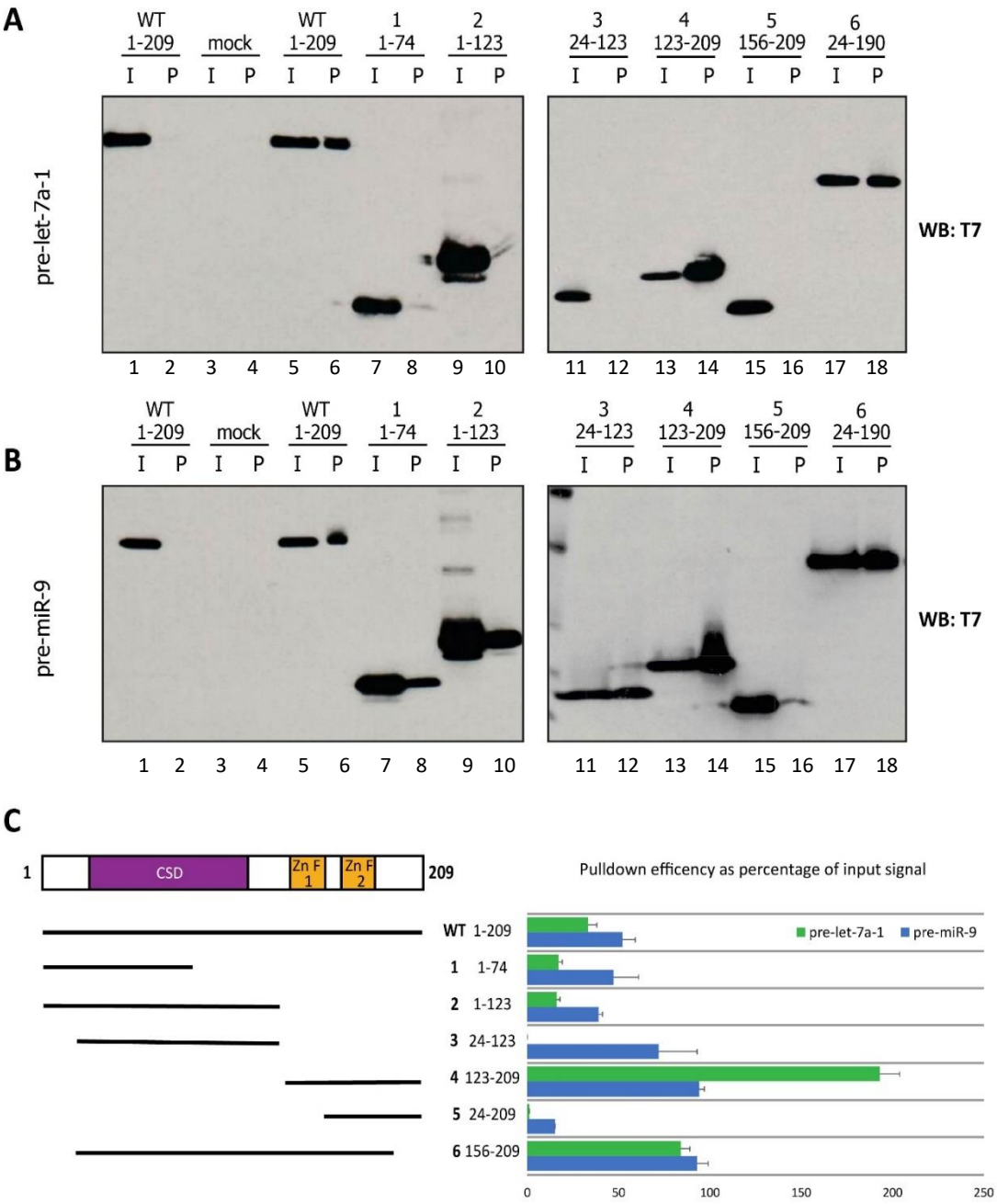

Figure 27 Differential binding of pre-let-7a-1 and pre-miR-9 to Lin28a truncations. *RNA pulldown assays carried out with beads coupled to pre-let-7a-1 (A) or pre-miR-9 (B). These beads were incubated with HeLa extracts overexpressing the respective Lin28a truncation, as indicated in the upper section of the panels with the numbers referring to the amino-acids present in that truncation (lanes 5-18). Above the lanes (I) indicates input (odd lanes) and (P) indicates pulldown (even lanes). Lanes 1-2 correspond to a beads-only control (no RNA), whilst lanes 3-4 marked as mock contained beads but no protein extract. (C) Quantification of Lin28a binding in RNA pulldown assays. Values are presented as percentage of input signal detected in the pulldown fraction and represent three independent experiments. The corresponding truncations and the domains they encompass are referenced in the schematic on the left of the panel.*

Changes in expression of other miRNAs upon constitutive expression of Lin28

Regulation of miR-9 by Lin28a during neuronal differentiation shows that its effects on neurogenesis are not limited to inhibiting processing of let-7 miRNAs. Lin28a has been shown to bind other pre-miRs[296,464,465,477,478], but the full extent of its regulatory role in miRNA biogenesis during neural differentiation is not known. To determine which other miRNAs are under control of Lin28a, small RNA sequencing was performed on undifferentiated (day 0) and differentiated (day 9) P19 cells. Control P19 cells were compared to cells constitutively expressing both GFP-tagged Lin28a and untagged Lin28a. The levels of mature miRNAs in differentiated and undifferentiated cells was determined and presented as a Day9/Day0 ratio. These ratios were then compared between FRT-P19 and GFP-P19 control cell lines and untagged and GFP-tagged Lin28a expressing cell lines (Figure 28).

The levels of many miRNAs were affected upon expression of untagged Lin28a; however, this was not the case for GFP-tagged Lin28a whose overexpression had a more modest effect which was restricted to a smaller number of miRNAs. This exclusive regulation by untagged but not GFP-tagged Lin28a is equivalent to what is observed for pre-miR-9. Importantly, small RNA seq data showed the expected reduction of let-7 levels upon constitutive expression of both untagged and GFP-tagged Lin28a relative to control cell lines, meanwhile reduction in miR-9 levels occurred upon induction of untagged but not GFP-tagged Lin28a. This is consistent

with all experiments up to this point and validates the data obtained from small RNA seq.

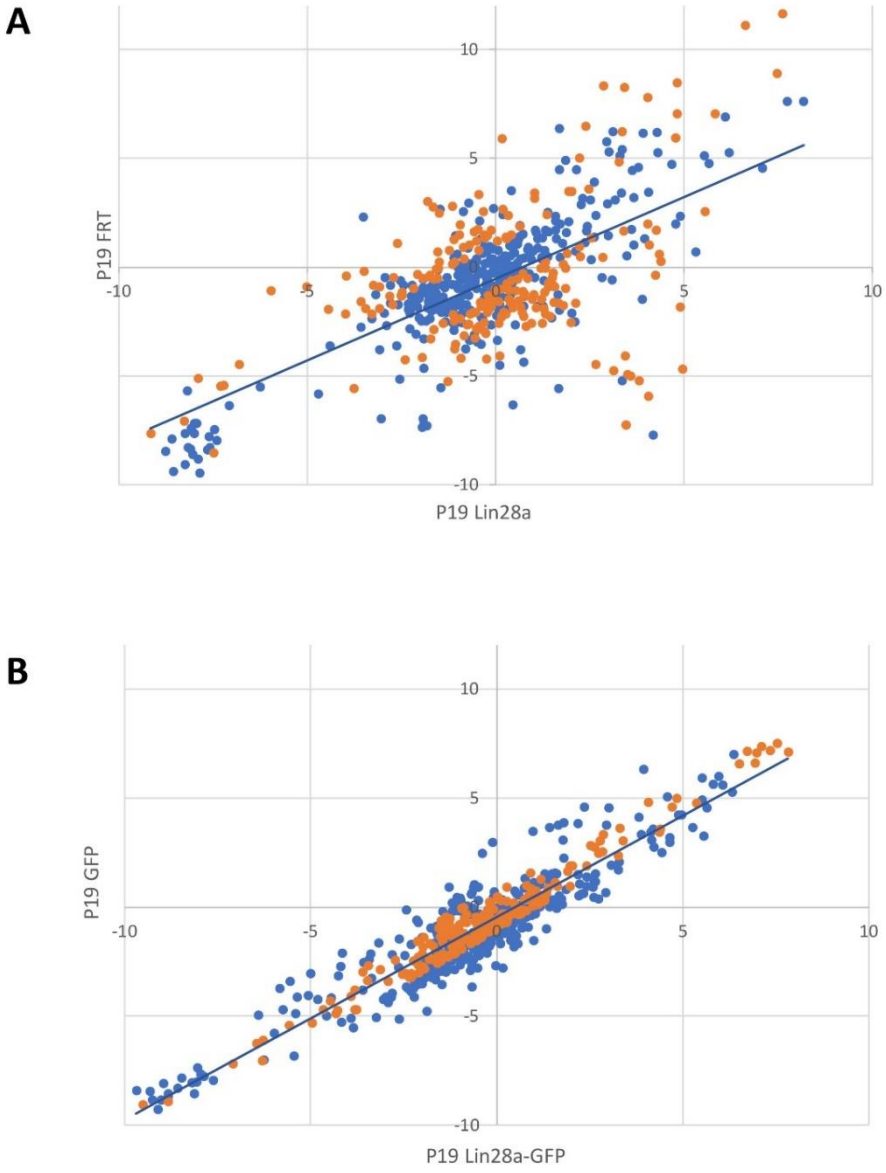

Data from Jakub Nowak

Figure 28 Lin28a regulates numerous miRNAs during neuronal differentiation. *miRNA levels in undifferentiated cells (Day 0) and differentiated cells (Day 9) were obtained by small RNA sequencing. Scatterplots represent the ratio (log2) of individual miRNA levels in Day 9 vs Day 0 for cells that constitutively express untagged Lin28a (A) or GFP-tagged Lin28a (B) compared to the same ratios in respective control cell lines. Data points in orange represent miRNAs which showed a difference in Day9/Day0 ratios between control and untagged-Lin28a greater than two-fold, but which were not affected by the expression of GFP-Lin28a.*

Positive regulation of miRNA levels by Lin28a

Surprisingly, small RNA seq data revealed that many miRNAs are positively regulated by Lin28a. Constitutive expression of untagged Lin28a resulted in higher levels of various miRNAs in differentiated cells compared to control P19 cell lines. Expression of GFP-tagged Lin28a left the levels of the same miRNAs unchanged. In order to validate these results, two upregulated miRNAs, miR-182 and miR-541 were selected. Small RNA-seq data showed that in control P19 cells, levels of these miRNAs decrease upon neural differentiation, however upon constitutive expression of untagged Lin28a this decrease was no longer seen with miR-541 and miR-182 levels maintained throughout differentiation(Figure 29). Expression of GFP-tagged Lin28a did not have the same effect. These results were validated by qRT-PCR (Figure 29). Importantly, RNA pulldown assays showed that both miRNAs could pull down Lin28a when incubated with Day 0 extracts (Figure 30). In contrast, pre-miR-16 could not pull down Lin28a, demonstrating that the interaction is specific.

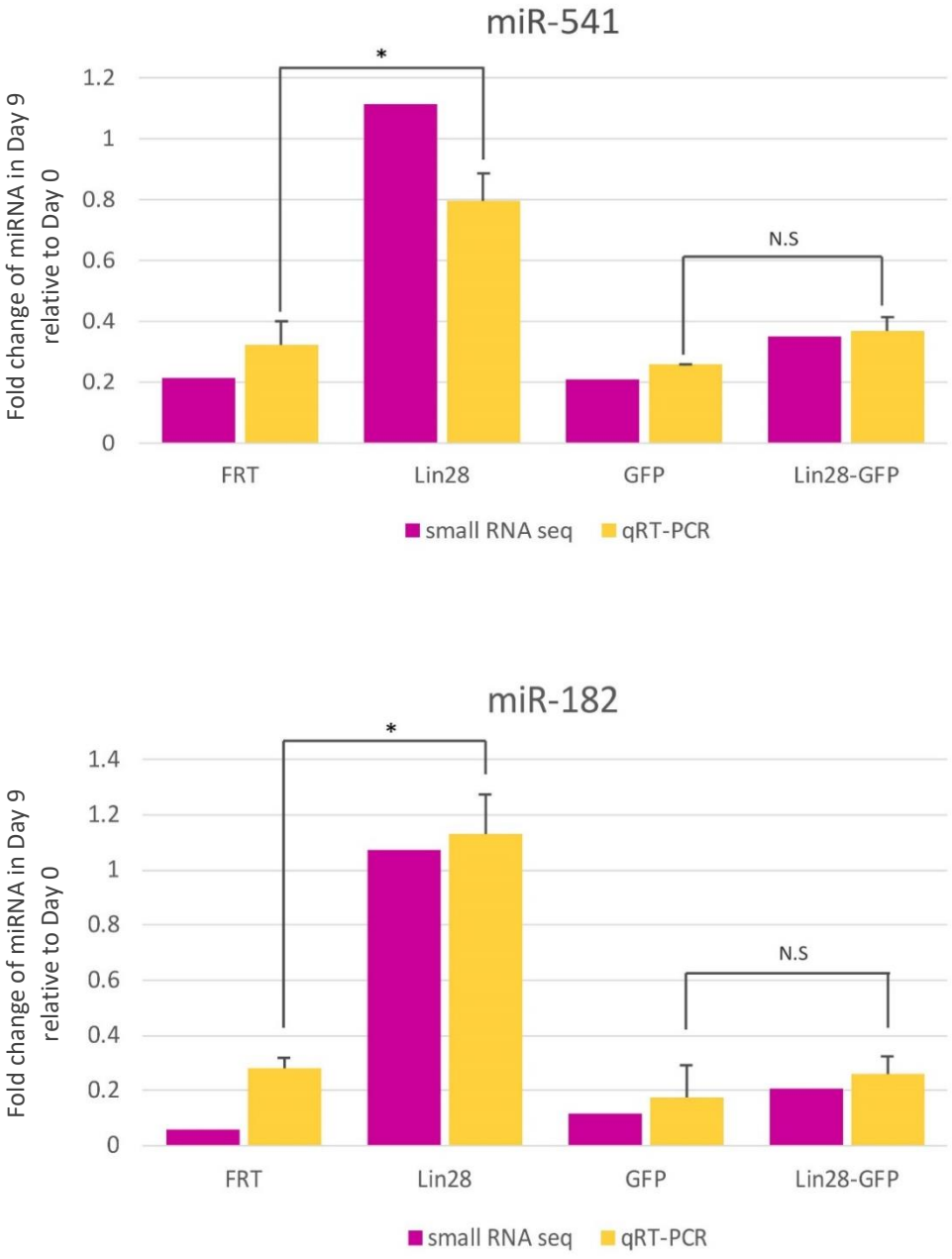

Figure 29 Upregulation of miR-541 and miR-182 by Lin28a. *qRT-PCR validation of small RNA seq data showing upregulation of miR-541 and miR-128 by untagged Lin28a but not GFP-tagged Lin28a. Values represent three independent experiments. Student's T-test was performed to determine statistical significance where *=p<0.05.*

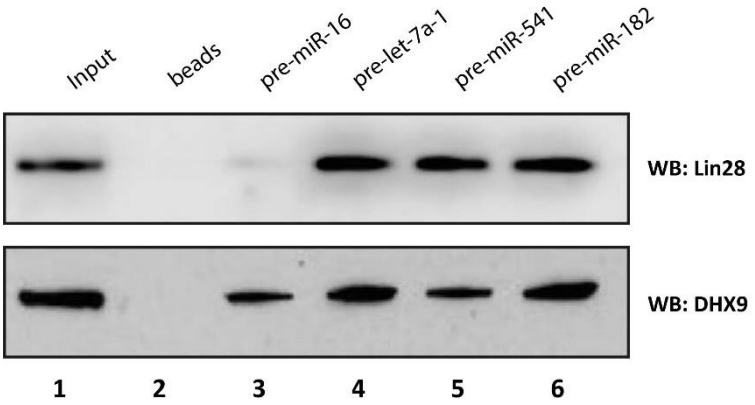

Figure 30 RNA pulldown showing Lin28a binding to miR-541 and miR-182. Western blot showing RNA pulldown assays carried out with beads coupled to pre-miR-541 or pre-miR-182 as indicated above the lanes. Additionally, beads coupled to pre-let-7a-1 were used as a positive control and pre-miR-16 coupled beads function as a negative control. Beads were incubated with undifferentiated (Day 0) P19 cell extracts. Lane 1 shows the input and lane 2 contains the uncoupled beads control. DHX9 blotting served as a positive binding control.

Regulation of 14q32 miRNAs by Lin28a during neural differentiation

One of the Lin28a upregulated miRNAs selected, miR-541, is part of cluster 14q32, previously shown to be subject to post-transcriptional regulation in this study. Whilst previous studies established a role for the 14q32 cluster during ischemia, this cluster also has important functions in neural differentiation with miRNAs in this cluster being enriched in the brain[243,489,490]. MiRNAs in this cluster vary in their temporal expression patterns in the brain; for instance, whilst miR-369 and miR-496 and miR-543 are abundant in both neural progenitors and neurons, miR-134 is poorly expressed in neural progenitors and is upregulated upon differentiation[243,247,248]. Within the cluster, miR-134 has the best studied roles in neurogenesis, playing an essential role in the regulation of dendritic outgrowth[243,247,491]. However other

miRNAs in the cluster have also been shown to be important in driving neural differentiation, including miR-369, miR-496, miR-543 and miR-376a[245,489]. MiR-541, shown here to be positively regulated by Lin28a, was shown to inhibit differentiation and neurite outgrowth through the targeting of Synapsin-I in a model of rat PC12 cells[492]. However, the mechanism of this regulation remains unknown.

Because of the roles of miRNA cluster 14q32 in neural development, as well as evidence of its post-transcriptional regulation and of upregulation of miR-541 by Lin28a, it was of interest to see if constitutive overexpression of Lin28a impacted other members of the cluster. For this, small RNA seq data for members of the cluster was analysed to obtain the ratio of these miRNAs in undifferentiated (Day 0) and differentiated cells (Day 9). These ratios were then compared between control cells and cells expressing constitutive untagged Lin28a (Figure 31).

Most miRNAs in the 14q32 cluster showed downregulation upon differentiation in control FRT P19 cells, with levels showing a greater than two-fold reduction from Day 0 to Day 9. However, some individual members showed little change or even a slight increase in their levels at Day 9 of differentiation with miR-496a being the only miRNA that exhibited a greater than two-fold increase upon differentiation. This is consistent with previous reports that show differences in the temporal expression of these miRNAs during neural development[248]. Interestingly, constitutive overexpression of Lin28a had a varied impact on 14q32 miRNAs. Three of the miRNAs were considered to be downregulated by Lin28a, meaning that the change in miRNA levels from day 0 to day 9 is at least twice as high in control cells compared to Lin28a expressing cells.

Half of the miRNAs in the cluster did not show any changes between cell lines, suggesting they are not subject to any regulation by Lin28a. Twenty-two miRNAs in the 14q32 cluster showed upregulation by Lin28a. The majority of these miRNAs showed a strong reduction in their levels upon differentiation in control FRT cells, however in Lin28a expressing cells their levels remain constant throughout differentiation.

However, miR-770 and miR-1180 showed constant levels in control cell lines but strong upregulation in Lin28a cells. Furthermore, miR-493 levels decreased by 75% in FRT cells, whilst in Lin28a cells they increased greater than two-fold.

Taken together, this indicates that Lin28a expression has a mostly positive effect in the levels of 14q32 miRNAs. Whilst further studies are needed to determine whether the effect observed is a product of direct or indirect regulation by Lin28a, it is known that this cluster is transcribed as a single polycistronic cluster and therefore the discrepancy in levels of individual miRNAs is due to post-transcriptional regulation.

miRNA	P19 FRT Day9/Day0 Fold change	Lin28a Day9/Day0 Fold change	Lin28 Fold change/ FRT Fold change
mir-496a	**2.473**	0.764	0.309
mir-381	1.337	**0.460**	0.344
mir-487b	1.931	0.807	0.418
mir-376a	1.147	0.582	0.508
mir-431	0.983	**0.500**	0.508
mir-341	1.125	0.581	0.517
mir-758	**0.229**	**0.129**	0.563
mir-323	0.536	**0.304**	0.566
mir-369	0.847	0.521	0.615
mir-380	1.287	0.899	0.699
mir-410	0.866	0.605	0.699
mir-136	0.713	0.536	0.753
mir-154	**0.179**	**0.136**	0.757
mir-376c	**0.388**	**0.319**	0.822
mir-1197	0.575	**0.490**	0.852
mir-376b	**0.229**	**0.205**	0.897
mir-412	1.433	1.308	0.913
mir-495	**0.388**	**0.377**	0.971
mir-370	1.085	1.060	0.977
mir-434	0.696	0.842	1.210
mir-382	1.013	1.263	1.247
mir-539	**0.408**	0.518	1.268
mir-300	1.088	1.466	1.347
mir-668	1.280	1.929	1.507
mir-667	0.551	0.995	1.808
mir-433	0.583	1.067	1.831
mir-377	0.538	1.049	1.948
mir-127	0.529	1.073	2.029
mir-770	1.177	**2.488**	2.114
mir-337	**0.371**	0.809	2.178
mir-665	**0.214**	**0.482**	2.249
mir-666	0.809	1.857	2.294
mir-411	**0.394**	0.936	2.372
mir-1193	**0.334**	0.797	2.382
mir-409	**0.218**	0.538	2.473
mir-485	**0.254**	0.629	2.476
mir-1188	1.664	**4.326**	2.599
mir-543	**0.177**	0.508	2.864
mir-494	**0.162**	**0.467**	2.890
mir-299a	**0.270**	0.867	3.215
mir-3072	**0.262**	0.874	3.329
mir-134	**0.234**	0.849	3.623
mir-379	**0.252**	1.053	4.176
mir-673	**0.340**	1.510	4.440
mir-540	**0.307**	1.412	4.601
mir-329	**0.213**	1.013	4.754
mir-541	**0.216**	1.113	5.166
mir-485	**0.161**	0.920	5.724
mir-493	**0.286**	**2.395**	8.374

Figure 31 Lin28a regulation of 14q32 miRNA cluster. Ratio of miRNA levels at Day 9 vs Day 0 of differentiation determined by small RNA seq. The first column represents the fold change in control FRT P19 cells whilst the second column shows the fold change in P19 cells constitutively expressing Lin28a. Red cells indicate an increase in miRNA levels from Day 0 to Day 9 whilst blue cells indicate a decrease in levels. Numbers in bold represent a change of at least 2-fold. The third column shows the fold difference in the Day 9/Day 0 ratios of miRNA levels in control and Lin28a expressing cell lines. Yellow cells indicate a difference greater than 2-fold in the ratios of control and Lin28a cell lines.

Discussion

Lin28a is well-known to regulate let-7 miRNAs during neurogenesis, in a uridylation dependent mechanism[101,472,478]. Whilst this mechanism is essential in the maintenance of ES cells, the roles of Lin28a in development are not limited to its regulation of let-7. Lin28a has been shown to directly bind mRNAs in ES cells enhancing the translation of genes involved in proliferation, survival and splicing[464,493,494].

Previously our group showed Lin28a to regulate brain-enriched miR-9 in a uridylation-independent manner[383]. Mir-9 also has important functions in regulating neural differentiation[481,483,484]. Interestingly, constitutively expressed GFP-tagged Lin28a could repress let-7 biogenesis but had no effect on miR-9 levels, suggesting involvement of different Lin28a domains in binding and regulating both miRNAs[383].

Here, Lin28a truncations with different domain configurations were generated to further study the involvement of the CSD and the zinc finger domain in binding these miRNA precursors. RNA pulldown assays with pre-let-7 and pre-miR-9 coupled to agarose beads showed differences in their binding to Lin28a domains. Pre-miR-9 bound to the Lin28a's CSD with much higher affinity than pre-let-7, whereas pre-let-7 pulled down the zinc finger domain twice as effectively as pre-miR-9 (Figure 27). These results were supported by further experiments showing the GGAG motif in the miR-9 CTL was not involved in Lin28a binding since the GGAG motif in the let-7 CTL has associates with the Lin28a zinc finger domain[486–488]. While GGAG is a preferred

Lin28a binding motif, previous work in our group has shown that a pre-let-7 mutant with a minimal CTL containing the GGAG motif could not bind Lin28a demonstrating that the structural context is important for this interaction[331]. This could explain why even though the GGAG motif is present in the miR-9 CTL, it is not involved in Lin28a binding.

Binding of Lin28a to the CTL of let-7 leads to the recruitment of TUT4/7 resulting in uridylation of its 3' end (Figure 7). This uridylation ultimately marks pre-let-7 for degradation by Dis3l2 exonuclease[329,330]. Previously, it was shown by our group that Lin28a regulates pre-miR-9 in a uridylation independent manner[383]. However, further experiments have shown that Dis3l2 is also involved in the regulation of miR-9, with *in vitro* studies showing it was capable of degrading miR-9. Furthermore, Dis3l2 knockdown resulted in an increase of miR-9 levels. This differs to let-7 where knockdown of Dis3l2 results in an increase in pre-let-7 but does not affect mature let-7 levels as Lin28a interaction can also directly block Dicer processing[478]. Again, this reveals differences in the mechanisms of regulation of Lin28a, showing it has a more robust control on let-7 levels. Further studies are necessary to fully elucidate the relationship between pre-miR-9, Lin28a and Dis3l2. Lin28a and Dis3l2 do not appear to interact in an RNA-independent manner[329]. In the case of pre-let-7, Lin28a mediated uridylation leads to recognition by Dis3l2 as this exonuclease favours uridylated substrates[495]. However, since regulation of miR-9 biogenesis is uridylation-independent it is unclear how Lin28a binding can affect pre-miR-9 degradation by Dis3l2.

Aside from further defining the details of miR-9 regulation by Lin28a, this study showed that constitutive expression of untagged Lin28a impacts the levels of many additional miRNAs during neural differentiation of P19 cells (Figure 28). Like miR-9 however, the levels of many of these miRNAs were not altered upon expression of GFP-tagged Lin28a, showing that interaction through the CSD could be important in their regulation. Additionally, unlike let-7 and miR-9 which are repressed by Lin28a, many miRNAs showed an increase in their levels in differentiated cells upon constitutive expression of untagged Lin28a. This suggest that Lin28a is carrying out a positive regulatory role. The levels of two Lin28a up-regulated miRNAs, miR-541 and miR-182 were validated through qRT-PCR (Figure 29). Additionally, RNA pulldown assays showed that these miRNAs interact with Lin28a. Whilst this suggests that at least some of the upregulated miRNAs could be directly regulated by Lin28a, the change in the levels of some miRNAs upon expression of Lin28a in differentiated cells could be a product of indirect regulation.

Lin28a is a pluripotency factor, quickly lost after the onset of differentiation. P19 cells are pluripotent embryonic carcinoma cells that constitutively express Lin28a, therefore overexpression of Lin28a should not affect their genetic programming. However, upon differentiation with RA forced expression of Lin28a could affect their differentiating potential, resulting in a state that is not fully differentiated which contributes to the alteration of miRNA levels with respect to wildtype P19 cells. Whilst the RA-mediated differentiation method used in this study does result in the formation of embryonic bodies at day 4 and subsequently cells with neuron-like morphology at day 9 in both wildtype and Lin28a overexpressing cells, differences

were observed. Specifically, the size of embryonic bodies of Lin28a but not Lin28a-GFP expressing cells were consistently found to be smaller[383].

Going forward it would be important to differentiate between direct regulation by Lin28a and changes brought about indirectly. Determining whether these miRNAs are able to interact with Lin28a through the use of RNA pulldown assays or RNA-immunoprecipitation would be useful in making this differentiation. Additionally, it would be informative to determine whether the addition of Lin28a to *in vitro* processing reactions with upregulated and downregulated pri-miRNAs, is sufficient to produce a positive or negative effect respectively on their processing

Additionally, it is of great interest to elucidate the mechanisms behind positive regulation by Lin28a, including the structural and sequence requirements of regulated miRNAs, the effect of Lin28a binding on pre-miR stability and the interacting partners of Lin28a. These are all intriguing questions that provide future research avenues.

Mir-541 is one of the miRNAs upregulated by Lin28a. It has been shown to be important in the differentiation of PC12 cells, through targeting of Synapsin-I[492]. PC12 cells are derived from a rat adrenal tumour and easily differentiate into neuron-like cells upon treatment with nerve growth factor (NGF). Treatment with NGF resulted in a reduction of miR-541 which led to decreased Synapsin-I levels and increased differentiation. MiR-451 forms part of the 14q32 cluster of miRNAs, a brain-enriched cluster that has been shown to be involved in various processes during neurogenesis[248].

In general, the cluster appeared to be downregulated upon differentiation (Figure 31). Because the cluster is transcribed as a single polycistronic unit, this could be an effect of transcriptional rather than post-transcriptional regulation. However, constitutive expression of Lin28a had different effects on individual members of the cluster. Approximately half of the miRNAs in the cluster showed increased levels in Lin28a expressing cells and three miRNAs in the cluster were negatively regulated by Lin28a with the rest of the members showing no effect.

Similarly, to what was previously observed after induction of HLI, this pattern of regulation was unrelated to the miRNAs position within the cluster (Figure 32). In the

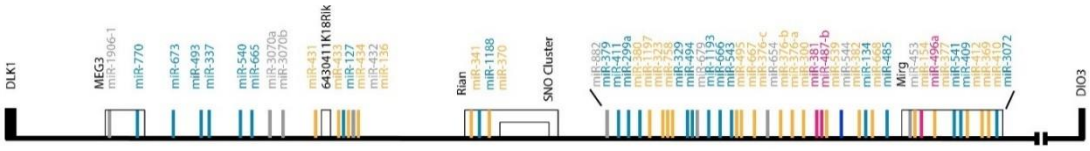

Figure 32 Lin28a regulation of 14q32 miRNAs is independent of their position within the cluster. *Schematic representation of 14q32 cluster colour coded by Lin28a regulation of individual miRNAs. Blue miRNAs are upregulated by Lin28a, red miRNAs are downregulated by Lin28a, and yellow miRNAs are unaffected. No data was available for miRNAs in grey.*

future it would be interesting to explore the sequence and structural motifs defining the effect of Lin28a on individual members of the cluster. The widespread effects of Lin28a expression on the levels of numerous miRNAs belonging to a cluster involved in neurogenesis pathways supports the idea that the roles of Lin28a in neural development are widespread and not yet fully understood.

Lin28a affected miRNAs are likely to be subject to additional levels of regulation. Previous studies showed that replacing the terminal loop of let-7 with the miR-16 terminal loop was sufficient to abolish Lin28a interaction and resulted in de-

repression of let-7. However, when the same experiments were conducted with miR-9, substitution of the terminal loop eliminated Lin28a binding but did not de-repress miR-9 processing[383]. This suggests that other factors are controlling the repression of mature miR-9. In a similar way, despite showing that Lin28a upregulates miR-541, knockdown of Lin28a did not repress miR-541 meaning it is likely other factors could be ensuring its processing. Because miRNA levels need to be carefully controlled during development, cells are likely to employ multiple regulatory mechanism to ensure correct temporal expression of miRNAs. Both upregulation and downregulation of miRNA levels can have significant developmental effects, for example both low and high levels of miR-134 during neurogenesis can compromise proper dendritic outgrowth[243]. Lin28a is unlikely to be the only factor controlling the regulation of the miRNAs affected by its constitutive expression. However, it is clear that Lin28a exerts important regulatory functions during neural differentiation and does so through various mechanisms. Elucidating the full details of these mechanisms is important in understanding the complex miRNA regulatory networks controlling neurogenesis.

Oleic acid regulation of miRNA biogenesis by inhibition of RNA binding activity of RBPs

As our knowledge of RBPs involved in miRNA biogenesis expands, we have also begun to better understand how RBP:miRNA interactions are modulated in a physiological context, allowing miRNA expression patterns to adapt according to the cellular environment. The RNA-binding activities of RBP proteins are often modulated via their interactions with proteins in cellular signalling pathways; examples of this are seen in miRNA biogenesis regulation in the inhibition of p72 binding to pri-miRs by YAP in the Hippo signalling pathway or contrarily by SMAD signalling proteins increasing the binding of p68 to pri-miRs[290,291]. But as the repertoire of known RBP grows, new mechanisms regulating their binding to RNA also emerge. This is seen with the increasingly growing group of metabolic enzymes that moonlight as RBPs; the RNA binding activity of these proteins is frequently regulated by the cellular metabolites that function as their substrates and co-factors[352,354].

Recently, Clingman *et al.* showed that Oleic Acid (OA) was able to inhibit the RNA binding of RNA-binding protein Musashi homolog 1 (MSI1)[382]. OA is a naturally occurring 18 carbon mono-unsaturated fatty acid with a *cis* double bond in the ω-9 position (Figure 33). It is the most common monounsaturated fatty acid in plants and animals, with a normal physiological serum concentration in humans ranging in the high µM to low mM range[496,497]. OA was identified in a screen of over 30,000 components as a specific inhibitor of MSI1, an RBP involved in neurogenesis. This

inhibition was mediated through binding of OA to the first of two RNA-recognition motifs (RRM)[382].

RRM domains are comprised of approximately 90 amino-acids and contain two consensus sequences termed RNP1 and RNP2 of eight and six conserved residues respectively. The RRM folds into a compact globular domain consisting of a β-sheet made up of four antiparallel β strands flanked on one side by two α-helixes. Conserved residues responsible for interaction with RNA are found on the β-sheet[498]. Clingman *et al.*[382] propose that OA binds in a hydrophobic cavity found in the surface of the MSI1 RRM1 α-helixes, opposite the RNA-binding surface. This binding then allosterically induces a conformational change that results in the inhibition of RNA binding by MSI1[382].

The inhibitory potential of OA was shared with other unsaturated fatty acids of 18-22 carbons in length which shared the ω-9 *cis* double bond; however, elaidic acid (EA), the *trans*-isoform of OA with similar molecular properties was unable to inhibit MSI1 RNA binding[382] .

MSI2 is a homologous protein to MSI1; they share 75% amino acid identity and are expressed in partially overlapping patterns[499]. RNA-binding inhibition by ω-9 fatty acids was conserved for MSI2[382]. It was previously shown in our group that MSI2 together with HuR, post-transcriptionally regulates the biogenesis of brain-enriched miR-7[296]. HuR is a ubiquitously expressed member of the Hu protein family, whose members possess three RRM motifs. HuR plays a role in stabilizing mRNA by binding to AU-rich elements (AREs)[500].

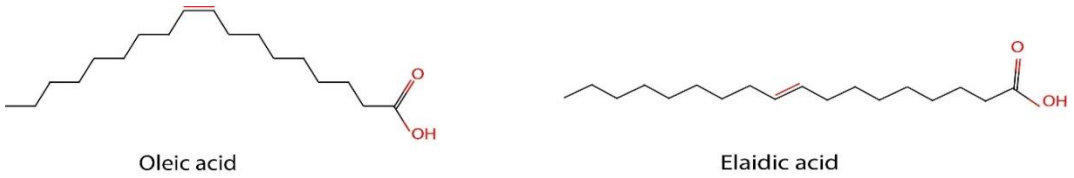

Figure 33 Structure of Oleic and Elaidic acid. Representation of the Structure of Oleic acid (OA) and Elaidic acid (EA). EA is a trans-isomer of OA, both are mono-unsaturated 18-carbon fatty acids with an ω-9 double bond.

MiR-7 is a known tumour suppressor, that targets oncogenic signalling proteins involved in diverse processes including cell cycle, proliferation and metastasis[501]. It directly regulates the epithelial growth factor receptor (EGFR) as well as upstream regulators of the Akt pathway, both of which are hyperactive in glioblastomas and are associated with aggressive phenotypes; in accordance miR-7 appears downregulated in glioblastoma[297]. MiR-7 has also been found to be downregulated in patients with Parkinson's disease (PD) as well as in PD animal models[180]. A role for miR-7 in PD has been attributed to its regulation of the *SNCA* gene which encodes α-SYN, a key protein in PD pathogenesis whose overexpression is deleterious to dopaminergic neurons[180,502].

MiR-7 resides in intron 15 of the hnRNP K mRNA and whilst this transcript is expressed ubiquitously, miR-7 is expressed predominantly in neural and pancreatic tissues[16,503]. Conversely, MSI2 is expressed across most tissues but is not found in the brain and is almost undetectable in the liver[296]. HuR mediates the recruitment of MSI2 to the CTL of pri-miR-7, where this complex increases the rigidity of the stem-loop structure which in turn inhibits microprocessor cleavage[296]. Given the inhibitory effect of OA on MSI2 RNA-binding, it was of interest to explore if it could disrupt the

binding of the HuR/MSI2 complex to the CTL of pri-miR-7, thereby allowing its processing (Figure 34).

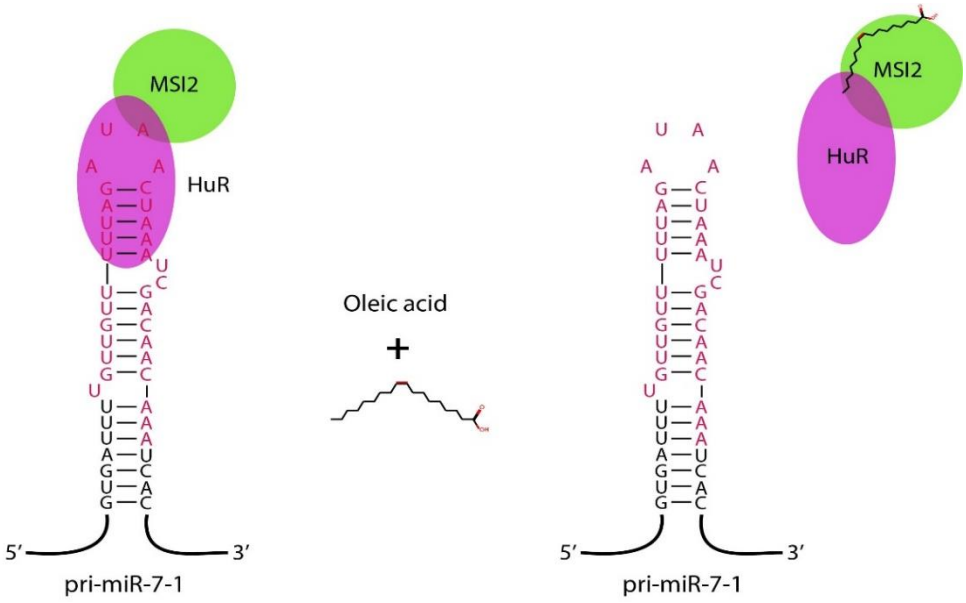

Figure 34 Regulation of pri-miR-7-1 processing by HuR and MSI2 and its inhibition by Oleic acid. *HuR and MSI2 form a complex that binds to pri-miR-7-1 CTL (in red) inhibiting its processing by the microprocessor. If oleic acid binding directly to MSI2 can displace the HuR/MSI2 complex from the pri-miR-7-1 CTL, this would in turn allow microprocessor processing.*

Inhibition of pre-miR-7/protein complexes by Oleic and Elaidic acid

As a first step in exploring the inhibition by OA of MSI2/HuR RNA-binding, an electrophoretic mobility shift assay (EMSA) was performed, incubating radiolabelled pre-miR-7 with HeLa whole cell extracts and increasing concentrations of OA. The same assay was carried out with EA, the *trans*-isoform of OA, which previously had been reported to be unable to inhibit MSI2 RNA-binding. Incubating pre-miR-7 with HeLa extracts in the absence of OA, resulted in a shift of the free RNA, indicating the formation of pre-miR-7,protein complexes. Upon addition of increasing concentrations of OA there was a corresponding decrease in the signal intensity of

the shifted complexes (Figure 35). This result suggests that OA is inhibiting the binding of proteins to pre-miR-7.

Contrary to what had been previously observed, increasing concentrations of EA had a similar effect on the signal intensity of the shifted free RNA, indicating a similar inhibition to that of OA. When densitometry analysis was performed on the EMSA results, the inhibitory effect of EA on complex formation was shown to be relatively weaker to that of OA at similar concentrations with a significantly lower signal in OA treated cells at concentrations of 500µM (Figure 36).

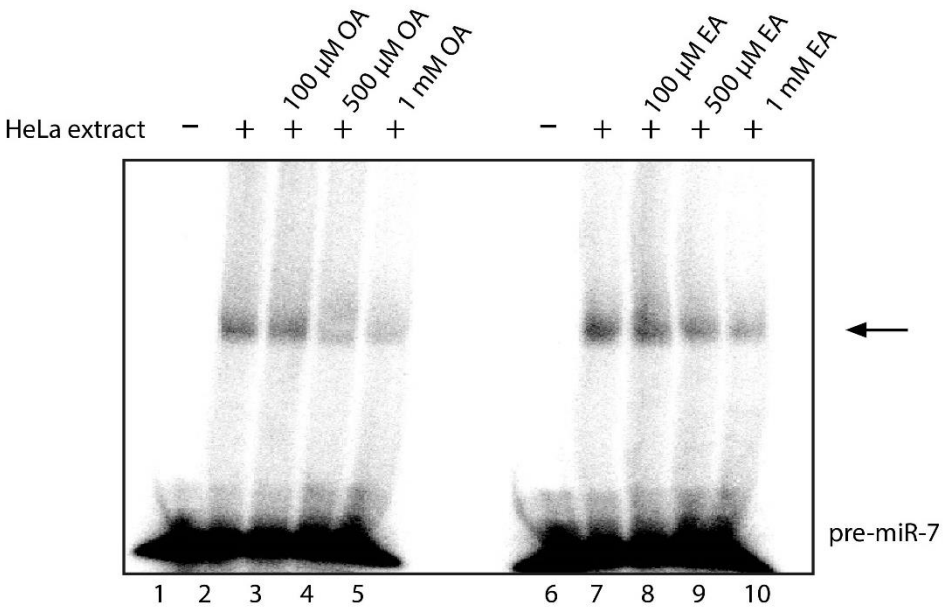

Figure 35 Inhibition of pre-miR-7/protein complexes by oleic and elaidic acid. EMSA was carried out with radiolabelled pre-miR-7 incubated with HeLa cell extracts and increasing concentrations of oleic acid (lanes 1-5) or elaidic acid (6-10). Lanes 1 and 6 represent controls incubated without cell extracts. Lanes 2 and 7 represent extracts incubated only with HeLa extracts but not OA/EA. The arrow highlights the shifted pre-miR-7/protein complexes.

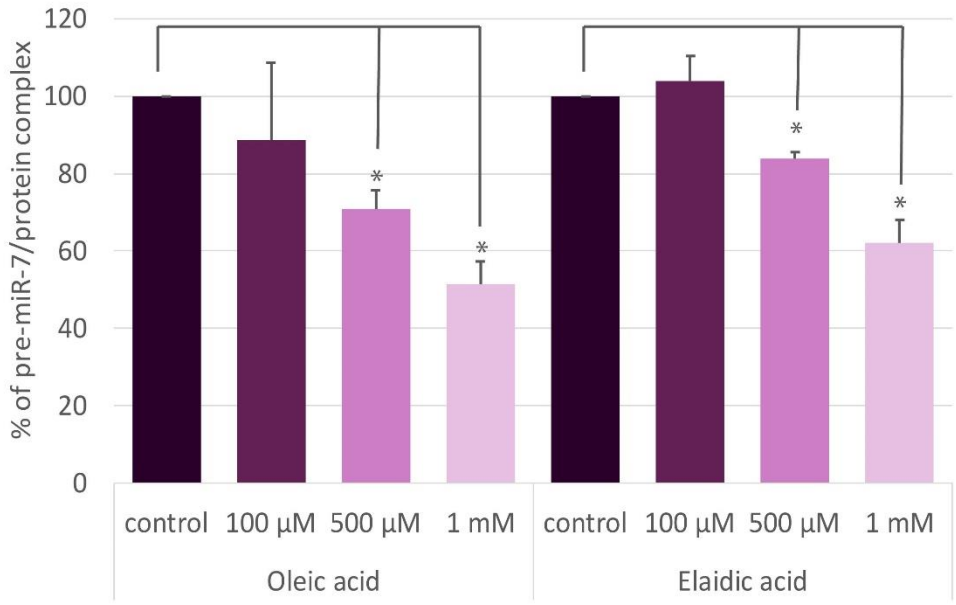

Figure 36. Quantification of pre-miR-7/protein complexes. *Densitometry analysis of EMSA. Controls represent the signal intensity of shifted pre-miR-7/protein complexes in the absence of fatty acids. Quantification of the signal of shifted pre-miR-7/protein complexes after treatment with oleic and elaidic acid is presented as a percentage relative to controls. These results represent three separate experiments. Students t-test was used to calculate significance with *=p<0.05*

Oleic and Elaidic acid inhibition of additional pri-miR/protein complexes

Additional EMSA experiments were carried out incubating HeLa extracts with three different radiolabelled pre-miRs, pre-let-7, pre-miR-16 and pre-miR-495, to determine whether the inhibitory effects of OA and EA treatment was specific to protein/RNA complexes with pre-miR-7. Incubation of all three pre-miRs with HeLa extracts produced a strong shifted signal, indicating the formation of pre-miR/protein complexes (Figure 37). Importantly, no reduction in the formation of pre-let-7/protein complexes was observed upon treatment with either OA or EA, whilst the signal for the shifted pre-miR-16/protein complexes was reduced at the high

concentrations of both OA and EA (Figure 37-38). This indicates some level of *in vitro* specificity, for the inhibitory actions of OA and EA.

In the assays carried out with pre-miR-495, a miRNA belonging to polycistronic miRNA cluster 14q32, a concentration dependent reduction in shifted complexes was observed upon treatment with OA (Figure 37 C). Although a slight reduction was also observed in samples incubated with EA, this was much smaller and remained constant for all concentrations of EA. This could suggest that these fatty acids are displacing a different set of proteins in the pre-miR-495/protein complexes (Figure 38 C).

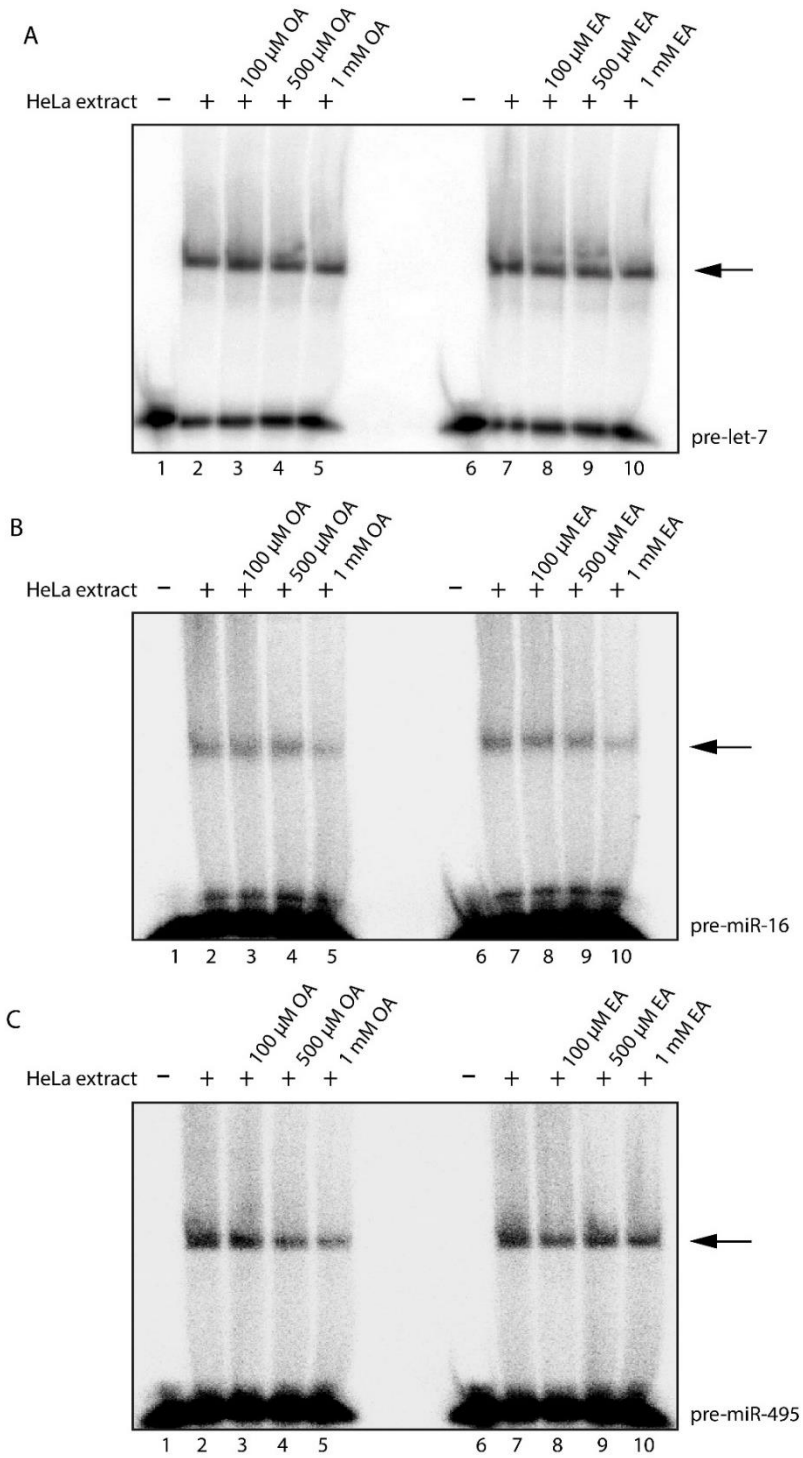

Figure 37 Inhibition of additional pre-miR/protein complexes by oleic and elaidic acid. EMSA with radiolabelled pre-let-7 (A), pre-miR-16 (B) and pre-miR-495 (C) incubated with HeLa extracts and increasing concentrations of OA (1-5) or EA (2-10). Lanes 1 and 6 are control EMSA with no protein extract. Lanes 2 and 6 are incubated with HeLa extract but no fatty acid. Images are representative of 3 experiments. Arrows highlight shifter pre-miR/protein complexes.

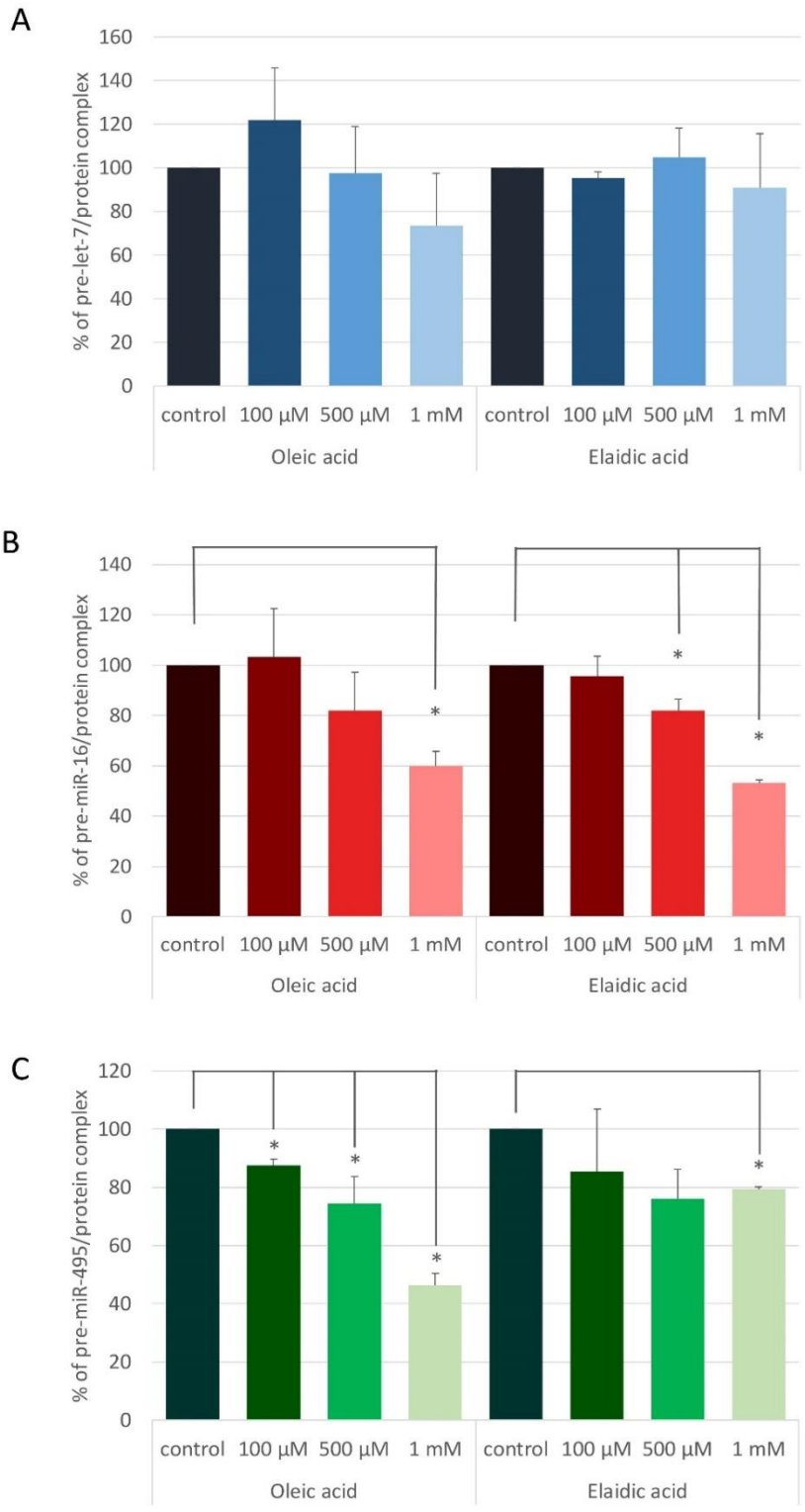

Figure 38 Quantification of pre-miR/protein complexes. *Densitometry analysis of EMSA with radiolabelled pre-let-7 (A), pre-miR-16 (B) and pre-miR-495 (C). Controls represent the signal intensity of shifted pre-miR/protein complexes in the absence of fatty acids. Quantification of the signal of shifted pre-miR/protein complexes after treatment with oleic and elaidic acid is presented as a percentage relative to controls. These results represent three separate experiments. Students t-test was used to calculate statistical significance with *=p<0.05*

Validation of specific RNA-binding proteins in pre-miR-7/protein complexes

Following the EMSA results, identification of HuR and MSI2 in the shifted pre-miR-7/protein complexes was sought. To do this, a modified EMSA assay termed western blot-combined EMSA (WEMSA) was performed. In this approach, EMSA assay were carried out incubating non-radiolabelled pre-miR-7 with HeLa whole cell extracts and increasing concentrations of OA or EA. Following separation of RNA complexes, the gel was then transferred onto a nitrocellulose membrane and probed with antibodies specific to selected proteins. The WEMSA showed a strong signal for HuR in the shifted band, positively identifying it as a component of the pre-miR-7 complexes. HuR signal decreased upon treatment with OA in a concentration dependent manner. Comparatively, treatment with EA showed a much smaller reduction in signal intensity of HuR in the protein/pri-miR-7 complexes (Figure 39 A). This discrepancy confirmed some degree of specificity in the RNA-binding inhibitory activity of fatty acids *in vitro.* Unfortunately, blotting against MSI2 produced a signal that was too low for detection and analysis.

Additionally, WEMSA was used to probe for DExD/H-box helicase DHX9. DHX9 is an NTP-dependent helicase with functions in multiple aspects of RNA biology, including miRNA biogenesis. Aside from its core helicase domain, DHX9 contains two double-stranded RNA binding domains (dsRBD) at its N-terminal[504]. OA and EA also resulted in a decrease in DHX9 present in the complexes, but did so to a smaller extent (Figure 39 B).

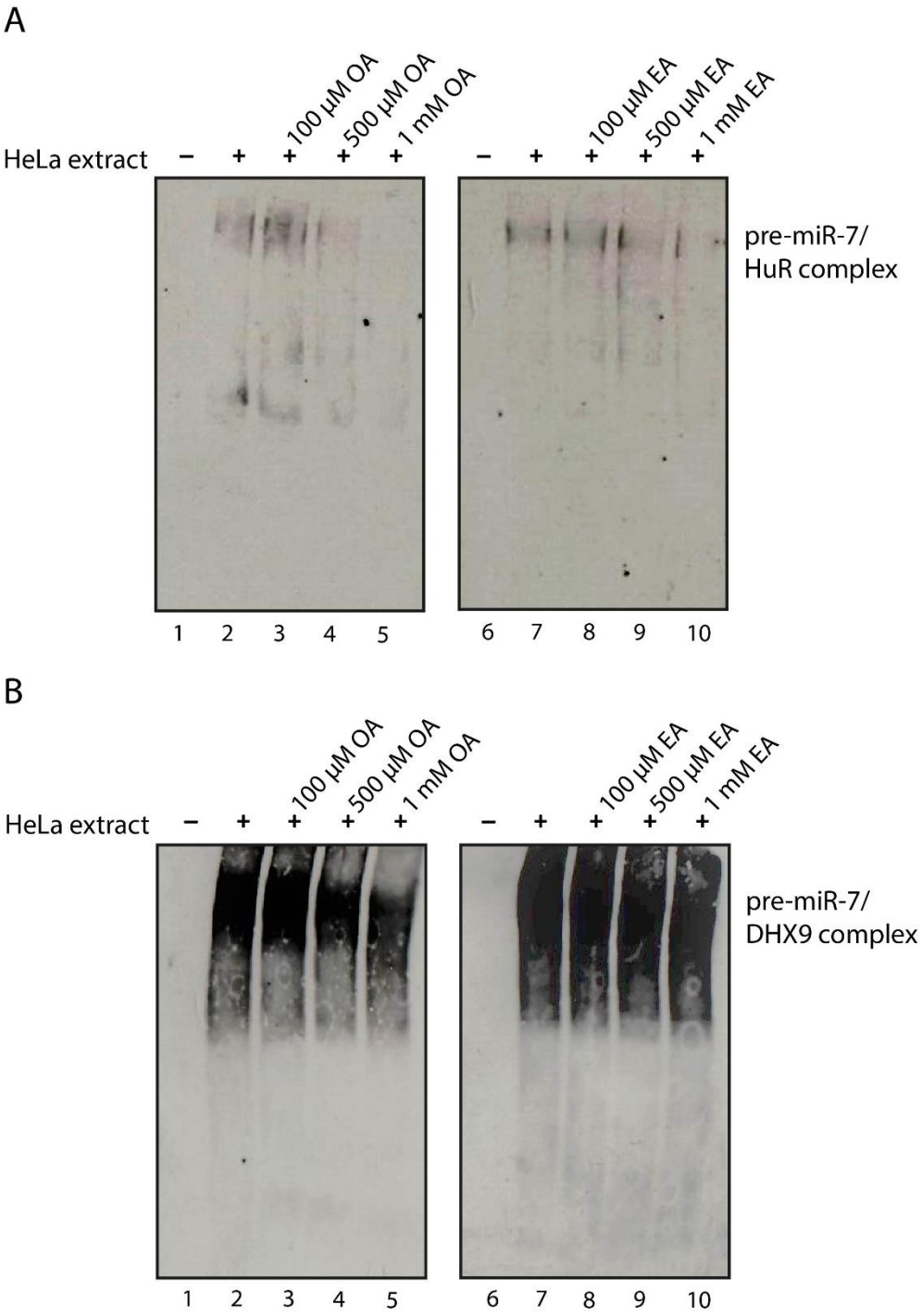

Figure 39 Validation of RNA-binding proteins in pre-miR-7/protein complex. *Western-blot combined EMSA (WEMSA) was performed on the EMSA in Figure 35. The EMSA gel was transferred unto a nitrocellulose membrane and blotted with antibodies against HuR (A) and DHX9 (B). Lanes 1 and 6 represent controls where no protein extracts were present. Lanes 2 and 7 represent pre-miR-7 incubated with protein extract but no fatty acids.*

RNA pulldown experiments corroborated the effects of OA and EA on the binding of RRM-containing proteins to the CTL of miR-7. HeLa whole cell extracts were incubated with miR-7 CTL coupled to agarose beads and increasing concentrations of OA and EA. This incubation was followed by stringent washes, permitting the identification of specific interactions. The binding of several RRM-containing proteins previously identified to bind specifically to the miR-7 CTL (namely HuR, MSI2 and hnRNP A1)[296] was then analysed by western blot (Figure 40). Incubation with 500µM concentrations of OA, but not lower concentrations, completely abolished the binding of all three proteins. EA similarly abolished binding of HuR and hnRNPA1 whilst reducing MSI2 binding at equivalent concentrations. Inhibition of DHX9 binding to miR-7 CTL was also probed and was unaffected by both OA and EA treatment. This suggests that the inhibitory effect of these fatty acids on RNA-binding could be specific to RRM-containing RBP.

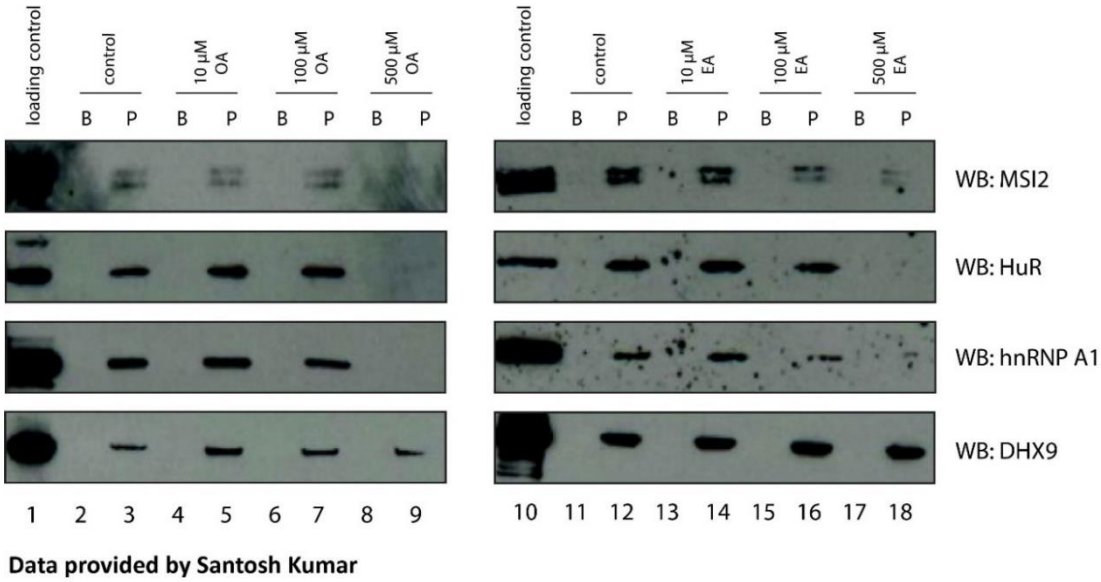

Figure 40 Inhibition by oleic and elaidic acid of RBPs binding miR-7-1 CTL. Western Blot analysis of RNA pulldown assays using miR-7-1-CTL coupled beads incubated with HeLa cell extracts and OA/EA treatment. Binding of RBPs MSI2, HuR, hnRNPA1 and DHX9, was analysed using specific antibodies as indicated on the left-hand side of the panel. Lanes 1-9 correspond to OA treatment and lanes 10-18 correspond to EA treatment. Lanes 1 and 10 represent loading control of HeLa extracts. In lanes marked B (Beads only), beads were not coupled to RNA, whereas in lanes marked P (pulldown) beads where coupled to miR-7-CTL. Concentrations of OA and EA used for each lane are indicated above the image were control indicates no fatty acid treatment.

Effects of oleic and elaidic acid on *in vitro* pri-miR-processing

Binding of an HuR/MSI2 complex regulates the biogenesis of miR-7 by binding to its CTL, stabilizing the stem-loop structure and inhibiting microprocessor processing[296]. Given this, it was analysed whether the displacement of this complex from the miR-7 CTL by OA rescued pri-miR-7 processing. This was done using *in vitro* processing assays, where radiolabelled pri-miR-7 was incubated with HeLa extracts and increasing concentrations of OA or EA. As expected, no processing of pri-miR-7 was observed in the absence of OA or EA, illustrated by the absence of pre-miR-7 in the samples. Upon incubation with 1mM concentrations of both OA and EA, a pre-miR-7 product could be detected, indicating rescued processing of pri-miR-7 (Figure 41 A-B). This displays specificity in the displacement of RBP by fatty acid treatment as the microprocessor was still able to bind and process pri-miR-7.

Equivalent assays were carried out with pri-miR-16; a miRNA with tumour suppressor roles that is ubiquitously expressed at high levels[16,230] and which remained unchanged after MSI2 and HuR knockdown in previous studies[296]. Intriguingly, treatment with OA or EA produced a concentration-dependent inhibitory effect on pri-miR-16 *in vitro* processing, contrary to the positive effect observed on pri-miR-7 processing (Figure 41 C-D). This effect could potentially be explained by OA and EA displacing RRM-containing RBPs that promote miR-16 processing. Indeed an example of an RRM containing RBP, RNA-binding protein 3 (RBM3), has been shown to bind pre-miR-16[313]. Additionally, overexpression and knockdown experiments show a positive correlation between levels of RBM3 and mature miR-16[313]. It is likely that

like RBM3, other yet unknown RRM-containing proteins can bind miR-16 precursors regulating their processing. In this way, the regulatory effects of long-chain fatty acids could extend far beyond the regulation of miR-7 biogenesis.

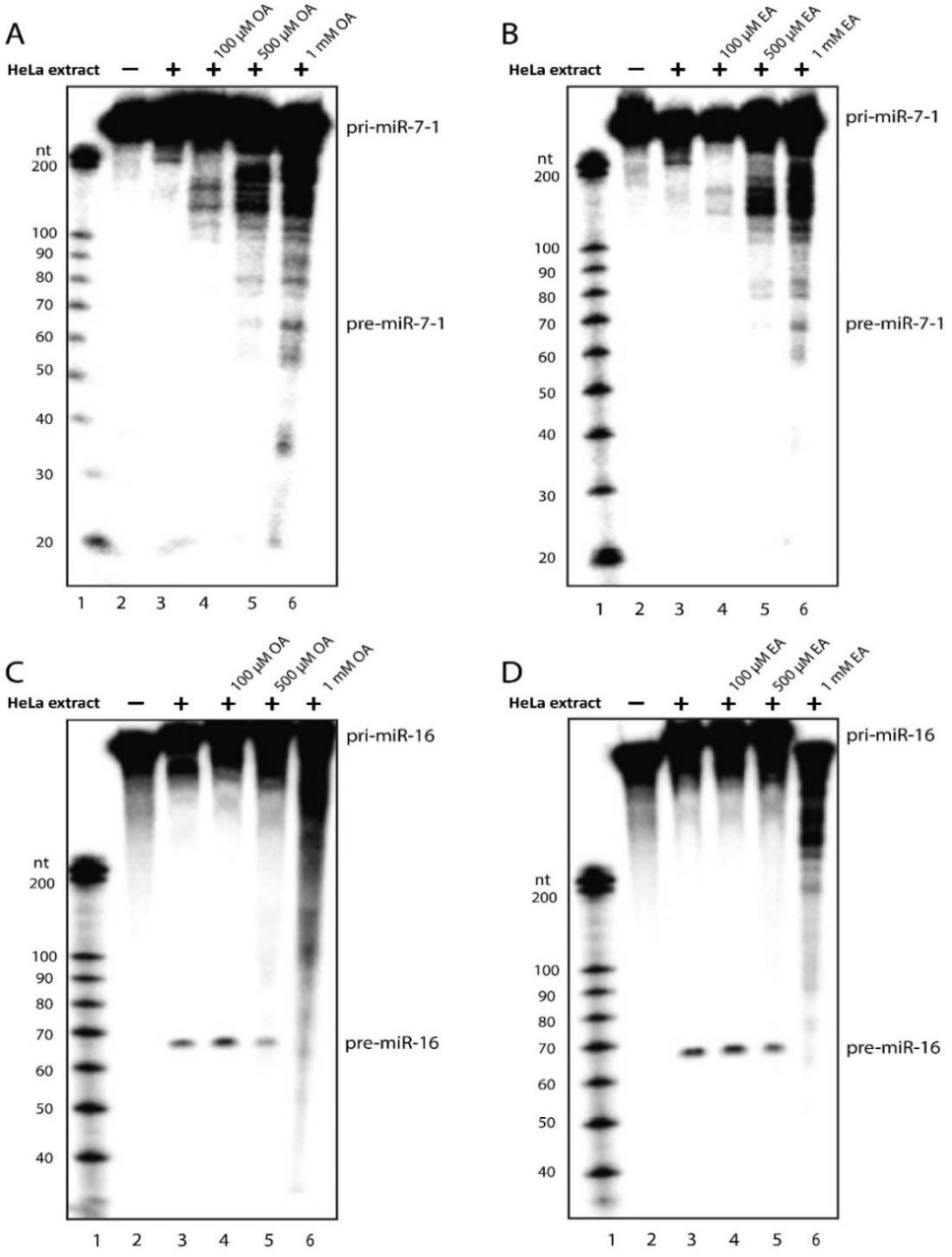

Data provided by Santosh Kumar

Figure 41 Induction of pri-miR-7 processing and inhibition of pri-miR-16 processing by oleic and elaidic acid. In vitro processing assays for pri-miR-7 (A-B) and pri-miR-16 (C-D). Lane 1 in all panels corresponds to MW ladder. Lane 2 in all panels corresponds to pri-miR-7/16 without HeLa extracts and lane 3 corresponds to pri-miR-7/16 and HeLa extract with no OA or EA treatment. In lanes 4-6 pri-miR-7/16 was incubated with HeLa extracts and increasing concentrations of OA (A,C) or EA (B,D).

Rescue of mature miR-7 production in cellular cultures by OA treatment

After establishing OA has the potential to inhibit the binding of MSI2 and HuR to miR-7 CTL as well as rescuing its processing *in vitro,* experiments were conducted to determine whether the same was true in a cellular culture. Previously it was shown that production of mature miR-7 is blocked in HeLa cells, and that this production was rescued by the knockdown of HuR or MSI2[296]. To determine whether displacement of these proteins by OA treatment could produce an analogous effect, levels of mature miR-7 were measured by qRT-PCR in HeLa extracts incubated with increasing concentrations of OA. Cells were grown for 24 hours before media was substituted for Opti-mem and OA was added in increasing concentrations. Because OA was resuspended in DMSO equivalent concentrations of DMSO were added to control cells.

A modest but significant increase in levels of mature miR-7 was observed at incubation with concentrations of 500µM and 1mM OA (Figure 42). Additionally, levels of two other miRNAs were monitored; let-7 for which EMSA analysis showed no reduction in protein/pre-let-7 complexes following OA treatment and miR-423 which is a stably expressed miRNA used as a control in qRT-PCR[420–423]. No change in the levels of either mature miR-423 or mature let-7 were detected reinforcing the observed specificity of the effect of OA treatment in miRNA biogenesis in cellular cultures and showing that general defects in miRNA processing were not present.

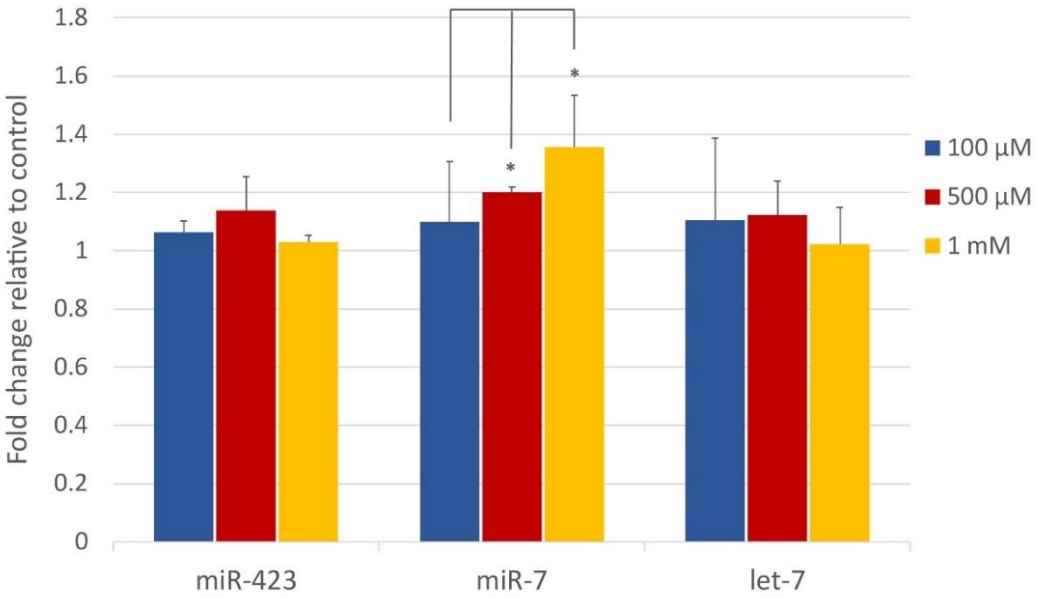

Figure 42 Increase in in vivo ***levels of miR-7 upon oleic acid treatment.*** *Total RNA was extracted from cells treated with increasing levels of OA. Levels of mature miRNAs in these samples were measured by qRT-PCR. The values presented correspond to the change in levels of miRNAs compared to control cells treated with DMSO. All values were normalized to miR-16. Students t-test was used to calculate statistical significance with *=p<0.05*

Discussion

OA was previously reported to inhibit binding of MSI1/MSI2 to RNA[382]; MSI2 in complex with HuR blocks processing of miR-7 contributing to its tissue-specificity[296]. Here, it was shown that OA can block the formation of miR-7 CTL/protein complexes observed in EMSA. Furthermore, HuR was positively identified in as a member of these shifted complexes showing that OA inhibits HuR binding to the CTL of miR-7. This was further confirmed by RNA pulldown experiments which additionally showed inhibition of MSI2 binding to miR-7 CTL. Along with inhibiting MSI2/HuR binding, OA treatment increased *in vitro* processing of pri-miR-7 and production of mature miR-7 in cellular cultures in a concentration dependent manner, suggesting that displacement of the MSI2/HuR complex can influence biogenesis of miR-7.

Unlike in the previous study by Clingman *et al*.[382] which showed no inhibition of MSI1/MSI2 binding by EA, a concentration-dependent reduction of the pre-miR-7/protein complexes upon EA treatment was also observed, although densitometry analysis revealed it was comparatively smaller, specifically at the 500µM concentrations. Similarly, in RNA pulldown experiments, high concentrations of EA completely displaced HuR and reduced MSI2 binding respectively.

This discrepancy could potentially be attributed to the higher concentrations of OA and EA used in our study. In the previous study other fatty acids of 18-22 carbons in length were also able to inhibit MSI1-RNA binding with varying strength, whilst saturated fatty acids or those with longer carbon chains were unable to inhibit RNA

binding[382]. This variation on inhibitory potential was proposed to depend on the ability of the given fatty acid to enter the hydrophobic cavity opposite the RNA-binding surface and establish extensive contact with the protein; the *trans*-bond in EA was suggested to diminish surface contact with MSI1. However, it is possible that this reduced contact is enough to produce inhibition of RNA-binding, although weaker, therefore requiring higher concentrations of EA.

Additionally, differences in RRM-containing proteins could make them more permissive to inhibition by *trans*-fatty acids. RRM-domains are conserved structurally but not in sequence, meaning the presence of differing side chains in the alpha-helical surface could impact their interaction with long-chain fatty acids. This is of particular relevance when considering the loss of pre-miR-7/protein complexes observed in EMSA upon treatment with EA since there are proteins other than MSI2 in these complexes, including HuR.

RRM domains are highly abundant in eukaryotic organisms, being present in >50% of human RBPs[505]. Here, RNA pulldown assays showed that OA and EA inhibited the binding of two RRM-containing proteins, HuR and hnRNP A1, to pre-miR-7 in addition to MSI2. This suggests that the inhibitory potential of long-chain fatty acids such as OA and EA could extend far beyond MSI1/MSI2. Similarly, EMSAs carried out with pre-miR-16 showed inhibition of miRNA/protein complexes by OA and EA in a concentration dependent manner, whilst OA additionally inhibited the formation of pre-miR-495/protein complexes. These EMSAs are insufficient to establish the identity of the proteins in the shifted pre-miR/protein complexes but is reasonable

to assume they are not restricted to MSI2 and HuR. This is further supported by *in vitro* processing assays for pri-miR-16 which show that contrary to that observed for pri-miR-7, incubation with OA and EA actually inhibit its processing. This suggests that the protein bound to pre-miR-16 being displaced by OA/EA are promoting rather than inhibitory factors. Additionally, miR-495 is a member of the 14q32 cluster, for which protein factors binding differentially upon starvation were previously sought in this study using RNA pulldown followed by SILAC mass spectrometry. Interestingly, one of the proteins validated to bind pre-miR-495 was CIRBP, a protein which possess an RRM domain in its N-terminus. Additionally, other RRM-containing proteins were identified to bind pre-miR-495 by mass spectrometry, including RBM3 and RBM27. In the future, it would be of interest to explore the presence of these protein in the pre-miR-495/protein complexes inhibited by OA.

These experiments revealed, the inhibitory potential of OA and EA against selected RRM-containing proteins. Whilst OA and EA also reduced binding of DHX9, a protein which does not contain an RRM domain, they had a weaker effect on this interaction. Importantly, *in vitro* processing assays showed the microprocessor remained functional in the presence of OA/EA, indicating it was still able to bind to pri-miR-7 and process it into pre-miR-7. Additionally, EMSA with pre-let-7 showed no inhibition of pre-let-7 protein complexes by OA/EA, showing that this inhibition is dependent on the RNA substrate. Finally, although both OA and EA were found to inhibit RNA binding of RRM containing proteins, they did exhibit some differences in doing so. Namely, only OA was able to inhibit pre-miR-495/protein complexes as well as producing a stronger inhibition of pre-miR-7/protein complexes than EA. In RNA

pulldown assays whilst EA showed a reduction in MSI2 binding to pre-miR-7, only OA completely abolished this binding. Altogether, this shows that the presence of long-chain fatty acids does not trigger a global inhibition of RNA-binding, but rather results in specific inhibition of RNA-binding dependent on the identity of the fatty-acid, the RNA-binding protein and the RNA substrate in question.

The results shown here confirm the initial reports of OA as a regulator of RNA-binding activity of MSI2 whilst presenting the possibility that this regulation could extend beyond what was first thought, influencing the RNA-binding activities of a larger set of RRM-containing proteins. Additionally, they show that OA can influence the biogenesis of at least miR-7, and potentially other miRNAs. This opens up the possibility of miRNAs as intermediaries between metabolism and gene expression, adding another component to this growingly interconnected regulatory network.

In glial cells, OA caused a decrease in lipogenesis and cholesterologenesis which coincided with a reduction in the expression of acetyl-coenzyme A carboxylase (ACC) and 3-hydroxy-3-methylglutaryl coenzyme A reductase (HMGCR), key enzymes in lipogenesis and cholesterologenesis respectively[506]. Similarly, a decrease in expression of lipogenic enzymes is observed in rats and mice fed with a diet rich in OA[507,508]. Whilst these changes are likely to partially mediated through direct activation by OA of the nuclear receptor transcription factor peroxisome proliferator-activated receptor alpha (PPARα)[508], this doesn't explain the full extent of changes seen in the levels of lipogenic and cholesterologenic enzymes and it is tempting to speculate that these are in part mediated indirectly, through changes in RNA

processing (including miRNA biogenesis). OA is further linked to a variety of pathological conditions. Colorectal cancer patients showed significantly higher proportions of OA compared to controls[509], whilst OA drove proliferation and chemoresistance in prostate cancer[510]. Reduced levels of OA were found in brains of patients with Alzheimer's disease[511,512]. Additionally, α-SYN, a protein genetically and pathologically linked with Parkinson's disease can cause an increase in OA production[513]. This protein has been identified as a miR-7 target[502], presenting the possibility of a positive feedback loop where an α-SYN mediated increase in OA leads to a decrease in miR-7 levels resulting in even higher levels of α-SYN.

It is hard to speculate what proportion of the effects of OA on cellular metabolism can be attributed to its impact on miRNA biogenesis, both under normal and pathological conditions. However, it would be of great interest in the future to further explore the impact of OA on global miRNA levels and further downstream changes in gene expression, to begin to answer these questions. It is likely that changes in miRNA profiles is one of many ways that OA regulates cellular metabolism, but when dealing with complex multifactorial diseases this could prove important clues as well as potential therapeutic targets.

Concluding remarks

This study has explored different aspects of the post-transcriptional regulation of miRNA biogenesis in specific contexts. By exploring the regulation of cluster 14q32 in response to ischemia and cellular starvation, HADHB and CIRBP were identified as novel factors involved in the regulation of miRNA biogenesis. These proteins showed specific regulation of the pre-miR to mature miRNA step of the miRNA biogenesis pathway.

As well as identifying novel proteins, this study further explored the roles of Lin28a in regulating miRNA biogenesis during neurogenesis of P19 cells. Lin28a has well described roles in the inhibition of let-7 biogenesis, however here it was shown that it regulates a second miRNA involved in neurogenesis, miR-9, and does so using a different mechanism. Extending this further, it was shown that Lin28a influences the levels of various miRNAs during neuronal differentiation, doing so in positive and negative manners.

Finally, this study also looked at the inhibitory effect of oleic and elaidic acid on the interaction of pre-miR terminal loops and regulatory protein complexes. Specifically, it was shown that oleic and elaidic acid are able to displace inhibitory factors from the miR-7 CTL, resulting in increased *in vitro* processing of pri-miR-7 and an increase of miR-7 levels in cultured cells. Additionally, oleic and elaidic acid were able were able to displace protein complexes from other pre-miR CTLs and, contrary to pri-miR-7, decreased *in vitro* processing of pri-miR-16.

Whilst the mechanisms described here were studied in specific cellular contexts, it is not known whether they operate in other scenarios, and it is of interest to understand the extent of their involvement in miRNA regulation. For example, HADHB is a metabolic enzyme that is ubiquitously expressed in cells and it would be interesting to know the context required for its involvement in miRNA regulation. Similarly, CIRBP is a stress response protein that is upregulated in response to various stimuli and that could have a role in remodelling the expression patterns of miRNAs in response to stress, including miRNAs outside of the 14q32 cluster.

On the other hand, levels of miRNAs in the 14q32 cluster are regulated in response to many cellular and extracellular conditions other than ischemia and therefore it is likely that other protein factors will be involved in their regulation. This is illustrated by the number of proteins identified to bind to pre-miR-329 and pre-miR-495 through RP-SMS, but also through regulation of the cluster by Lin28a during neurogenesis. Lin28a was shown to upregulate various members of the cluster and specifically was shown to bind miR-541. However, knockdown of Lin28a was not sufficient to reduce the levels of miR-541, once again showing that an individual miRNA is likely to be subject to various forms of regulation simultaneously.

The regulation of miRNA biogenesis by RBPs is also dependent on the cellular environment, as seen by studying the effects of oleic acid on these interactions. Whilst in this study the focus was around the displacement of regulatory complexes from the miR-7 CTL, it was also shown that oleic acid has an effect on other protein complexes, and the full regulatory potential of oleic acid is unknown.

Regulation of miRNA biogenesis by individual protein factors is always context specific, with all these factors interacting in complex regulatory networks to fine-tune the levels of miRNAs, and by increasing our understanding of the details involved in miRNA-protein interactions we can better understand the larger regulatory networks at play. In the future this knowledge could be used to design novel miRNA-based therapeutic approaches.

References

1. Bartel, D. P. MicroRNAs: Genomics, Biogenesis, Mechanism, and Function. *Cell* **116**, 281–297 (2004).

2. Kim, V. N., Han, J. & Siomi, M. C. Biogenesis of small RNAs in animals. *Nat. Rev. Mol. Cell Biol.* **10**, 126–129 (2009).

3. Hammond, S. M., Bernstein, E., Beach, D. & Hannon, G. J. An RNA-directed nuclease mediates post-transcriptional gene silencing in *Drosophila* cells. *Nature* **404**, 293–296 (2000).

4. Bartel, D. P. MicroRNAs: Target Recognition and Regulatory Functions. *Cell* **136**, 215–233 (2009).

5. Guo, H., Ingolia, N. T., Weissman, J. S. & Bartel, D. P. Mammalian microRNAs predominantly act to decrease target mRNA levels. *Nature* **466**, 835–840 (2010).

6. Lee, R. C., Feinbaum, R. L. & Ambros, V. The C. elegans heterochronic gene lin-4 encodes small RNAs with antisense complementarity to lin-14. *Cell* **75**, 843–854 (1993).

7. Wightman, B., Ha, I. & Ruvkun, G. Posttranscriptional regulation of the heterochronic gene lin-14 by lin-4 mediates temporal pattern formation in C. elegans. *Cell* **75**, 855–862 (1993).

8. Reinhart, B. J. *et al.* The 21-nucleotide *let-7* RNA regulates developmental timing in *Caenorhabditis elegans*. *Nature* **403**, 901–906 (2000).

9. Pasquinelli, A. E. *et al.* Conservation of the sequence and temporal expression of let-7 heterochronic regulatory RNA. *Nature* **408**, 86–89 (2000).

10. Lagos-Quintana, M., Rauhut, R., Lendeckel, W. & Tuschl, T. Identification of Novel Genes Coding for Small Expressed RNAs. *Science* **294**, 853–858 (2001).

11. Lee, R. C. & Ambros, V. An Extensive Class of Small RNAs in Caenorhabditis elegans. *Science* **294**, 862–864 (2001).

12. Lau, N. C., Lim, L. P., Weinstein, E. G. & Bartel, D. P. An Abundant Class of Tiny RNAs with Probable Regulatory Roles in Caenorhabditis elegans. *Science* **294**, 858–862 (2001).

13. Kozomara, A. & Griffiths-Jones, S. miRBase: annotating high confidence microRNAs using deep sequencing data. *Nucleic Acids Res.* **42**, D68–D73 (2014).

14. Friedman, R. C., Farh, K. K.-H., Burge, C. B. & Bartel, D. P. Most mammalian mRNAs are conserved targets of microRNAs. *Genome Res.* **19**, 92–105 (2009).

15. Bartel, D. P. Metazoan MicroRNAs. *Cell* **173**, 20–51 (2018).

16. Landgraf, P. *et al.* A mammalian microRNA expression atlas based on small RNA library sequencing. *Cell* **129**, 1401–14 (2007).

17. Lu, J. *et al.* MicroRNA expression profiles classify human cancers. *Nature* **435**, 834–838 (2005).

18. Nelson, P. T., Wang, W.-X. & Rajeev, B. W. MicroRNAs (miRNAs) in Neurodegenerative Diseases. *Brain Pathol. Zurich Switz.* **18**, 130–138 (2008).

19. Lujambio, A. & Lowe, S. W. The microcosmos of cancer. *Nature* **482**, 347–355 (2012).

20. Barwari, T., Joshi, A. & Mayr, M. MicroRNAs in Cardiovascular Disease. *J. Am. Coll. Cardiol.* **68**, 2577–2584 (2016).

21. Fernández-Hernando, C., Ramírez, C. M., Goedeke, L. & Suárez, Y. MicroRNAs in Metabolic Disease. *Arterioscler. Thromb. Vasc. Biol.* **33**, 178–185 (2013).

22. Chong, M. M. W. *et al.* Canonical and alternate functions of the microRNA biogenesis machinery. *Genes Dev.* **24**, 1951–1960 (2010).

23. Bernstein, E. *et al.* Dicer is essential for mouse development. *Nat. Genet.* **35**, 215–217 (2003).

24. Lee, Y., Jeon, K., Lee, J.-T., Kim, S. & Kim, V. N. MicroRNA maturation: stepwisee processing and subcellular localization. *EMBO J.* **21**, 4663–4670 (2002).

25. Lee, Y. *et al.* The nuclear RNase III Drosha initiates microRNA processing. *Nature* **425**, 415–419 (2003).

26. Carmell, M. A. & Hannon, G. J. RNase III enzymes and the initiation of gene silencing. *Nat. Struct. Mol. Biol.* **11**, 214–218 (2004).

27. Denli, A. M., Tops, B. B. J., Plasterk, R. H. A., Ketting, R. F. & Hannon, G. J. Processing of primary microRNAs by the Microprocessor complex. *Nature* **432**, 231–5 (2004).

28. Cai, X., Hagedorn, C. H. & Cullen, B. R. Human microRNAs are processed from capped, polyadenylated transcripts that can also function as mRNAs. *RNA* **10**, 1957–1966 (2004).

29. Lee, Y. *et al.* MicroRNA genes are transcribed by RNA polymerase II. *EMBO J.* **23**, 4051–60 (2004).

30. Bogerd, H. P. *et al.* A Mammalian Herpesvirus Uses Noncanonical Expression and Processing Mechanisms to Generate Viral MicroRNAs. *Mol. Cell* **37**, 135–142 (2010).

31. Kincaid, R. P. & Sullivan, C. S. Virus-Encoded microRNAs: An Overview and a Look to the Future. *PLOS Pathog.* **8**, e1003018 (2012).

32. Gregory, R. I. *et al.* The Microprocessor complex mediates the genesis of microRNAs. *Nature* **432**, 235–240 (2004).

33. Han, J. *et al.* The Drosha-DGCR8 complex in primary microRNA processing. *Genes Dev.* **18**, 3016–27 (2004).

34. Herbert, K. M. *et al.* A heterotrimer model of the complete Microprocessor complex revealed by single-molecule subunit counting. *RNA* **22**, 175–183 (2016).

35. Nguyen, T. A. *et al.* Functional Anatomy of the Human Microprocessor. *Cell* **161**, 1374–1387 (2015).

36. Shiohama, A., Sasaki, T., Noda, S., Minoshima, S. & Shimizu, N. Nucleolar localization of DGCR8 and identification of eleven DGCR8-associated proteins. *Exp. Cell Res.* **313**, 4196–4207 (2007).

37. Heras, S. R. *et al.* The Microprocessor controls the activity of mammalian retrotransposons. *Nat. Struct. Mol. Biol.* **20**, 1173–1181 (2013).

38. Macias, S. *et al.* DGCR8 HITS-CLIP reveals novel functions for the Microprocessor. *Nat. Struct. Mol. Biol.* **19**, 760–766 (2012).

39. Marinaro, F. *et al.* MicroRNA-independent functions of DGCR8 are essential for neocortical development and TBR1 expression. *EMBO Rep.* **18**, 603–618 (2017).

40. Knuckles, P. *et al.* Drosha regulates neurogenesis by controlling Neurogenin 2 expression independent of microRNAs. *Nat. Neurosci.* **15**, 962–969 (2012).

41. Macias, S., Cordiner, R. A., Gautier, P., Plass, M. & Cáceres, J. F. DGCR8 Acts as an Adaptor for the Exosome Complex to Degrade Double-Stranded Structured RNAs. *Mol. Cell* **60**, 873–885 (2015).

42. Han, J. *et al.* Molecular Basis for the Recognition of Primary microRNAs by the Drosha-DGCR8 Complex. *Cell* **125**, 887–901 (2006).

43. Fang, W. & Bartel, D. P. The Menu of Features that Define Primary MicroRNAs and Enable De Novo Design of MicroRNA Genes. *Mol. Cell* **60**, 131–145 (2015).

44. Auyeung, V. C., Ulitsky, I., McGeary, S. E. & Bartel, D. P. Beyond Secondary Structure: Primary-Sequence Determinants License Pri-miRNA Hairpins for Processing. *Cell* **152**, 844–858 (2013).

45. Louloupi, A., Ntini, E., Liz, J. & Ørom, U. A. Microprocessor dynamics shows co- and post-transcriptional processing of pri-miRNAs. *RNA* **23**, 892–898 (2017).

46. Kim, Y.-K. & Kim, V. N. Processing of intronic microRNAs. *EMBO J.* **26**, 775–783 (2007).

47. Morlando, M. *et al.* Primary microRNA transcripts are processed co-transcriptionally. *Nat. Struct. Mol. Biol.* **15**, 902–909 (2008).

48. Yi, R., Qin, Y., Macara, I. G. & Cullen, B. R. Exportin-5 mediates the nuclear export of pre-microRNAs and short hairpin RNAs. *Genes Dev.* **17**, 3011–6 (2003).

49. Hutvágner, G. *et al.* A cellular function for the RNA-interference enzyme Dicer in the maturation of the let-7 small temporal RNA. *Science* **293**, 834–8 (2001).

50. Bernstein, E., Caudy, A. A., Hammond, S. M. & Hannon, G. J. Role for a bidentate ribonuclease in the initiation step of RNA interference. *Nature* **409**, 363–366 (2001).

51. Iwasaki, S. *et al.* Hsc70/Hsp90 chaperone machinery mediates ATP-dependent RISC loading of small RNA duplexes. *Mol. Cell* **39**, 292–299 (2010).

52. Kobayashi, H. & Tomari, Y. RISC assembly: Coordination between small RNAs and Argonaute proteins. *Biochim. Biophys. Acta BBA - Gene Regul. Mech.* **1859**, 71–81 (2016).

53. Ruby, J. G., Jan, C. H. & Bartel, D. P. Intronic microRNA precursors that bypass Drosha processing. *Nature* **448**, 83–86 (2007).

54. Okamura, K., Hagen, J. W., Duan, H., Tyler, D. M. & Lai, E. C. The Mirtron Pathway Generates microRNA-Class Regulatory RNAs in Drosophila. *Cell* **130**, 89–100 (2007).

55. Babiarz, J. E., Ruby, J. G., Wang, Y., Bartel, D. P. & Blelloch, R. Mouse ES cells express endogenous shRNAs, siRNAs, and other Microprocessor-independent, Dicer-dependent small RNAs. *Genes Dev.* **22**, 2773–2785 (2008).

56. Xie, M. *et al.* Mammalian 5'-Capped MicroRNA Precursors that Generate a Single MicroRNA. *Cell* **155**, 1568–1580 (2013).

57. Röther, S. & Meister, G. Small RNAs derived from longer non-coding RNAs. *Biochimie* **93**, 1905–1915 (2011).

58. Ender, C. *et al.* A human snoRNA with microRNA-like functions. *Mol. Cell* **32**, 519–528 (2008).

59. Scott, M. S. & Ono, M. From snoRNA to miRNA: Dual function regulatory non-coding RNAs. *Biochimie* **93**, 1987–1992 (2011).

60. Brameier, M., Herwig, A., Reinhardt, R., Walter, L. & Gruber, J. Human box C/D snoRNAs with miRNA like functions: expanding the range of regulatory RNAs. *Nucleic Acids Res.* **39**, 675–686 (2011).

61. Ono, M. *et al.* Identification of human miRNA precursors that resemble box C/D snoRNAs. *Nucleic Acids Res.* **39**, 3879–3891 (2011).

62. Taft, R. J. *et al.* Small RNAs derived from snoRNAs. *RNA* (2009) doi:10.1261/rna.1528909.

63. Bellutti, F., Kauer, M., Kneidinger, D., Lion, T. & Klein, R. Identification of RISC-Associated Adenoviral MicroRNAs, a Subset of Their Direct Targets, and Global Changes in the Targetome upon Lytic Adenovirus 5 Infection. *J. Virol.* **89**, 1608–1627 (2015).

64. Cheloufi, S., Dos Santos, C. O., Chong, M. M. W. & Hannon, G. J. A dicer-independent miRNA biogenesis pathway that requires Ago catalysis. *Nature* **465**, 584–589 (2010).

65. Cifuentes, D. *et al.* A Novel miRNA Processing Pathway Independent of Dicer Requires Argonaute2 Catalytic Activity. *Science* **328**, 1694–1698 (2010).

66. Meister, G. *et al.* Human Argonaute2 Mediates RNA Cleavage Targeted by miRNAs and siRNAs. *Mol. Cell* **15**, 185–197 (2004).

67. Hammond, S. M., Boettcher, S., Caudy, A. A., Kobayashi, R. & Hannon, G. J. Argonaute2, a Link Between Genetic and Biochemical Analyses of RNAi. *Science* **293**, 1146–1150 (2001).

68. Liu, J. *et al.* Argonaute2 Is the Catalytic Engine of Mammalian RNAi. *Science* **305**, 1437–1441 (2004).

69. Sasaki, T., Shiohama, A., Minoshima, S. & Shimizu, N. Identification of eight members of the Argonaute family in the human genome☆. *Genomics* **82**, 323–330 (2003).

70. Karginov, F. V. *et al.* Diverse endonucleolytic cleavage sites in the mammalian transcriptome depend upon microRNAs, Drosha, and additional nucleases. *Mol. Cell* **38**, 781–788 (2010).

71. Stark, A., Brennecke, J., Russell, R. B. & Cohen, S. M. Identification of Drosophila MicroRNA Targets. *PLoS Biol.* **1**, (2003).

72. Lai, E. C. Micro RNAs are complementary to 3' UTR sequence motifs that mediate negative post-transcriptional regulation. *Nat. Genet.* **30**, 363–364 (2002).

73. Lewis, B. P., Shih, I., Jones-Rhoades, M. W., Bartel, D. P. & Burge, C. B. Prediction of Mammalian MicroRNA Targets. *Cell* **115**, 787–798 (2003).

74. Grimson, A. *et al.* MicroRNA Targeting Specificity in Mammals: Determinants beyond Seed Pairing. *Mol. Cell* **27**, 91–105 (2007).

75. Schirle, N. T., Sheu-Gruttadauria, J. & MacRae, I. J. Structural basis for microRNA targeting. *Science* **346**, 608–613 (2014).

76. Hendrickson, D. G. *et al.* Concordant Regulation of Translation and mRNA Abundance for Hundreds of Targets of a Human microRNA. *PLOS Biol.* **7**, e1000238 (2009).

77. Selbach, M. *et al.* Widespread changes in protein synthesis induced by microRNAs. *Nature* **455**, 58–63 (2008).

78. Baek, D. *et al.* The impact of microRNAs on protein output. *Nature* **455**, 64–71 (2008).

79. Lim, L. P. *et al.* Microarray analysis shows that some microRNAs downregulate large numbers of target mRNAs. *Nature* **433**, 769–773 (2005).

80. Wu, L., Fan, J. & Belasco, J. G. MicroRNAs direct rapid deadenylation of mRNA. *Proc. Natl. Acad. Sci.* **103**, 4034–4039 (2006).

81. Hutvágner, G. & Zamore, P. D. A microRNA in a Multiple-Turnover RNAi Enzyme Complex. *Science* **297**, 2056–2060 (2002).

82. Eulalio, A. *et al.* Deadenylation is a widespread effect of miRNA regulation. *RNA* **15**, 21–32 (2009).

83. Giraldez, A. J. *et al.* Zebrafish MiR-430 Promotes Deadenylation and Clearance of Maternal mRNAs. *Science* **312**, 75–79 (2006).

84. Jonas, S. & Izaurralde, E. Towards a molecular understanding of microRNA-mediated gene silencing. *Nat. Rev. Genet.* **16**, 421–433 (2015).

85. Behm-Ansmant, I. *et al.* mRNA degradation by miRNAs and GW182 requires both CCR4:NOT deadenylase and DCP1:DCP2 decapping complexes. *Genes Dev.* **20**, 1885–1898 (2006).

86. Sheu-Gruttadauria, J. & MacRae, I. J. Structural Foundations of RNA Silencing by Argonaute. *J. Mol. Biol.* **429**, 2619–2639 (2017).

87. Wahle, E. & Winkler, G. S. RNA decay machines: Deadenylation by the Ccr4–Not and Pan2–Pan3 complexes. *Biochim. Biophys. Acta BBA - Gene Regul. Mech.* **1829**, 561–570 (2013).

88. Jonas, S. & Izaurralde, E. The role of disordered protein regions in the assembly of decapping complexes and RNP granules. *Genes Dev.* **27**, 2628–2641 (2013).

89. Chen, C.-Y. A. & Shyu, A.-B. Mechanisms of deadenylation-dependent decay. *Wiley Interdiscip. Rev. RNA* **2**, 167–183 (2011).

90. Ebert, M. S. & Sharp, P. A. Roles for MicroRNAs in Conferring Robustness to Biological Processes. *Cell* **149**, 515–524 (2012).

91. Stark, A., Brennecke, J., Bushati, N., Russell, R. B. & Cohen, S. M. Animal MicroRNAs Confer Robustness to Gene Expression and Have a Significant Impact on 3'UTR Evolution. *Cell* **123**, 1133–1146 (2005).

92. Vidigal, J. A. & Ventura, A. The biological functions of miRNAs: lessons from in vivo studies. *Trends Cell Biol.* **25**, 137–147 (2015).

93. Tsang, J., Zhu, J. & van Oudenaarden, A. MicroRNA-Mediated Feedback and Feedforward Loops Are Recurrent Network Motifs in Mammals. *Mol. Cell* **26**, 753–767 (2007).

94. Maiorano, N. A. & Mallamaci, A. The pro-differentiating role of miR-124: Indicating the road to become a neuron. *RNA Biol.* **7**, 528–533 (2010).

95. Cao, Y. *et al.* Global and gene-specific analyses show distinct roles for Myod and Myog at a common set of promoters. *EMBO J.* **25**, 502–511 (2006).

96. Cheng, L.-C., Pastrana, E., Tavazoie, M. & Doetsch, F. miR-124 regulates adult neurogenesis in the subventricular zone stem cell niche. *Nat. Neurosci.* **12**, 399–408 (2009).

97. Visvanathan, J., Lee, S., Lee, B., Lee, J. W. & Lee, S.-K. The microRNA miR-124 antagonizes the anti-neural REST/SCP1 pathway during embryonic CNS development. *Genes Dev.* **21**, 744–749 (2007).

98. Hayes, G. D. & Ruvkun, G. Misexpression of the Caenorhabditis elegans miRNA let-7 Is Sufficient to Drive Developmental Programs. *Cold Spring Harb. Symp. Quant. Biol.* **71**, 21–27 (2006).

99. Roush, S. & Slack, F. J. The let-7 family of microRNAs. *Trends Cell Biol.* **18**, 505–516 (2008).

100. Viswanathan, S. R., Daley, G. Q. & Gregory, R. I. Selective blockade of microRNA processing by Lin28. *Science* **320**, 97–100 (2008).

101. Newman, M. A., Thomson, J. M. & Hammond, S. M. Lin-28 interaction with the Let-7 precursor loop mediates regulated microRNA processing. *RNA* **14**, 1539–1549 (2008).

102. Rybak, A. *et al.* A feedback loop comprising lin-28 and let-7 controls pre-let-7 maturation during neural stem-cell commitment. *Nat. Cell Biol.* **10**, 987–993 (2008).

103. Heo, I. *et al.* Lin28 mediates the terminal uridylation of let-7 precursor MicroRNA. *Mol. Cell* **32**, 276–284 (2008).

104. Melton, C., Judson, R. L. & Blelloch, R. Opposing microRNA families regulate self-renewal in mouse embryonic stem cells. *Nature* **463**, 621–626 (2010).

105. Cao, X., Yeo, G., Muotri, A. R., Kuwabara, T. & Gage, F. H. Noncoding Rnas in the Mammalian Central Nervous System. *Annu. Rev. Neurosci.* **29**, 77–103 (2006).

106. Sempere, L. F., Cole, C. N., Mcpeek, M. A. & Peterson, K. J. The phylogenetic distribution of metazoan microRNAs: insights into evolutionary complexity and constraint. *J. Exp. Zoolog. B Mol. Dev. Evol.* **306B**, 575–588 (2006).

107. Bicker, S. & Schratt, G. microRNAs: tiny regulators of synapse function in development and disease. *J. Cell. Mol. Med.* **12**, 1466–1476 (2008).

108. Follert, P., Cremer, H. & Béclin, C. MicroRNAs in brain development and function: a matter of flexibility and stability. *Front. Mol. Neurosci.* **7**, (2014).

109. Yang, Z., Cappello, T. & Wang, L. Emerging role of microRNAs in lipid metabolism. *Acta Pharm. Sin. B* **5**, 145–150 (2015).

110. Adlakha, Y. K. *et al.* Pro-apoptotic miRNA-128-2 modulates ABCA1, ABCG1 and RXRα expression and cholesterol homeostasis. *Cell Death Dis.* **4**, e780 (2013).

111. Melkman-Zehavi, T. *et al.* miRNAs control insulin content in pancreatic β-cells via downregulation of transcriptional repressors. *EMBO J.* **30**, 835–845 (2011).

112. Poy, M. N. *et al.* A pancreatic islet-specific microRNA regulates insulin secretion. *Nature* **432**, 226–230 (2004).

113. Frost, R. J. A. & Olson, E. N. Control of glucose homeostasis and insulin sensitivity by the Let-7 family of microRNAs. *Proc. Natl. Acad. Sci. U. S. A.* **108**, 21075–21080 (2011).

114. Ouaamari, A. E. *et al.* miR-375 Targets 3'-Phosphoinositide–Dependent Protein Kinase-1 and Regulates Glucose-Induced Biological Responses in Pancreatic β-Cells. *Diabetes* **57**, 2708–2717 (2008).

115. Poy, M. N. *et al.* miR-375 maintains normal pancreatic α- and β-cell mass. *Proc. Natl. Acad. Sci.* **106**, 5813–5818 (2009).

116. Trajkovski, M. *et al.* MicroRNAs 103 and 107 regulate insulin sensitivity. *Nature* **474**, 649–653 (2011).

117. O'Connell, R. M., Rao, D. S., Chaudhuri, A. A. & Baltimore, D. Physiological and pathological roles for microRNAs in the immune system. *Nat. Rev. Immunol.* **10**, 111–122 (2010).

118. O'Connell, R. M., Taganov, K. D., Boldin, M. P., Cheng, G. & Baltimore, D. MicroRNA-155 is induced during the macrophage inflammatory response. *Proc. Natl. Acad. Sci.* **104**, 1604–1609 (2007).

119. Taganov, K. D., Boldin, M. P., Chang, K.-J. & Baltimore, D. NF-κB-dependent induction of microRNA miR-146, an inhibitor targeted to signaling proteins of innate immune responses. *Proc. Natl. Acad. Sci.* **103**, 12481–12486 (2006).

120. Sheedy, F. J. *et al.* Negative regulation of TLR4 via targeting of the proinflammatory tumor suppressor PDCD4 by the microRNA miR-21. *Nat. Immunol.* **11**, 141–147 (2010).

121. Liu, G. *et al.* miR-147, a microRNA that is induced upon Toll-like receptor stimulation, regulates murine macrophage inflammatory responses. *Proc. Natl. Acad. Sci.* **106**, 15819–15824 (2009).

122. Bazzoni, F. *et al.* Induction and regulatory function of miR-9 in human monocytes and neutrophils exposed to proinflammatory signals. *Proc. Natl. Acad. Sci.* **106**, 5282–5287 (2009).

123. Ostermann, E. *et al.* Deregulation of Type I IFN-Dependent Genes Correlates with Increased Susceptibility to Cytomegalovirus Acute Infection of Dicer Mutant Mice. *PLoS ONE* **7**, (2012).

124. Ceppi, M. *et al.* MicroRNA-155 modulates the interleukin-1 signaling pathway in activated human monocyte-derived dendritic cells. *Proc. Natl. Acad. Sci.* **106**, 2735–2740 (2009).

125. Rodriguez, A. *et al.* Requirement of bic/microRNA-155 for Normal Immune Function. *Science* **316**, 608–611 (2007).

126. O'Connell, R. M., Chaudhuri, A. A., Rao, D. S. & Baltimore, D. Inositol phosphatase SHIP1 is a primary target of miR-155. *Proc. Natl. Acad. Sci.* **106**, 7113–7118 (2009).

127. Witteveldt, J., Ivens, A. & Macias, S. Inhibition of Microprocessor Function during the Activation of the Type I Interferon Response. *Cell Rep.* **23**, 3275–3285 (2018).

128. Rooij, E. van *et al.* Control of Stress-Dependent Cardiac Growth and Gene Expression by a MicroRNA. *Science* **316**, 575–579 (2007).

129. Calin, G. A. *et al.* Human microRNA genes are frequently located at fragile sites and genomic regions involved in cancers. *Proc. Natl. Acad. Sci. U. S. A.* **101**, 2999–3004 (2004).

130. Suzuki, H., Maruyama, R., Yamamoto, E. & Kai, M. Epigenetic alteration and microRNA dysregulation in cancer. *Front. Genet.* **4**, (2013).

131. Lin, S. & Gregory, R. I. MicroRNA biogenesis pathways in cancer. *Nat. Rev. Cancer* **15**, 321–333 (2015).

132. Chang, T.-C. *et al.* Widespread microRNA repression by Myc contributes to tumorigenesis. *Nat. Genet.* **40**, 43–50 (2008).

133. Feng, Z., Zhang, C., Wu, R. & Hu, W. Tumor suppressor p53 meets microRNAs. *J. Mol. Cell Biol.* **3**, 44–50 (2011).

134. Karube, Y. *et al.* Reduced expression of Dicer associated with poor prognosis in lung cancer patients. *Cancer Sci.* **96**, 111–115 (2005).

135. Zhu, D.-X. *et al.* Downregulated Dicer expression predicts poor prognosis in chronic lymphocytic leukemia. *Cancer Sci.* **103**, 875–881 (2012).

136. Pampalakis, G., Diamandis, E. P., Katsaros, D. & Sotiropoulou, G. Down-regulation of dicer expression in ovarian cancer tissues. *Clin. Biochem.* **43**, 324–327 (2010).

137. O'Donnell, K. A., Wentzel, E. A., Zeller, K. I., Dang, C. V. & Mendell, J. T. c-Myc-regulated microRNAs modulate E2F1 expression. *Nature* **435**, 839–843 (2005).

138. He, L. *et al.* A microRNA polycistron as a potential human oncogene. *Nature* **435**, 828–833 (2005).

139. Hayashita, Y. *et al.* A Polycistronic MicroRNA Cluster, miR-17-92, Is Overexpressed in Human Lung Cancers and Enhances Cell Proliferation. *Cancer Res.* **65**, 9628–9632 (2005).

140. Dews, M. *et al.* Augmentation of tumor angiogenesis by a Myc-activated microRNA cluster. *Nat. Genet.* **38**, 1060–1065 (2006).

141. Olive, V. *et al.* miR-19 is a key oncogenic component of mir-17-92. *Genes Dev.* **23**, 2839–2849 (2009).

142. Hong, L. *et al.* The miR-17-92 Cluster of MicroRNAs Confers Tumorigenicity by Inhibiting Oncogene-Induced Senescence. *Cancer Res.* **70**, 8547–8557 (2010).

143. Volinia, S. *et al.* Reprogramming of miRNA networks in cancer and leukemia. *Genome Res.* **20**, 589–599 (2010).

144. Pan, X., Wang, Z.-X. & Wang, R. MicroRNA-21: A novel therapeutic target in human cancer. *Cancer Biol. Ther.* **10**, 1224–1232 (2010).

145. Medina, P. P., Nolde, M. & Slack, F. J. OncomiR addiction in an *in vivo* model of microRNA-21-induced pre-B-cell lymphoma. *Nature* **467**, 86–90 (2010).

146. Boyerinas, B., Park, S.-M., Hau, A., Murmann, A. E. & Peter, M. E. The role of let-7 in cell differentiation and cancer. *Endocr. Relat. Cancer* **17**, F19–F36 (2010).

147. Wang, H., Zhao, Q., Deng, K., Guo, X. & Xia, J. Lin28: an emerging important oncogene connecting several aspects of cancer. *Tumor Biol.* **37**, 2841–2848 (2016).

148. Kalinowski, F. C. *et al.* microRNA-7: A tumor suppressor miRNA with therapeutic potential. *Int. J. Biochem. Cell Biol.* **54**, 312–317 (2014).

149. Liu, Z. *et al.* MiR-7-5p is frequently downregulated in glioblastoma microvasculature and inhibits vascular endothelial cell proliferation by targeting RAF1. *Tumor Biol.* **35**, 10177–10184 (2014).

150. Nakanishi, N. *et al.* The up-regulation of microRNA-335 is associated with lipid metabolism in liver and white adipose tissue of genetically obese mice. *Biochem. Biophys. Res. Commun.* **385**, 492–496 (2009).

151. Takanabe, R. *et al.* Up-regulated expression of microRNA-143 in association with obesity in adipose tissue of mice fed high-fat diet. *Biochem. Biophys. Res. Commun.* **376**, 728–732 (2008).

152. Xie, H., Lim, B. & Lodish, H. F. MicroRNAs Induced During Adipogenesis that Accelerate Fat Cell Development Are Downregulated in Obesity. *Diabetes* **58**, 1050–1057 (2009).

153. Guay, C., Roggli, E., Nesca, V., Jacovetti, C. & Regazzi, R. Diabetes mellitus, a microRNA-related disease? *Transl. Res.* **157**, 253–264 (2011).

154. Lynn, F. C. *et al.* MicroRNA Expression Is Required for Pancreatic Islet Cell Genesis in the Mouse. *Diabetes* **56**, 2938–2945 (2007).

155. Baffy, G. MicroRNAs in Nonalcoholic Fatty Liver Disease. *J. Clin. Med.* **4**, 1977–1988 (2015).

156. Rottiers, V. & Näär, A. M. MicroRNAs in metabolism and metabolic disorders. *Nat. Rev. Mol. Cell Biol.* **13**, 239–250 (2012).

157. Lee, J. *et al.* A Pathway Involving Farnesoid X Receptor and Small Heterodimer Partner Positively Regulates Hepatic Sirtuin 1 Levels via MicroRNA-34a Inhibition. *J. Biol. Chem.* **285**, 12604–12611 (2010).

158. McKinsey, T. A. & Olson, E. N. Toward transcriptional therapies for the failing heart: chemical screens to modulate genes. *J. Clin. Invest.* **115**, 538–546 (2005).

159. Dirkx, E. *et al.* Nfat and miR-25 cooperate to reactivate the transcription factor Hand2 in heart failure. *Nat. Cell Biol.* **15**, 1282–1293 (2013).

160. Carè, A. *et al. MicroRNA-133* controls cardiac hypertrophy. *Nat. Med.* **13**, 613–618 (2007).

161. da Costa Martins, P. A. *et al.* MicroRNA-199b targets the nuclear kinase Dyrk1a in an auto-amplification loop promoting calcineurin/NFAT signalling. *Nat. Cell Biol.* **12**, 1220–1227 (2010).

162. Ganesan Jayavarshni *et al.* MiR-378 Controls Cardiac Hypertrophy by Combined Repression of Mitogen-Activated Protein Kinase Pathway Factors. *Circulation* **127**, 2097–2106 (2013).

163. Castaldi Alessandra *et al.* MicroRNA-133 Modulates the β1-Adrenergic Receptor Transduction Cascade. *Circ. Res.* **115**, 273–283 (2014).

164. Karakikes Ioannis *et al.* Therapeutic Cardiac-Targeted Delivery of miR-1 Reverses Pressure Overload–Induced Cardiac Hypertrophy and Attenuates Pathological Remodeling. *J. Am. Heart Assoc.* **2**, e000078.

165. Elia Leonardo *et al.* Reciprocal Regulation of MicroRNA-1 and Insulin-Like Growth Factor-1 Signal Transduction Cascade in Cardiac and Skeletal Muscle in Physiological and Pathological Conditions. *Circulation* **120**, 2377–2385 (2009).

166. Wahlquist, C. *et al.* Inhibition of *miR-25* improves cardiac contractility in the failing heart. *Nature* **508**, 531–535 (2014).

167. Li, H. *et al.* Alteration in microRNA-25 expression regulate cardiac function via renin secretion. *Exp. Cell Res.* **365**, 119–128 (2018).

168. Lovren Fina *et al.* MicroRNA-145 Targeted Therapy Reduces Atherosclerosis. *Circulation* **126**, S81–S90 (2012).

169. Schober, A. *et al.* MicroRNA-126-5p promotes endothelial proliferation and limits atherosclerosis by suppressing Dlk1. *Nat. Med.* **20**, 368–376 (2014).

170. Eulalio, A. *et al.* Functional screening identifies miRNAs inducing cardiac regeneration. *Nature* **492**, 376–381 (2012).

171. Zhao, Y. *et al.* Dysregulation of Cardiogenesis, Cardiac Conduction, and Cell Cycle in Mice Lacking miRNA-1-2. *Cell* **129**, 303–317 (2007).

172. Thum, T. *et al.* MicroRNA-21 contributes to myocardial disease by stimulating MAP kinase signalling in fibroblasts. *Nature* **456**, 980–984 (2008).

173. Ling, S., Zhou, J., Rudd, J. A., Hu, Z. & Fang, M. The Recent Updates of Therapeutic Approaches Against Aβ for the Treatment of Alzheimer's Disease. *Anat. Rec.* **294**, 1307–1318 (2011).

174. Wang, W.-X. *et al.* The Expression of MicroRNA miR-107 Decreases Early in Alzheimer's Disease and May Accelerate Disease Progression through Regulation of β-Site Amyloid Precursor Protein-Cleaving Enzyme 1. *J. Neurosci. Off. J. Soc. Neurosci.* **28**, 1213–1223 (2008).

175. Yao, J. *et al.* MicroRNA-Related Cofilin Abnormality in Alzheimer's Disease. *PLOS ONE* **5**, e15546 (2010).

176. Cox, M. B. *et al.* MicroRNAs miR-17 and miR-20a Inhibit T Cell Activation Genes and Are Under-Expressed in MS Whole Blood. *PLOS ONE* **5**, e12132 (2010).

177. Moreau, M. P., Bruse, S. E., David-Rus, R., Buyske, S. & Brzustowicz, L. M. Altered MicroRNA Expression Profiles in Postmortem Brain Samples from Individuals with Schizophrenia and Bipolar Disorder. *Biol. Psychiatry* **69**, 188–193 (2011).

178. Santarelli, D. M., Beveridge, N. J., Tooney, P. A. & Cairns, M. J. Upregulation of Dicer and MicroRNA Expression in the Dorsolateral Prefrontal Cortex Brodmann Area 46 in Schizophrenia. *Biol. Psychiatry* **69**, 180–187 (2011).

179. Beveridge, N. J., Gardiner, E., Carroll, A. P., Tooney, P. A. & Cairns, M. J. Schizophrenia is associated with an increase in cortical microRNA biogenesis. *Mol. Psychiatry* **15**, 1176–1189 (2010).

180. Leggio, L. *et al.* microRNAs in Parkinson's Disease: From Pathogenesis to Novel Diagnostic and Therapeutic Approaches. *Int. J. Mol. Sci.* **18**, (2017).

181. Cerutti, H. & Casas-Mollano, J. A. On the origin and functions of RNA-mediated silencing: from protists to man. *Curr. Genet.* **50**, 81–99 (2006).

182. Grimson, A. *et al.* Early origins and evolution of microRNAs and Piwi-interacting RNAs in animals. *Nature* **455**, 1193–1197 (2008).

183. Pfeffer, S. *et al.* Identification of Virus-Encoded MicroRNAs. *Science* **304**, 734–736 (2004).

184. Sullivan, C. S., Grundhoff, A. T., Tevethia, S., Pipas, J. M. & Ganem, D. SV40-encoded microRNAs regulate viral gene expression and reduce susceptibility to cytotoxic T cells. *Nature* **435**, 682 (2005).

185. Pfeffer, S. Herpesviruses Encode Their Own MicroRNAs. *Clin. Chem.* **60**, 791–792 (2014).

186. Jones-Rhoades, M. W., Bartel, D. P. & Bartel, B. MicroRNAs AND THEIR REGULATORY ROLES IN PLANTS. *Annu. Rev. Plant Biol.* **57**, 19–53 (2006).

187. Reinhart, B. J., Weinstein, E. G., Rhoades, M. W., Bartel, B. & Bartel, D. P. MicroRNAs in plants. *Genes Dev.* **16**, 1616–1626 (2002).

188. Papp, I. *et al.* Evidence for Nuclear Processing of Plant Micro RNA and Short Interfering RNA Precursors. *Plant Physiol.* **132**, 1382–1390 (2003).

189. Rhoades, M. W. *et al.* Prediction of Plant MicroRNA Targets. *Cell* **110**, 513–520 (2002).

190. Vaucheret, H. Gene silencing: Mode of miRNA biogenesis matters. *Nat. Plants* **1**, 15019 (2015).

191. Llave, C., Xie, Z., Kasschau, K. D. & Carrington, J. C. Cleavage of Scarecrow-like mRNA Targets Directed by a Class of Arabidopsis miRNA. *Science* **297**, 2053–2056 (2002).

192. German, M. A. *et al.* Global identification of microRNA–target RNA pairs by parallel analysis of RNA ends. *Nat. Biotechnol.* **26**, 941–946 (2008).

193. Prochnik, S. E., Rokhsar, D. S. & Aboobaker, A. A. Evidence for a microRNA expansion in the bilaterian ancestor. *Dev. Genes Evol.* **217**, 73–77 (2007).

194. Hertel, J. *et al.* The expansion of the metazoan microRNA repertoire. *BMC Genomics* **7**, 25 (2006).

195. Guerra-Assunção, J. A. & Enright, A. J. Large-scale analysis of microRNA evolution. *BMC Genomics* **13**, 218 (2012).

196. Heimberg, A. M., Sempere, L. F., Moy, V. N., Donoghue, P. C. J. & Peterson, K. J. MicroRNAs and the advent of vertebrate morphological complexity. *Proc. Natl. Acad. Sci.* **105**, 2946–2950 (2008).

197. Berezikov, E. Evolution of microRNA diversity and regulation in animals. *Nat. Rev. Genet.* **12**, 846–860 (2011).

198. Bentwich, I. *et al.* Identification of hundreds of conserved and nonconserved human microRNAs. *Nat. Genet.* **37**, 766–770 (2005).

199. Smalheiser, N. R. & Torvik, V. I. Mammalian microRNAs derived from genomic repeats. *Trends Genet.* **21**, 322–326 (2005).

200. Berezikov, E. *et al.* Deep annotation of Drosophila melanogaster microRNAs yields insights into their processing, modification, and emergence. *Genome Res.* **21**, 203–215 (2011).

201. Campo-Paysaa, F., Sémon, M., Cameron, R. A., Peterson, K. J. & Schubert, M. microRNA complements in deuterostomes: origin and evolution of microRNAs. *Evol. Dev.* **13**, 15–27 (2011).

202. Farh, K. K.-H. *et al.* The Widespread Impact of Mammalian MicroRNAs on mRNA Repression and Evolution. *Science* **310**, 1817–1821 (2005).

203. Olena, A. F. & Patton, J. G. Genomic organization of microRNAs. *J. Cell. Physiol.* **222**, 540–545 (2010).

204. França, G. S., Vibranovski, M. D. & Galante, P. A. F. Host gene constraints and genomic context impact the expression and evolution of human microRNAs. *Nat. Commun.* **7**, 11438 (2016).

205. Hinske, L. C. G., Galante, P. A., Kuo, W. P. & Ohno-Machado, L. A potential role for intragenic miRNAs on their hosts' interactome. *BMC Genomics* **11**, 533 (2010).

206. Hinske, L. C. *et al.* miRIAD—integrating microRNA inter- and intragenic data. *Database J. Biol. Databases Curation* **2014**, (2014).

207. Rodriguez, A., Griffiths-Jones, S., Ashurst, J. L. & Bradley, A. Identification of Mammalian microRNA Host Genes and Transcription Units. *Genome Res.* **14**, 1902–1910 (2004).

208. Baskerville, S. & Bartel, D. P. Microarray profiling of microRNAs reveals frequent coexpression with neighboring miRNAs and host genes. *RNA* **11**, 241–247 (2005).

209. Ozsolak, F. *et al.* Chromatin structure analyses identify miRNA promoters. *Genes Dev.* **22**, 3172–3183 (2008).

210. Zhou, X., Ruan, J., Wang, G. & Zhang, W. Characterization and Identification of MicroRNA Core Promoters in Four Model Species. *PLOS Comput. Biol.* **3**, e37 (2007).

211. Saini, H. K., Griffiths-Jones, S. & Enright, A. J. Genomic analysis of human microRNA transcripts. *Proc. Natl. Acad. Sci. U. S. A.* **104**, 17719–17724 (2007).

212. Wang, Y., Luo, J., Zhang, H. & Lu, J. microRNAs in the Same Clusters Evolve to Coordinately Regulate Functionally Related Genes. *Mol. Biol. Evol.* **33**, 2232–2247 (2016).

213. Kabekkodu, S. P. *et al.* Clustered miRNAs and their role in biological functions and diseases: Biological regulation by miRNA clusters. *Biol. Rev.* **93**, 1955–1986 (2018).

214. Yuan, X. *et al.* Clustered microRNAs' coordination in regulating protein-protein interaction network. *BMC Syst. Biol.* **3**, 65 (2009).

215. Wang, J. *et al.* Regulatory coordination of clustered microRNAs based on microRNA-transcription factor regulatory network. *BMC Syst. Biol.* **5**, 199 (2011).

216. Ryazansky, S. S., Gvozdev, V. A. & Berezikov, E. Evidence for post-transcriptional regulation of clustered microRNAs in Drosophila. *BMC Genomics* **12**, 371 (2011).

217. Mohammed, J., Siepel, A. & Lai, E. C. Diverse modes of evolutionary emergence and flux of conserved microRNA clusters. *RNA* **20**, 1850–1863 (2014).

218. Marco, A., Ninova, M. & Griffiths-Jones, S. Multiple products from microRNA transcripts. *Biochem. Soc. Trans.* **41**, 850–4 (2013).

219. Sass, S. *et al.* MicroRNAs coordinately regulate protein complexes. *BMC Syst. Biol.* **5**, 136 (2011).

220. Xu, J. & Wong, C. A computational screen for mouse signaling pathways targeted by microRNA clusters. *RNA* **14**, 1276–1283 (2008).

221. Mogilyansky, E. & Rigoutsos, I. The miR-17/92 cluster: a comprehensive update on its genomics, genetics, functions and increasingly important and numerous roles in health and disease. *Cell Death Differ.* **20**, 1603–1614 (2013).

222. de Pontual, L. *et al.* Germline deletion of the miR-17-92 cluster causes growth and skeletal defects in humans. *Nat. Genet.* **43**, 1026–1030 (2011).

223. Wang, J. *et al.* Bmp Signaling Regulates Myocardial Differentiation from Cardiac Progenitors Through a MicroRNA-Mediated Mechanism. *Dev. Cell* **19**, 903–912 (2010).

224. Cordes, K. R. *et al.* miR-145 and miR-143 regulate smooth muscle cell fate and plasticity. *Nature* **460**, 705–710 (2009).

225. Wu, J. *et al.* Two miRNA clusters, miR-34b/c and miR-449, are essential for normal brain development, motile ciliogenesis, and spermatogenesis. *Proc. Natl. Acad. Sci.* **111**, E2851–E2857 (2014).

226. Mi, S. *et al.* Aberrant overexpression and function of the miR-17-92 cluster in MLL-rearranged acute leukemia. *Proc. Natl. Acad. Sci.* **107**, 3710–3715 (2010).

227. Olive, V., Li, Q. & He, L. mir-17-92: a polycistronic oncomir with pleiotropic functions. *Immunol. Rev.* **253**, 158–166 (2013).

228. Fuziwara, C. S. & Kimura, E. T. Insights into Regulation of the miR-17-92 Cluster of miRNAs in Cancer. *Front. Med.* **2**, (2015).

229. Weeraratne, S. D. *et al.* Pleiotropic effects of miR-183~96~182 converge to regulate cell survival, proliferation and migration in medulloblastoma. *Acta Neuropathol. (Berl.)* **123**, 539–552 (2012).

230. Aqeilan, R. I., Calin, G. A. & Croce, C. M. *miR-15a* and *miR-16-1* in cancer: discovery, function and future perspectives. *Cell Death Differ.* **17**, 215–220 (2010).

231. Bonci, D. *et al.* The *miR-15a–miR-16-1* cluster controls prostate cancer by targeting multiple oncogenic activities. *Nat. Med.* **14**, 1271–1277 (2008).

232. Bottoni, A. *et al.* miR-15a and miR-16-1 down-regulation in pituitary adenomas. *J. Cell. Physiol.* **204**, 280–285 (2005).

233. Furuta, M. *et al.* The Tumor-Suppressive miR-497-195 Cluster Targets Multiple Cell-Cycle Regulators in Hepatocellular Carcinoma. *PLOS ONE* **8**, e60155 (2013).

234. Almen, G. C. van *et al.* MicroRNA-18 and microRNA-19 regulate CTGF and TSP-1 expression in age-related heart failure. *Aging Cell* **10**, 769–779 (2011).

235. Dai, R. *et al.* Identification of a Common Lupus Disease-Associated microRNA Expression Pattern in Three Different Murine Models of Lupus. *PLOS ONE* **5**, e14302 (2010).

236. Pichler, S. *et al.* The miRNome of Alzheimer's disease: consistent downregulation of the miR-132/212 cluster. *Neurobiol. Aging* **50**, 167.e1-167.e10 (2017).

237. Lau, P. *et al.* Alteration of the microRNA network during the progression of Alzheimer's disease. *EMBO Mol. Med.* **5**, 1613–1634 (2013).

238. Finnerty, J. R. *et al.* The miR-15/107 Group of MicroRNA Genes: Evolutionary Biology, Cellular Functions, and Roles in Human Diseases. *J. Mol. Biol.* **402**, 491–509 (2010).

239. Seitz, H. *et al.* A Large Imprinted microRNA Gene Cluster at the Mouse Dlk1-Gtl2 Domain. *Genome Res.* 1741–1748 (2004) doi:10.1101/gr.2743304.

240. Glazov, E. a., McWilliam, S., Barris, W. C. & Dalrymple, B. P. Origin, evolution, and biological role of miRNA cluster in DLK-DIO3 genomic region in placental mammals. *Mol. Biol. Evol.* **25**, 939–948 (2008).

241. Tierling, S. *et al.* High-resolution map and imprinting analysis of the Gtl2-Dnchc1 domain on mouse chromosome 12. *Genomics* **87**, 225–35 (2006).

242. Benetatos, L., Vartholomatos, G. & Hatzimichael, E. MEG3 imprinted gene contribution in tumorigenesis. *Int. J. Cancer* **129**, 773–779 (2011).

243. Fiore, R. *et al.* Mef2-mediated transcription of the miR379–410 cluster regulates activity-dependent dendritogenesis by fine-tuning Pumilio2 protein levels. *EMBO J.* **28**, 697–710 (2009).

244. Snyder, C. M. *et al.* MEF2A regulates the Gtl2-Dio3 microRNA mega-cluster to modulate WNT signaling in skeletal muscle regeneration. *Dev. Camb. Engl.* **140**, 31–42 (2013).

245. Rago, L., Beattie, R., Taylor, V. & Winter, J. miR379–410 cluster miRNAs regulate neurogenesis and neuronal migration by fine-tuning N-cadherin. *EMBO J.* **33**, 906–920 (2014).

246. Gao, J. *et al.* A novel pathway regulates memory and plasticity via SIRT1 and miR-134. *Nature* **466**, 1105–1109 (2010).

247. Schratt, G. M. *et al.* A brain-specific microRNA regulates dendritic spine development. *Nature* **439**, 283–9 (2006).

248. Winter, J. MicroRNAs of the miR379–410 cluster: New players in embryonic neurogenesis and regulators of neuronal function. *Neurogenesis* **2**, (2015).

249. Abuhatzira, L. *et al.* Multiple microRNAs within the 14q32 cluster target the mRNAs of major type 1 diabetes autoantigens IA-2, IA-2β, and GAD65. *FASEB J. Off. Publ. Fed. Am. Soc. Exp. Biol.* **29**, 4374–83 (2015).

250. Gardiner, E. *et al.* Imprinted DLK1-DIO3 region of 14q32 defines a schizophrenia-associated miRNA signature in peripheral blood mononuclear cells. *Mol. Psychiatry* **17**, 827–40 (2012).

251. Welten, S. M. J. *et al.* Inhibition of 14q32 microRNAs miR-329, miR-487b, miR-494, and miR-495 increases neovascularization and blood flow recovery after ischemia. *Circ. Res.* **115**, 696–708 (2014).

252. Luk, J. M. *et al.* DLK1-DIO3 genomic imprinted microRNA cluster at 14q32.2 defines a stemlike subtype of hepatocellular carcinoma associated with poor survival. *J. Biol. Chem.* **286**, 30706–30713 (2011).

253. Bandrés, E. *et al.* Identification by Real-time PCR of 13 mature microRNAs differentially expressed in colorectal cancer and non-tumoral tissues. *Mol. Cancer* **5**, 29 (2006).

254. Haller, F. *et al.* Localization- and mutation-dependent microRNA (miRNA) expression signatures in gastrointestinal stromal tumours (GISTs), with a cluster of co-expressed miRNAs located at 14q32.31. *J. Pathol.* **220**, 71–86 (2010).

255. Zhang, L. *et al.* Genomic and epigenetic alterations deregulate microRNA expression in human epithelial ovarian cancer. *Proc Natl Acad Sci* **105**, 7004–7009 (2008).

256. Gattolliat, C.-H. *et al.* Expression of miR-487b and miR-410 encoded by 14q32.31 locus is a prognostic marker in neuroblastoma. *Br. J. Cancer* **105**, 1352–1361 (2011).

257. Guo, L. *et al.* Gene expression profiling of drug-resistant small cell lung cancer cells by combining microRNA and cDNA expression analysis. *Eur. J. Cancer* **46**, 1692–1702 (2010).

258. Williams, A. E., Moschos, S. A., Perry, M. M., Barnes, P. J. & Lindsay, M. A. Maternally imprinted microRNAs are differentially expressed during mouse and human lung development. *Dev. Dyn. Off. Publ. Am. Assoc. Anat.* **236**, 572–80 (2007).

259. Castilla, M. Á. *et al.* Micro-RNA signature of the epithelial–mesenchymal transition in endometrial carcinosarcoma. *J. Pathol.* **223**, 72–80 (2011).

260. Guled, M. *et al.* CDKN2A, NF2, and JUN are dysregulated among other genes by miRNAs in malignant mesothelioma—A miRNA microarray analysis. *Genes. Chromosomes Cancer* **48**, 615–623 (2009).

261. Yan, L.-X. *et al.* MicroRNA miR-21 overexpression in human breast cancer is associated with advanced clinical stage, lymph node metastasis and patient poor prognosis. *RNA* **14**, 2348–2360 (2008).

262. Bockmeyer, C. L. *et al.* MicroRNA profiles of healthy basal and luminal mammary epithelial cells are distinct and reflected in different breast cancer subtypes. *Breast Cancer Res. Treat.* **130**, 735–745 (2011).

263. Hwang-Verslues, W. W. *et al.* miR-495 is upregulated by E12/E47 in breast cancer stem cells, and promotes oncogenesis and hypoxia resistance via downregulation of E-cadherin and REDD1. *Oncogene* **30**, 2463–2474 (2011).

264. Lowery, A. J. *et al.* MicroRNA signatures predict oestrogen receptor, progesterone receptor and HER2/neureceptor status in breast cancer. *Breast Cancer Res.* **11**, R27 (2009).

265. Hill, K. E. *et al.* An imprinted non-coding genomic cluster at 14q32 defines clinically relevant molecular subtypes in osteosarcoma across multiple independent datasets. *J. Hematol. Oncol.J Hematol Oncol* **10**, (2017).

266. Ha, M. & Kim, V. N. Regulation of microRNA biogenesis. *Nat. Rev. Mol. Cell Biol.* **15**, 509–524 (2014).

267. Michlewski, G. & Caceres, J. F. Post-transcriptional control of miRNA biogenesis. *RNA* rna.068692.118 (2018) doi:10.1261/rna.068692.118.

268. Lee, Y. S. & Dutta, A. The tumor suppressor microRNA let-7 represses the HMGA2 oncogene. *Genes Dev.* **21**, 1025–1030 (2007).

269. Corcoran, D. L. *et al.* Features of Mammalian microRNA Promoters Emerge from Polymerase II Chromatin Immunoprecipitation Data. *PLOS ONE* **4**, e5279 (2009).

270. Bosia, C., Osella, M., Baroudi, M. E., Corà, D. & Caselle, M. Gene autoregulation via intronic microRNAs and its functions. *BMC Syst. Biol.* **6**, 131 (2012).

271. Megraw, M. *et al.* Isoform specific gene auto-regulation via miRNAs: a case study on miR-128b and ARPP-21. *Theor. Chem. Acc.* **125**, 593–598 (2010).

272. Rao, P. K., Kumar, R. M., Farkhondeh, M., Baskerville, S. & Lodish, H. F. Myogenic factors that regulate expression of muscle-specific microRNAs. *Proc. Natl. Acad. Sci.* **103**, 8721–8726 (2006).

273. Zhao, Y., Samal, E. & Srivastava, D. Serum response factor regulates a muscle-specific microRNA that targets *Hand2* during cardiogenesis. *Nature* **436**, 214–220 (2005).

274. Conaco, C., Otto, S., Han, J.-J. & Mandel, G. Reciprocal actions of REST and a microRNA promote neuronal identity. *Proc. Natl. Acad. Sci.* **103**, 2422–2427 (2006).

275. Kim, J. *et al.* A MicroRNA Feedback Circuit in Midbrain Dopamine Neurons. *Science* **317**, 1220–1224 (2007).

276. Ben-Ami, O., Pencovich, N., Lotem, J., Levanon, D. & Groner, Y. A regulatory interplay between miR-27a and Runx1 during megakaryopoiesis. *Proc. Natl. Acad. Sci.* **106**, 238–243 (2009).

277. Zhao, H., Kalota, A., Jin, S. & Gewirtz, A. M. The c-myb proto-oncogene and microRNA-15a comprise an active autoregulatory feedback loop in human hematopoietic cells. *Blood* **113**, 505–516 (2009).

278. He, L., He, X., Lowe, S. W. & Hannon, G. J. microRNAs join the p53 network — another piece in the tumour-suppression puzzle. *Nat. Rev. Cancer* **7**, 819–822 (2007).

279. Ma, L. *et al.* miR-9, a MYC/MYCN-activated microRNA, regulates E-cadherin and cancer metastasis. *Nat. Cell Biol.* **12**, 247–256 (2010).

280. Han, L., Witmer, P. D. W., Casey, E., Valle, D. & Sukumar, S. DNA methylation regulates microRNA expression. *Cancer Biol. Ther.* **6**, 1290–1294 (2007).

281. Lujambio, A. *et al.* A microRNA DNA methylation signature for human cancer metastasis. *Proc. Natl. Acad. Sci.* **105**, 13556–13561 (2008).

282. Bueno, M. J. *et al.* Genetic and Epigenetic Silencing of MicroRNA-203 Enhances ABL1 and BCR-ABL1 Oncogene Expression. *Cancer Cell* **13**, 496–506 (2008).

283. Saito, Y. *et al.* Specific activation of microRNA-127 with downregulation of the proto-oncogene BCL6 by chromatin-modifying drugs in human cancer cells. *Cancer Cell* **9**, 435–443 (2006).

284. Brueckner, B. *et al.* The Human let-7a-3 Locus Contains an Epigenetically Regulated MicroRNA Gene with Oncogenic Function. *Cancer Res.* **67**, 1419–1423 (2007).

285. Conrad, T., Marsico, A., Gehre, M. & Ørom, U. A. Microprocessor Activity Controls Differential miRNA Biogenesis In Vivo. *Cell Rep.* **9**, 542–554 (2014).

286. Creugny, A., Fender, A. & Pfeffer, S. Regulation of primary microRNA processing. *FEBS Lett.* **592**, 1980–1996 (2018).

287. Chaulk, S. G. *et al.* Role of pri-miRNA tertiary structure in miR-17~92 miRNA biogenesis. *RNA Biol.* **8**, 1105–1114 (2011).

288. Contrant, M. *et al.* Importance of the RNA secondary structure for the relative accumulation of clustered viral microRNAs. *Nucleic Acids Res.* **42**, 7981–7996 (2014).

289. Suzuki, H. I. *et al.* Modulation of microRNA processing by p53. *Nature* **460**, 529–533 (2009).

290. Davis, B. N., Hilyard, A. C., Lagna, G. & Hata, A. SMAD proteins control DROSHA-mediated microRNA maturation. *Nature* **454**, 56–61 (2008).

291. Mori, M. *et al.* Hippo Signaling Regulates Microprocessor and Links Cell-Density-Dependent miRNA Biogenesis to Cancer. *Cell* **156**, 893–906 (2014).

292. Kawai, S. & Amano, A. BRCA1 regulates microRNA biogenesis via the DROSHA microprocessor complex. *J Cell Biol* **197**, 201–208 (2012).

293. Sakamoto, S. *et al.* The NF90-NF45 Complex Functions as a Negative Regulator in the MicroRNA Processing Pathway. *Mol. Cell. Biol.* **29**, 3754–3769 (2009).

294. Todaka, H. *et al.* Overexpression of NF90-NF45 Represses Myogenic MicroRNA Biogenesis, Resulting in Development of Skeletal Muscle Atrophy and Centronuclear Muscle Fibers. *Mol. Cell. Biol.* **35**, 2295–2308 (2015).

295. Higuchi, T. *et al.* Suppression of MicroRNA-7 (miR-7) Biogenesis by Nuclear Factor 90-Nuclear Factor 45 Complex (NF90-NF45) Controls Cell Proliferation in Hepatocellular Carcinoma. *J. Biol. Chem.* **291**, 21074–21084 (2016).

296. Choudhury, N. R. *et al.* Tissue-specific control of brain-enriched miR-7 biogenesis. *Genes Dev.* **27**, 24–38 (2013).

297. Kefas, B. *et al.* microRNA-7 inhibits the epidermal growth factor receptor and the akt pathway and is down-regulated in glioblastoma. *Cancer Res.* **68**, 3566–3572 (2008).

298. Michlewski, G., Guil, S., Semple, C. A. & Cáceres, J. F. Posttranscriptional regulation of miRNAs harboring conserved terminal loops. *Mol. Cell* **32**, 383–93 (2008).

299. Guil, S. & Cáceres, J. F. The multifunctional RNA-binding protein hnRNP A1 is required for processing of miR-18a. *Nat. Struct. Mol. Biol.* **14**, 591–596 (2007).

300. Michlewski, G. & Cáceres, J. F. Antagonistic role of hnRNP A1 and KSRP in the regulation of let-7a biogenesis. *Nat. Struct. Mol. Biol.* **17**, 1011–8 (2010).

301. Trabucchi, M. *et al.* The RNA-binding protein KSRP promotes the biogenesis of a subset of microRNAs. *Nature* **459**, 1010–4 (2009).

302. Park, J.-E. *et al.* Dicer recognizes the 5′ end of RNA for efficient and accurate processing. *Nature* **475**, 201–205 (2011).

303. Heo, I. *et al.* Mono-Uridylation of Pre-MicroRNA as a Key Step in the Biogenesis of Group II let-7 MicroRNAs. *Cell* **151**, 521–532 (2012).

304. Xhemalce, B., Robson, S. C. & Kouzarides, T. Human RNA Methyltransferase BCDIN3D Regulates MicroRNA Processing. *Cell* **151**, 278–288 (2012).

305. Chendrimada, T. P. *et al.* TRBP recruits the Dicer complex to Ago2 for microRNA processing and gene silencing. *Nature* **436**, 740–744 (2005).

306. Haase, A. D. *et al.* TRBP, a regulator of cellular PKR and HIV-1 virus expression, interacts with Dicer and functions in RNA silencing. *EMBO Rep.* **6**, 961–967 (2005).

307. Lee, Y. *et al.* The role of PACT in the RNA silencing pathway. *EMBO J.* **25**, 522–32 (2006).

308. Chakravarthy, S., Sternberg, S. H., Kellenberger, C. & Doudna, J. A. Substrate-specific kinetics of Dicer-catalyzed RNA Processing. *J. Mol. Biol.* **404**, 392–402 (2010).

309. Lee, H. Y. & Doudna, J. A. TRBP alters human precursor microRNA processing in vitro. *RNA N. Y. N* **18**, 2012–2019 (2012).

310. Fukunaga, R. *et al.* Dicer Partner Proteins Tune the Length of Mature miRNAs in Flies and Mammals. *Cell* **151**, 533–546 (2012).

311. Lee, H. Y., Zhou, K., Smith, A. M., Noland, C. L. & Doudna, J. A. Differential roles of human Dicer-binding proteins TRBP and PACT in small RNA processing. *Nucleic Acids Res.* **41**, 6568–6576 (2013).

312. Wilson, R. C. *et al.* Dicer-TRBP Complex Formation Ensures Accurate Mammalian MicroRNA Biogenesis. *Mol. Cell* **57**, 397–407 (2015).

313. Pilotte, J., Dupont-Versteegden, E. E. & Vanderklish, P. W. Widespread Regulation of miRNA Biogenesis at the Dicer Step by the Cold-Inducible RNA-Binding Protein, RBM3. *PLoS ONE* **6**, (2011).

314. Rau, F. *et al.* Misregulation of miR-1 processing is associated with heart defects in myotonic dystrophy. *Nat. Struct. Mol. Biol.* **18**, 840–845 (2011).

315. Kawahara, Y. & Mieda-Sato, A. TDP-43 promotes microRNA biogenesis as a component of the Drosha and Dicer complexes. *Proc. Natl. Acad. Sci. U. S. A.* **109**, 3347–52 (2012).

316. Wu, S.-L. *et al.* Genome-wide analysis of YB-1-RNA interactions reveals a novel role of YB-1 in miRNA processing in glioblastoma multiforme. *Nucleic Acids Res.* **43**, 8516–8528 (2015).

317. Mayr, C., Hemann, M. T. & Bartel, D. P. Disrupting the Pairing Between let-7 and Hmga2 Enhances Oncogenic Transformation. *Science* **315**, 1576–1579 (2007).

318. Johnson, S. M. *et al.* RAS Is Regulated by the let-7 MicroRNA Family. *Cell* **120**, 635–647 (2005).

319. Kumar, M. S., Lu, J., Mercer, K. L., Golub, T. R. & Jacks, T. Impaired microRNA processing enhances cellular transformation and tumorigenesis. *Nat. Genet.* **39**, 673–677 (2007).

320. Suh, M.-R. *et al.* Human embryonic stem cells express a unique set of microRNAs. *Dev. Biol.* **270**, 488–498 (2004).

321. Wulczyn, F. G. *et al.* Post-transcriptional regulation of the let-7 microRNA during neural cell specification. *FASEB J.* **21**, 415–426 (2006).

322. Yu, J. *et al.* Induced Pluripotent Stem Cell Lines Derived from Human Somatic Cells. *Science* **318**, 1917–1920 (2007).

323. Viswanathan, S. R. & Daley, G. Q. Lin28: A MicroRNA Regulator with a Macro Role. *Cell* **140**, 445–449 (2010).

324. Guo, Y. *et al.* Identification and characterization of lin-28 homolog B (LIN28B) in human hepatocellular carcinoma. *Gene* **384**, 51–61 (2006).

325. Piskounova, E. *et al.* Determinants of MicroRNA Processing Inhibition by the Developmentally Regulated RNA-binding Protein Lin28. *J. Biol. Chem.* **283**, 21310–21314 (2008).

326. Lightfoot, H. L. *et al.* A LIN28-Dependent Structural Change in pre-let-7g Directly Inhibits Dicer Processing. *Biochemistry* **50**, 7514–7521 (2011).

327. Heo, I. *et al.* TUT4 in Concert with Lin28 Suppresses MicroRNA Biogenesis through Pre-MicroRNA Uridylation. *Cell* **138**, 696–708 (2009).

328. Hagan, J. P., Piskounova, E. & Gregory, R. I. Lin28 recruits the TUTase Zcchc11 to inhibit let-7 maturation in mouse embryonic stem cells. *Nat. Struct. Mol. Biol.* **16**, 1021–1025 (2009).

329. Chang, H.-M., Triboulet, R., Thornton, J. E. & Gregory, R. I. A role for the Perlman syndrome exonuclease Dis3l2 in the Lin28–let-7 pathway. *Nature* **497**, 244–248 (2013).

330. Ustianenko, D. *et al.* Mammalian DIS3L2 exoribonuclease targets the uridylated precursors of let-7 miRNAs. *RNA* **19**, 1632–1638 (2013).

331. Choudhury, N. R. *et al.* Trim25 Is an RNA-Specific Activator of Lin28a/TuT4-Mediated Uridylation. *Cell Rep.* **9**, 1265–1272 (2014).

332. Yang, W. *et al.* Modulation of microRNA processing and expression through RNA editing by ADAR deaminases. *Nat. Struct. Mol. Biol.* **13**, 13–21 (2006).

333. Vesely, C. *et al.* ADAR2 induces reproducible changes in sequence and abundance of mature microRNAs in the mouse brain. *Nucleic Acids Res.* **42**, 12155–12168 (2014).

334. Kawahara, Y. *et al.* Redirection of Silencing Targets by Adenosine-to-Inosine Editing of miRNAs. *Science* **315**, 1137–1140 (2007).

335. Kawahara, Y. *et al.* Frequency and fate of microRNA editing in human brain. *Nucleic Acids Res.* **36**, 5270–5280 (2008).

336. Choudhury, Y. *et al.* Attenuated adenosine-to-inosine editing of microRNA-376a* promotes invasiveness of glioblastoma cells. *J. Clin. Invest.* **122**, 4059–4076 (2012).

337. Kawahara, Y. *et al.* RNA editing of the microRNA-151 precursor blocks cleavage by the Dicer-TRBP complex. *EMBO Rep.* **8**, 763–9 (2007).

338. Blow, M. J. *et al.* RNA editing of human microRNAs. *Genome Biol.* **7**, R27 (2006).

339. Ota, H. *et al.* ADAR1 forms a complex with Dicer to promote microRNA processing and RNA-induced gene silencing. *Cell* **153**, 575–589 (2013).

340. Heale, B. S. E. *et al.* Editing independent effects of ADARs on the miRNA/siRNA pathways. *EMBO J.* **28**, 3145–3156 (2009).

341. Gantier, M. P. *et al.* Analysis of microRNA turnover in mammalian cells following Dicer1 ablation. *Nucleic Acids Res.* **39**, 5692–5703 (2011).

342. Baccarini, A. *et al.* Kinetic analysis reveals the fate of a microRNA following target regulation in mammalian cells. *Curr. Biol. CB* **21**, 369–376 (2011).

343. Katoh, T. *et al.* Selective stabilization of mammalian microRNAs by 3' adenylation mediated by the cytoplasmic poly(A) polymerase GLD-2. *Genes Dev.* **23**, 433–438 (2009).

344. Backes, S. *et al.* Degradation of Host MicroRNAs by Poxvirus Poly(A) Polymerase Reveals Terminal RNA Methylation as a Protective Antiviral Mechanism. *Cell Host Microbe* **12**, 200–210 (2012).

345. Rüegger, S. & Großhans, H. MicroRNA turnover: when, how, and why. *Trends Biochem. Sci.* **37**, 436–446 (2012).

346. Ameres, S. L. *et al.* Target RNA-directed trimming and tailing of small silencing RNAs. *Science* **328**, 1534–1539 (2010).

347. Haas, G. *et al.* Identification of factors involved in target RNA-directed microRNA degradation. *Nucleic Acids Res.* **44**, 2873–2887 (2016).

348. Scherrer, T., Mittal, N., Janga, S. C. & Gerber, A. P. A Screen for RNA-Binding Proteins in Yeast Indicates Dual Functions for Many Enzymes. *PLoS ONE* **5**, e15499 (2010).

349. Tsvetanova, N. G., Klass, D. M., Salzman, J. & Brown, P. O. Proteome-Wide Search Reveals Unexpected RNA-Binding Proteins in Saccharomyces cerevisiae. *PLoS ONE* **5**, e12671 (2010).

350. Baltz, A. G. *et al.* The mRNA-bound proteome and its global occupancy profile on protein-coding transcripts. *Mol. Cell* **46**, 674–90 (2012).

351. Castello, A. *et al.* Insights into RNA Biology from an Atlas of Mammalian mRNA-Binding Proteins. *Cell* **149**, 1393–1406 (2012).

352. Castello, A., Hentze, M. W. & Preiss, T. Metabolic Enzymes Enjoying New Partnerships as RNA-Binding Proteins. *Trends Endocrinol. Metab. TEM* **26**, 746–57 (2015).

353. Hentze, M. W. Enzymes as RNA-binding proteins: a role for (di)nucleotide-binding domains? *Trends Biochem. Sci.* **19**, 101–103 (1994).

354. Cieśla, J. Metabolic enzymes that bind RNA: yet another level of cellular regulatory network? *Acta Biochim. Pol.* (2006).

355. Panda, S. *et al.* Coordinated Transcription of Key Pathways in the Mouse by the Circadian Clock. *Cell* **109**, 307–320 (2002).

356. Hong, S.-H. *et al.* Nuclear receptors and metabolism: from feast to famine. *Diabetologia* **57**, 860–867 (2014).

357. Reddy, A. B. *et al.* Circadian Orchestration of the Hepatic Proteome. *Curr. Biol.* **16**, 1107–1115 (2006).

358. Eckel-Mahan, K. & Sassone-Corsi, P. Metabolism and the Circadian Clock Converge. *Physiol. Rev.* **93**, 107–135 (2013).

359. Jeffery, C. J. Moonlighting proteins. *Trends Biochem. Sci.* **24**, 8–11 (1999).

360. Hentze, M. W. & Argos, P. Homology between IRE-BP, a regulatory RNA-binding protein, aconitase, and isopropylmalate isomerase. *Nucleic Acids Res.* **19**, 1739–1740 (1991).

361. Hentze, M. W. & Kühn, L. C. Molecular control of vertebrate iron metabolism: mRNA-based regulatory circuits operated by iron, nitric oxide, and oxidative stress. *Proc. Natl. Acad. Sci. U. S. A.* **93**, 8175–8182 (1996).

362. Rouault, T. A., Stout, C. D., Kaptain, S., Harford, J. B. & Klausner, R. D. Structural relationship between an iron-regulated RNA-binding protein (IRE-BP) and aconitase: Functional implications. *Cell* **64**, 881–883 (1991).

363. Klausner, R. D. & Rouault, T. A. A double life: cytosolic aconitase as a regulatory RNA binding protein. *Mol. Biol. Cell* **4**, 1–5 (1993).

364. Nagy, E. & Rigby, W. F. C. Glyceraldehyde-3-phosphate Dehydrogenase Selectively Binds AU-rich RNA in the NAD+-binding Region (Rossmann Fold). *J. Biol. Chem.* **270**, 2755–2763 (1995).

365. Nagy, E. *et al.* Identification of the NAD+-Binding Fold of Glyceraldehyde-3-Phosphate Dehydrogenase as a Novel RNA-Binding Domain. *Biochem. Biophys. Res. Commun.* **275**, 253–260 (2000).

366. Espel, E. The role of the AU-rich elements of mRNAs in controlling translation. *Semin. Cell Dev. Biol.* **16**, 59–67 (2005).

367. Qi, M.-Y. *et al.* AU-Rich-Element-Dependent Translation Repression Requires the Cooperation of Tristetraprolin and RCK/P54. *Mol. Cell. Biol.* **32**, 913–928 (2012).

368. Chang, C.-H. *et al.* Posttranscriptional Control of T Cell Effector Function by Aerobic Glycolysis. *Cell* **153**, 1239–1251 (2013).

369. Nakagawa, J. *et al.* AUH, a gene encoding an AU-specific RNA binding protein with intrinsic enoyl-CoA hydratase activity. *Proc. Natl. Acad. Sci. U. S. A.* **92**, 2051–2055 (1995).

370. Mack, M. *et al.* Biochemical characterization of human 3-methylglutaconyl-CoA hydratase and its role in leucine metabolism. *FEBS J.* **273**, 2012–2022 (2006).

371. Kurimoto, K., Fukai, S., Nureki, O., Muto, Y. & Yokoyama, S. Crystal Structure of Human AUH Protein, a Single-Stranded RNA Binding Homolog of Enoyl-CoA Hydratase. *Structure* **9**, 1253–1263 (2001).

372. Richman, T. R. *et al.* A bifunctional protein regulates mitochondrial protein synthesis. *Nucleic Acids Res.* **42**, 5483–5494 (2014).

373. Holzmann, J. *et al.* RNase P without RNA: Identification and Functional Reconstitution of the Human Mitochondrial tRNA Processing Enzyme. *Cell* **135**, 462–474 (2008).

374. Chatfield, K. C. *et al.* Mitochondrial energy failure in HSD10 disease is due to defective mtDNA transcript processing. *Mitochondrion* **21**, 1–10 (2015).

375. Adams, D. J. *et al.* HADHB, HuR, and CP1 Bind to the Distal 3'-Untranslated Region of Human Renin mRNA and Differentially Modulate Renin Expression. *J. Biol. Chem.* **278**, 44894–44903 (2003).

376. Elzinga, S. D., Bednarz, A. L., van Oosterum, K., Dekker, P. J. & Grivell, L. A. Yeast mitochondrial NAD(+)-dependent isocitrate dehydrogenase is an RNA-binding protein. *Nucleic Acids Res.* **21**, 5328–5331 (1993).

377. Anderson, S. L., Minard, K. I. & McAlister-Henn, L. Allosteric Inhibition of NAD+-Specific Isocitrate Dehydrogenase by a Mitochondrial mRNA. *Biochemistry* **39**, 5623–5629 (2000).

378. Xing, S. & Poirier, Y. The protein acetylome and the regulation of metabolism. *Trends Plant Sci.* **17**, 423–430 (2012).

379. Blee, T. K. P., Gray, N. K. & Brook, M. Modulation of the cytoplasmic functions of mammalian post-transcriptional regulatory proteins by methylation and acetylation: a key layer of regulation waiting to be uncovered? *Biochem. Soc. Trans.* **43**, 1285–1295 (2015).

380. Babic, I., Jakymiw, A. & Fujita, D. J. The RNA binding protein Sam68 is acetylated in tumor cell lines, and its acetylation correlates with enhanced RNA binding activity. *Oncogene* **23**, 3781–3789 (2004).

381. Kumar, S. & Maiti, S. The Effect of N-acetylation and N-methylation of Lysine Residue of Tat Peptide on its Interaction with HIV-1 TAR RNA. *PLOS ONE* **8**, e77595 (2013).

382. Clingman, C. C. *et al.* Allosteric inhibition of a stem cell RNA-binding protein by an intermediary metabolite. *eLife* **3**, (2014).

383. Nowak, J. S., Choudhury, N. R., de Lima Alves, F., Rappsilber, J. & Michlewski, G. Lin28a regulates neuronal differentiation and controls miR-9 production. *Nat. Commun.* **5**, 3687 (2014).

384. Nowak-Sliwinska, P. *et al.* Consensus guidelines for the use and interpretation of angiogenesis assays. (2018) doi:PG/10/94/28651.

385. Nossent, A. Y. *et al.* CCR7-CCL19/CCL21 Axis is Essential for Effective Arteriogenesis in a Murine Model of Hindlimb Ischemia. *J. Am. Heart Assoc. Cardiovasc. Cerebrovasc. Dis.* **6**, (2017).

386. Tuffy, K. M. & Planey, S. L. Cytoskeleton-Associated Protein 4: Functions Beyond the Endoplasmic Reticulum in Physiology and Disease. *International Scholarly Research Notices* https://www.hindawi.com/journals/isrn/2012/142313/ (2012) doi:10.5402/2012/142313.

387. Zhong, P. & Huang, H. Recent progress in the research of cold-inducible RNA-binding protein. *Future Sci. OA* **3**, (2017).

388. Liao, Y., Tong, L., Tang, L. & Wu, S. The role of cold-inducible RNA binding protein in cell stress response. *Int. J. Cancer* **141**, 2164–2173 (2017).

389. Ngoc-Tung, T., Su, H., Lu, Y., Leslie, C. S. & Zhao, X. RBM15-Mediated RNA Splicing Fine-Tunes Epigenetic Program through Interaction with SF3B1. *Blood* **126**, 4110–4110 (2015).

390. Lesbirel, S. & Wilson, S. A. The m6A-methylase complex and mRNA export. *Biochim. Biophys. Acta BBA - Gene Regul. Mech.* **1862**, 319–328 (2019).

391. Moindrot, B. *et al.* A Pooled shRNA Screen Identifies Rbm15, Spen, and Wtap as Factors Required for Xist RNA-Mediated Silencing. *Cell Rep.* **12**, 562–572 (2015).

392. Li, J. Y., Daniels, G., Wang, J. & Zhang, X. TBL1XR1 in physiological and pathological states. *Am. J. Clin. Exp. Urol.* **3**, 13–23 (2015).

393. Liang, K. *et al.* Cryo-EM structure of human mitochondrial trifunctional protein. *Proc. Natl. Acad. Sci.* **115**, 7039–7044 (2018).

394. Wilkinson, B. & Gilbert, H. F. Protein disulfide isomerase. *Biochim. Biophys. Acta BBA - Proteins Proteomics* **1699**, 35–44 (2004).

395. Damianov, A., Kann, M., Lane, W. S. & Bindereif, A. Human RBM28 protein is a specific nucleolar component of the spliceosomal snRNPs. *Biol. Chem.* **387**, (2006).

396. Israelsen, W. J. & Vander Heiden, M. G. Pyruvate kinase: Function, regulation and role in cancer. *Semin. Cell Dev. Biol.* **43**, 43–51 (2015).

397. Fu, X. *et al.* Mitochondrial trifunctional protein deficiency due to HADHB gene mutation in a Chinese family. *Mol. Genet. Metab. Rep.* **5**, 80–84 (2015).

398. Orii, K. E. *et al.* Genomic and Mutational Analysis of the Mitochondrial Trifunctional Protein β-Subunit (HADHB) Gene in Patients with Trifunctional Protein Deficiency. *Hum. Mol. Genet.* **6**, 1215–1224 (1997).

399. Xia, C., Fu, Z., Battaile, K. P. & Kim, J.-J. P. Crystal structure of human mitochondrial trifunctional protein, a fatty acid β-oxidation metabolon. *Proc. Natl. Acad. Sci.* **116**, 6069–6074 (2019).

400. Venkatesan, R. & Wierenga, R. K. Structure of Mycobacterial β-Oxidation Trifunctional Enzyme Reveals Its Altered Assembly and Putative Substrate Channeling Pathway. *ACS Chem. Biol.* **8**, 1063–1073 (2013).

401. Morris, B. J. *et al.* cAMP controls human renin mRNA stability via specific RNA-binding proteins. *Acta Physiol. Scand.* **181**, 369–373 (2004).

402. Nishiyama, H. *et al.* A Glycine-rich RNA-binding Protein Mediating Cold-inducible Suppression of Mammalian Cell Growth. *J. Cell Biol.* **137**, 899–908 (1997).

403. Sheikh, M. S. *et al.* Identification of Several Human Homologs of Hamster DNA Damage-inducible Transcripts CLONING AND CHARACTERIZATION OF A NOVEL UV-INDUCIBLE cDNA THAT CODES FOR A PUTATIVE RNA-BINDING PROTEIN. *J. Biol. Chem.* **272**, 26720–26726 (1997).

404. Wellmann, S. *et al.* Oxygen-regulated expression of the RNA-binding proteins RBM3 and CIRP by a HIF-1-independent mechanism. *J. Cell Sci.* **117**, 1785–94 (2004).

405. Sumitomo, Y. *et al.* Identification of a novel enhancer that binds Sp1 and contributes to induction of cold-inducible RNA-binding protein (cirp) expression in mammalian cells. *BMC Biotechnol.* **12**, 72 (2012).

406. Gotic, I. *et al.* Temperature regulates splicing efficiency of the cold-inducible RNA-binding protein gene Cirbp. *Genes Dev.* **30**, 2005–2017 (2016).

407. Al-Fageeh, M. B. & Smales, C. M. Cold-inducible RNA binding protein (CIRP) expression is modulated by alternative mRNAs. *RNA* **15**, 1164–1176 (2009).

408. De Leeuw, F. *et al.* The cold-inducible RNA-binding protein migrates from the nucleus to cytoplasmic stress granules by a methylation-dependent mechanism and acts as a translational repressor. *Exp. Cell Res.* **313**, 4130–4144 (2007).

409. Zhou, M., Yang, W.-L., Ji, Y., Qiang, X. & Wang, P. Cold-inducible RNA-binding protein mediates neuroinflammation in cerebral ischemia. *Biochim. Biophys. Acta BBA - Gen. Subj.* **1840**, 2253–2261 (2014).

410. Yang, R., Weber, D. J. & Carrier, F. Post-transcriptional regulation of thioredoxin by the stress inducible heterogenous ribonucleoprotein A18. *Nucleic Acids Res.* **34**, 1224–1236 (2006).

411. Tang, C. *et al.* Analysis of gene expression profiles reveals the regulatory network of cold-inducible RNA-binding protein mediating the growth of BHK-21 cells. *Cell Biol. Int.* **39**, 678–689 (2015).

412. Xia, Z. *et al.* Cold-inducible RNA-binding protein (CIRP) regulates target mRNA stabilization in the mouse testis. *FEBS Lett.* **586**, 3299–3308 (2012).

413. Chang, E. T., Parekh, P. R., Yang, Q., Nguyen, D. M. & Carrier, F. Heterogenous ribonucleoprotein A18 (hnRNP A18) promotes tumor growth by increasing protein translation of selected transcripts in cancer cells. *Oncotarget* **7**, 10578–10593 (2016).

414. Chen, X. *et al.* Cold Inducible RNA Binding Protein Is Involved in Chronic Hypoxia Induced Neuron Apoptosis by Down-Regulating HIF-1α Expression and Regulated By microRNA-23a. *Int. J. Biol. Sci.* **13**, 518–531 (2017).

415. Yang, C. & Carrier, F. The UV-inducible RNA-binding Protein A18 (A18 hnRNP) Plays a Protective Role in the Genotoxic Stress Response. *J. Biol. Chem.* **276**, 47277–47284 (2001).

416. Yang, R. *et al.* Functional Significance for a Heterogenous Ribonucleoprotein A18 Signature RNA Motif in the 3'-Untranslated Region of Ataxia Telangiectasia Mutated and Rad3-related (ATR) Transcript. *J. Biol. Chem.* **285**, 8887–8893 (2010).

417. Liu, Y. *et al.* Cold-induced RNA-binding proteins regulate circadian gene expression by controlling alternative polyadenylation. *Sci. Rep.* **3**, (2013).

418. Zhang, Q. *et al.* Involvement of Cold Inducible RNA-Binding Protein in Severe Hypoxia-Induced Growth Arrest of Neural Stem Cells In Vitro. *Mol. Neurobiol.* **54**, 2143–2153 (2017).

419. Masuda, T. *et al.* Cold-inducible RNA-binding protein (Cirp) interacts with Dyrk1b/Mirk and promotes proliferation of immature male germ cells in mice. *Proc. Natl. Acad. Sci. U. S. A.* **109**, 10885–10890 (2012).

420. Gharbi, S. *et al.* Identification of Reliable Reference Genes for Quantification of MicroRNAs in Serum Samples of Sulfur Mustard-Exposed Veterans. *Cell J. Yakhteh* **17**, 494–501 (2015).

421. Liang, Y., Ridzon, D., Wong, L. & Chen, C. Characterization of microRNA expression profiles in normal human tissues. *BMC Genomics* **8**, 166 (2007).

422. Babion, I., Snoek, B. C., van de Wiel, M. A., Wilting, S. M. & Steenbergen, R. D. M. A Strategy to Find Suitable Reference Genes for miRNA Quantitative PCR Analysis and Its Application to Cervical Specimens. *J. Mol. Diagn.* **19**, 625–637 (2017).

423. Abraham, S., Montoya, R. T., Edelstein, L. C., McKenzie, S. E. & Bray, P. F. Identification of Reference Genes for miRNA Profiling in Hematopoietic Cell Lineages. *Blood* **120**, 3330–3330 (2012).

424. Lu, M. *et al.* CIRBP is a novel oncogene in human bladder cancer inducing expression of HIF-1α. *Cell Death Dis.* **9**, 1046 (2018).

425. Solomon, S. S., Majumdar, G., Martinez-Hernandez, A. & Raghow, R. A critical role of Sp1 transcription factor in regulating gene expression in response to insulin and other hormones. *Life Sci.* **83**, 305–312 (2008).

426. Chu, S. Transcriptional regulation by post-transcriptional modification—Role of phosphorylation in Sp1 transcriptional activity. *Gene* **508**, 1–8 (2012).

427. Yeh, S. H. *et al.* Translational and transcriptional control of Sp1 against ischaemia through a hydrogen peroxide-activated internal ribosomal entry site pathway. *Nucleic Acids Res.* **39**, 5412–5423 (2011).

428. Udelhoven, M., Pasieka, M., Leeser, U., Krone, W. & Schubert, M. Neuronal insulin receptor substrate 2 (IRS2) expression is regulated by ZBP89 and SP1 binding to the IRS2 promoter. *J. Endocrinol.* **204**, 199–208 (2010).

429. Koizume, S. & Miyagi, Y. Anti-apoptotic genes are synergistically activated in OVSAYO cells cultured under conditions of serum starvation and hypoxia. *Genomics Data* **5**, 129–131 (2015).

430. Ming, L. *et al.* Sp1 and p73 activate PUMA following serum starvation. *Carcinogenesis* **29**, 1878–1884 (2008).

431. Woo, S. K. *et al.* Sequential activation of hypoxia-inducible factor 1 and specificity protein 1 is required for hypoxia-induced transcriptional stimulation of Abcc8. *J. Cereb. Blood Flow Metab.* **32**, 525–536 (2012).

432. Miki, N., Ikuta, M. & Matsui, T. Hypoxia-induced Activation of the Retinoic Acid Receptor-related Orphan Receptor α4 Gene by an Interaction between Hypoxia-inducible Factor-1 and Sp1. *J. Biol. Chem.* **279**, 15025–15031 (2004).

433. Jin, H.-O. *et al.* Hypoxic condition- and high cell density-induced expression of Redd1 is regulated by activation of hypoxia-inducible factor-1alpha and Sp1 through the phosphatidylinositol 3-kinase/Akt signaling pathway. *Cell. Signal.* **19**, 1393–1403 (2007).

434. Qiang, X. *et al.* Cold-inducible RNA-binding protein (CIRP) triggers inflammatory responses in hemorrhagic shock and sepsis. *Nat. Med.* **19**, 1489–1495 (2013).

435. Aoki, K., Ishii, Y., Matsumoto, K. & Tsujimoto, M. Methylation of Xenopus CIRP2 regulates its arginine- and glycine-rich region-mediated nucleocytoplasmic distribution. *Nucleic Acids Res.* **30**, 5182–5192 (2002).

436. Lim, S. K. *et al.* Activation of PRMT1 and PRMT5 mediates hypoxia- and ischemia-induced apoptosis in human lung epithelial cells and the lung of miniature pigs: The role of p38 and JNK mitogen-activated protein kinases. *Biochem. Biophys. Res. Commun.* **440**, 707–713 (2013).

437. Loberg, R. D., Vesely, E. & Brosius, F. C. Enhanced glycogen synthase kinase-3beta activity mediates hypoxia-induced apoptosis of vascular smooth muscle cells and is prevented by glucose transport and metabolism. *J. Biol. Chem.* **277**, 41667–41673 (2002).

438. Mottet, D. *et al.* Regulation of Hypoxia-inducible Factor-1α Protein Level during Hypoxic Conditions by the Phosphatidylinositol 3-Kinase/Akt/Glycogen

Synthase Kinase 3β Pathway in HepG2 Cells. *J. Biol. Chem.* **278**, 31277–31285 (2003).

439. Chen, E. Y., Mazure, N. M., Cooper, J. A. & Giaccia, A. J. Hypoxia Activates a Platelet-derived Growth Factor Receptor/Phosphatidylinositol 3-Kinase/Akt Pathway That Results in Glycogen Synthase Kinase-3 Inactivation. *Cancer Res.* **61**, 2429–2433 (2001).

440. Zhu, X., Bührer, C. & Wellmann, S. Cold-inducible proteins CIRP and RBM3, a unique couple with activities far beyond the cold. *Cell. Mol. Life Sci.* (2016) doi:10.1007/s00018-016-2253-7.

441. Wong, J. J.-L. *et al.* RBM3 regulates temperature sensitive miR-142–5p and miR-143 (thermomiRs), which target immune genes and control fever. *Nucleic Acids Res.* **44**, 2888–2897 (2016).

442. Kakumani, P. K. *et al.* Association of HADHA with human RNA silencing machinery. *Biochem. Biophys. Res. Commun.* **466**, 481–485 (2015).

443. Kantor Paul F., Lucien Arnaud, Kozak Raymond & Lopaschuk Gary D. The Antianginal Drug Trimetazidine Shifts Cardiac Energy Metabolism From Fatty Acid Oxidation to Glucose Oxidation by Inhibiting Mitochondrial Long-Chain 3-Ketoacyl Coenzyme A Thiolase. *Circ. Res.* **86**, 580–588 (2000).

444. Liu, X. *et al.* Characterization of mitochondrial trifunctional protein and its inactivation study for medicine development. *Biochim. Biophys. Acta BBA - Proteins Proteomics* **1784**, 1742–1749 (2008).

445. Chrusciel, P., Rysz, J. & Banach, M. Defining the Role of Trimetazidine in the Treatment of Cardiovascular Disorders: Some Insights on Its Role in Heart Failure and Peripheral Artery Disease. *Drugs* **74**, 971–980 (2014).

446. MacInnes Alan *et al.* The Antianginal Agent Trimetazidine Does Not Exert Its Functional Benefit via Inhibition of Mitochondrial Long-Chain 3-Ketoacyl Coenzyme A Thiolase. *Circ. Res.* **93**, e26–e32 (2003).

447. Hans, F. P., Moser, M., Bode, C. & Grundmann, S. MicroRNA Regulation of Angiogenesis and Arteriogenesis. *Trends Cardiovasc. Med.* **20**, 253–262 (2010).

448. Sun, L., Li, W., Lei, F. & Li, X. The regulatory role of microRNAs in angiogenesis-related diseases. *J. Cell. Mol. Med.* **22**, 4568–4587 (2018).

449. Lei, Z. *et al.* MicroRNA-132/212 family enhances arteriogenesis after hindlimb ischaemia through modulation of the Ras-MAPK pathway. *J. Cell. Mol. Med.* **19**, 1994–2005 (2015).

450. Landskroner-Eiger, S. *et al.* Endothelial miR-17∼92 cluster negatively regulates arteriogenesis via miRNA-19 repression of WNT signaling. *Proc. Natl. Acad. Sci.* **112**, 12812–12817 (2015).

451. Lujan, D. A., Ochoa, J. L. & Hartley, R. S. Cold-inducible RNA binding protein in cancer and inflammation. *Wiley Interdiscip. Rev. RNA* **9**, e1462 (2018).

452. LLeonart, M. E. A new generation of proto-oncogenes: Cold-inducible RNA binding proteins. *Biochim. Biophys. Acta BBA - Rev. Cancer* **1805**, 43–52 (2010).

453. Lee, H., Han, S., Kwon, C. S. & Lee, D. Biogenesis and regulation of the let-7 miRNAs and their functional implications. *Protein Cell* **7**, 100–113 (2016).

454. Sokol, N. S., Xu, P., Jan, Y.-N. & Ambros, V. Drosophila let-7 microRNA is required for remodeling of the neuromusculature during metamorphosis. *Genes Dev.* **22**, 1591–1596 (2008).

455. Worringer, K. A. *et al.* The let-7/LIN-41 Pathway Regulates Reprogramming to Human Induced Pluripotent Stem Cells by Controlling Expression of Prodifferentiation Genes. *Cell Stem Cell* **14**, 40–52 (2014).

456. Zhao, C. *et al.* MicroRNA let-7b regulates neural stem cell proliferation and differentiation by targeting nuclear receptor TLX signaling. *Proc. Natl. Acad. Sci. U. S. A.* **107**, 1876–1881 (2010).

457. Zhao, C., Sun, G., Ye, P., Li, S. & Shi, Y. MicroRNA let-7d regulates the TLX/microRNA-9 cascade to control neural cell fate and neurogenesis. *Sci. Rep.* **3**, (2013).

458. Nishino, J., Kim, S., Zhu, Y., Zhu, H. & Morrison, S. J. A network of heterochronic genes including Imp1 regulates temporal changes in stem cell properties. *eLife* **2**, e00924 (2013).

459. Sempere, L. F. *et al.* Expression profiling of mammalian microRNAs uncovers a subset of brain-expressed microRNAs with possible roles in murine and human neuronal differentiation. *Genome Biol.* **5**, R13 (2004).

460. Moss, E. G., Lee, R. C. & Ambros, V. The Cold Shock Domain Protein LIN-28 Controls Developmental Timing in C. elegans and Is Regulated by the lin-4 RNA. *Cell* **88**, 637–646 (1997).

461. Moss, E. G. & Tang, L. Conservation of the heterochronic regulator Lin-28, its developmental expression and microRNA complementary sites. *Dev. Biol.* **258**, 432–442 (2003).

462. Darr, H. & Benvenisty, N. Genetic Analysis of the Role of the Reprogramming Gene LIN-28 in Human Embryonic Stem Cells. *STEM CELLS* **27**, 352–362 (2009).

463. Yang, D.-H. & Moss, E. G. Temporally regulated expression of Lin-28 in diverse tissues of the developing mouse. *Gene Expr. Patterns* **3**, 719–726 (2003).

464. Wilbert, M. L. *et al.* LIN28 Binds Messenger RNAs at GGAGA Motifs and Regulates Splicing Factor Abundance. *Mol. Cell* **48**, 195–206 (2012).

465. Cho, J. *et al.* LIN28A Is a Suppressor of ER-Associated Translation in Embryonic Stem Cells. *Cell* **151**, 765–777 (2012).

466. Xu, B., Zhang, K. & Huang, Y. Lin28 modulates cell growth and associates with a subset of cell cycle regulator mRNAs in mouse embryonic stem cells. *RNA* **15**, 357–361 (2009).

467. Takamizawa, J. *et al.* Reduced Expression of the let-7 MicroRNAs in Human Lung Cancers in Association with Shortened Postoperative Survival. *Cancer Res.* **64**, 3753–3756 (2004).

468. Dahiya, N. *et al.* MicroRNA Expression and Identification of Putative miRNA Targets in Ovarian Cancer. *PLOS ONE* **3**, e2436 (2008).

469. O'Hara, A. J. *et al.* Tumor suppressor microRNAs are underrepresented in primary effusion lymphoma and Kaposi sarcoma. *Blood* **113**, 5938–5941 (2009).

470. Mi, S. *et al.* MicroRNA expression signatures accurately discriminate acute lymphoblastic leukemia from acute myeloid leukemia. *Proc. Natl. Acad. Sci.* **104**, 19971–19976 (2007).

471. Koscianska, E. *et al.* Prediction and preliminary validation of oncogene regulation by miRNAs. *BMC Mol. Biol.* **8**, 79 (2007).

472. Viswanathan, S. R. *et al.* Lin28 promotes transformation and is associated with advanced human malignancies. *Nat. Genet.* **41**, 843–848 (2009).

473. Dangi-Garimella, S. *et al.* Raf kinase inhibitory protein suppresses a metastasis signalling cascade involving LIN28 and let-7. *EMBO J.* **28**, 347–358 (2009).

474. Hagan, J. P., O'Neill, B. L., Stewart, C. L., Kozlov, S. V. & Croce, C. M. At least ten genes define the imprinted Dlk1-Dio3 cluster on mouse chromosome 12qF1. *PloS One* **4**, e4352 (2009).

475. Thornton, J. E., Chang, H.-M., Piskounova, E. & Gregory, R. I. Lin28-mediated control of let-7 microRNA expression by alternative TUTases Zcchc11 (TUT4) and Zcchc6 (TUT7). *RNA N. Y. N* **18**, 1875–1885 (2012).

476. Piskounova, E. *et al.* Oncogenic Lin28A and Lin28B inhibit let-7 microRNA biogenesis by distinct mechanisms. *Cell* **147**, 1066–1079 (2011).

477. Towbin, H. *et al.* Systematic screens of proteins binding to synthetic microRNA precursors. *Nucleic Acids Res.* **41**, e47–e47 (2013).

478. Heo, I. *et al.* TUT4 in Concert with Lin28 Suppresses MicroRNA Biogenesis through Pre-MicroRNA Uridylation. *Cell* **138**, 696–708 (2009).

479. Yuva-Aydemir, Y., Simkin, A., Gascon, E. & Gao, F.-B. MicroRNA-9. *RNA Biol.* **8**, 557–564 (2011).

480. He, M. *et al.* Cell-Type-Based Analysis of MicroRNA Profiles in the Mouse Brain. *Neuron* **73**, 35–48 (2012).

481. Krichevsky, A. M., Sonntag, K.-C., Isacson, O. & Kosik, K. S. Specific MicroRNAs Modulate Embryonic Stem Cell–Derived Neurogenesis. *STEM CELLS* **24**, 857–864 (2006).

482. Shibata, M., Nakao, H., Kiyonari, H., Abe, T. & Aizawa, S. MicroRNA-9 Regulates Neurogenesis in Mouse Telencephalon by Targeting Multiple Transcription Factors. *J. Neurosci.* **31**, 3407–3422 (2011).

483. Zhao, C., Sun, G., Li, S. & Shi, Y. A feedback regulatory loop involving microRNA-9 and nuclear receptor TLX in neural stem cell fate determination. *Nat. Struct. Mol. Biol.* **16**, 365–371 (2009).

484. Yoo, A. S. *et al.* MicroRNA-mediated conversion of human fibroblasts to neurons. *Nature* **476**, 228–231 (2011).

485. Laneve, P. *et al.* A minicircuitry involving REST and CREB controls miR-9-2 expression during human neuronal differentiation. *Nucleic Acids Res.* **38**, 6895–6905 (2010).

486. Nam, Y., Chen, C., Gregory, R. I., Chou, J. J. & Sliz, P. Molecular Basis for Interaction of let-7 MicroRNAs with Lin28. *Cell* **147**, 1080–1091 (2011).

487. Desjardins, A., Yang, A., Bouvette, J., Omichinski, J. G. & Legault, P. Importance of the NCp7-like domain in the recognition of pre-let-7g by the pluripotency factor Lin28. *Nucleic Acids Res.* **40**, 1767–1777 (2012).

488. Loughlin, F. E. *et al.* Structural basis of pre-let-7 miRNA recognition by the zinc knuckles of pluripotency factor Lin28. *Nat. Struct. Mol. Biol.* **19**, 84–89 (2011).

489. Jovičić, A. *et al.* Comprehensive Expression Analyses of Neural Cell-Type-Specific miRNAs Identify New Determinants of the Specification and Maintenance of Neuronal Phenotypes. *J. Neurosci.* **33**, 5127–5137 (2013).

490. Huang, B. *et al.* MicroRNA expression profiling during neural differentiation of mouse embryonic carcinoma P19 cells. *Acta Biochim. Biophys. Sin.* **41**, 231–236 (2009).

491. Gaughwin, P., Ciesla, M., Yang, H., Lim, B. & Brundin, P. Stage-Specific Modulation of Cortical Neuronal Development by Mmu-miR-134. *Cereb. Cortex* **21**, 1857–1869 (2011).

492. Zhang, J. *et al.* Effects of miR-541 on neurite outgrowth during neuronal differentiation. *Cell Biochem. Funct.* **29**, 279–286 (2011).

493. Xu, B. & Huang, Y. Histone H2a mRNA interacts with Lin28 and contains a Lin28-dependent posttranscriptional regulatory element. *Nucleic Acids Res.* **37**, 4256–4263 (2009).

494. Peng, S. *et al.* Genome-Wide Studies Reveal That Lin28 Enhances the Translation of Genes Important for Growth and Survival of Human Embryonic Stem Cells. *STEM CELLS* **29**, 496–504 (2011).

495. Malecki, M. *et al.* The exoribonuclease Dis3L2 defines a novel eukaryotic RNA degradation pathway. *EMBO J.* **32**, 1842–1854 (2013).

496. Abdelmagid, S. A. *et al.* Comprehensive Profiling of Plasma Fatty Acid Concentrations in Young Healthy Canadian Adults. *PLOS ONE* **10**, e0116195 (2015).

497. Rustan, A. C. & Drevon, C. A. Fatty Acids: Structures and Properties. in *Encyclopedia of Life Sciences* (ed. John Wiley & Sons, Ltd) (John Wiley & Sons, Ltd, 2005). doi:10.1038/npg.els.0003894.

498. Maris, C., Dominguez, C. & Allain, F. H.-T. The RNA recognition motif, a plastic RNA-binding platform to regulate post-transcriptional gene expression. *FEBS J.* **272**, 2118–2131 (2005).

499. Sakakibara, S., Nakamura, Y., Satoh, H. & Okano, H. RNA-Binding Protein Musashi2: Developmentally Regulated Expression in Neural Precursor Cells and Subpopulations of Neurons in Mammalian CNS. *J. Neurosci.* **21**, 8091–8107 (2001).

500. Chen, C.-Y. A., Xu, N. & Shyu, A.-B. Highly Selective Actions of HuR in Antagonizing AU-Rich Element-Mediated mRNA Destabilization. *Mol. Cell. Biol.* **22**, 7268–7278 (2002).

501. Horsham, J. L. *et al.* Clinical Potential of microRNA-7 in Cancer. *J. Clin. Med.* **4**, 1668–1687 (2015).

502. Junn, E. *et al.* Repression of α-synuclein expression and toxicity by microRNA-7. *Proc. Natl. Acad. Sci. U. S. A.* **106**, 13052–13057 (2009).

503. Yanai, I. *et al.* Genome-wide midrange transcription profiles reveal expression level relationships in human tissue specification. *Bioinformatics* **21**, 650–659 (2005).

504. Lee, T. & Pelletier, J. The biology of DHX9 and its potential as a therapeutic target. *Oncotarget* **7**, 42716–42739 (2016).

505. Tsai, Y. S., Gomez, S. M. & Wang, Z. Prevalent RNA recognition motif duplication in the human genome. *RNA* **20**, 702–712 (2014).

506. Natali, F., Siculella, L., Salvati, S. & Gnoni, G. V. Oleic acid is a potent inhibitor of fatty acid and cholesterol synthesis in C6 glioma cells. *J. Lipid Res.* **48**, 1966–1975 (2007).

507. Pan, J. H. *et al.* Inhibition of the lipogenesis in liver and adipose tissue of diet-induced obese C57BL/6 mice by feeding oleic acid-rich sesame oil. *Food Sci. Biotechnol.* **24**, 1115–1121 (2015).

508. Hsu, S.-C. & Huang, C. Reduced Fat Mass in Rats Fed a High Oleic Acid–Rich Safflower Oil Diet Is Associated with Changes in Expression of Hepatic PPARα and Adipose SREBP-1c–Regulated Genes,2. *J. Nutr.* **136**, 1779–1785 (2006).

509. Baró, L., Hermoso, J.-C., Núñez, M.-C., Jiménez-Rios, J.-A. & Gil, A. Abnormalities in plasma and red blood cell fatty acid profiles of patients with colorectal cancer. *Br. J. Cancer* **77**, 1978–1983 (1998).

510. Liotti, A. *et al.* Oleic acid promotes prostate cancer malignant phenotype via the G protein-coupled receptor FFA1/GPR40. *J. Cell. Physiol.* **233**, 7367–7378 (2018).

511. Snowden, S. G. *et al.* Association between fatty acid metabolism in the brain and Alzheimer disease neuropathology and cognitive performance: A nontargeted metabolomic study. *PLoS Med.* **14**, (2017).

512. Fonteh, A. N., Cipolla, M., Chiang, J., Arakaki, X. & Harrington, M. G. Human Cerebrospinal Fluid Fatty Acid Levels Differ between Supernatant Fluid and Brain-Derived Nanoparticle Fractions, and Are Altered in Alzheimer's Disease. *PLOS ONE* **9**, e100519 (2014).

513. Fanning, S. *et al.* Lipidomic Analysis of α-Synuclein Neurotoxicity Identifies Stearoyl CoA Desaturase as a Target for Parkinson Treatment. *Mol. Cell* **73**, 1001-1014.e8 (2019).